remote sensing

MDPI

Review

Imaging Cultural Heritage at Different Scales: Part II, the Meso-Scale (Sites)

Luca Piroddi [1,2,*], Nasser Abu Zeid [3,†], Sergio Vincenzo Calcina [1], Patrizia Capizzi [4], Luigi Capozzoli [5], Ilaria Catapano [6], Marilena Cozzolino [7], Sebastiano D'Amico [2], Rosa Lasaponara [5] and Deodato Tapete [8]

1 Department of Civil, Environmental Engineering and Architecture, University of Cagliari, Via Marengo 2, 09123 Cagliari, Italy; sergiocalcina@virgilio.it
2 Department of Geosciences, University of Malta, MSD 208 0 Msida, Malta; sebastiano.damico@um.edu.mt
3 Department of Physics and Earth Sciences, University of Ferrara, Via Saragat 1, 44122 Ferrara, Italy; a.nasser@unife.it
4 Department of Earth and Sea Sciences, University of Palermo, Via Archirafi, 22, 90123 Palermo, Italy; patrizia.capizzi@unipa.it
5 Institute of Methodologies for Environmental Analysis—National Research Council of Italy (CNR-IMAA), C.da S. Loja-Zona Industriale, 85050 Tito Scalo, Italy; luigi.capozzoli@imaa.cnr.it (L.C.); rosa.lasaponara@imaa.cnr.it (R.L.)
6 Institute for Electromagnetic Sensing of the Environment—National Research Council of Italy (CNR-IREA), Via Diocleziano 328, 80127 Napoli, Italy; catapano.i@irea.cnr.it
7 Department of Agricultural, Environmental and Food Sciences, University of Molise, Via De Sanctis snc, 86100 Campobasso, Italy; marilena.cozzolino@unimol.it
8 Italian Space Agency (ASI), Via del Politecnico snc, 00133 Rome, Italy; deodato.tapete@asi.it
* Correspondence: lucapiroddi@yahoo.it
† Current address: TeamGeofisica.CEG, Via G. Fabbri, 342, 44124 Ferrara, Italy.

Abstract: Non-invasive sensing techniques have become a cornerstone in the study and preservation of Cultural Heritage. These techniques offer a means to investigate the internal structure and surface properties of precious and delicate objects without causing damage. This article is the second of three review articles exploring contact and non-contact imaging methods applied to Cultural Heritage at various scales encompassing micro- (i.e., manufacts), meso- (sites), and macro-scales (landscapes). The unifying factor of these techniques is their ability to infer variations in geometrical and physical properties across inspected surfaces or volumes. This allows researchers to discover new historical sites, map their spatial extent, and characterize their material features at different scales, from landscapes to artifacts. This second part focuses on the meso-scale, encompassing the inspection, documentation, study, and characterization of historical and archeological sites, monuments, and submerged sites, using both contact and remote sensing techniques.

Keywords: geophysical prospections; historical/archeological sites; monuments and submerged sites; risk management; archeological prospection; surveying; drones; close range sensors; Cultural Heritage

check for updates

Academic Editor: Henrique Lorenzo

Received: 4 January 2025
Revised: 2 February 2025
Accepted: 6 February 2025
Published: 10 February 2025

Citation: Piroddi, L.; Abu Zeid, N.; Calcina, S.V.; Capizzi, P.; Capozzoli, L.; Catapano, I.; Cozzolino, M.; D'Amico, S.; Lasaponara, R.; Tapete, D. Imaging Cultural Heritage at Different Scales: Part II, the Meso-Scale (Sites). *Remote Sens.* **2025**, *17*, 598. https://doi.org/10.3390/rs17040598/

Copyright: © 2025 by the authors. Licensee MDPI, Basel, Switzerland. This article is an open access article distributed under the terms and conditions of the Creative Commons Attribution (CC BY) license (https://creativecommons.org/licenses/by/4.0/).

1. Introduction

Conservation science of Cultural Heritage is nowadays a multidisciplinary research field where remote sensing techniques play a key role, primarily due to their capabilities to inspect the surface and internal structure of fragile objects with high artistic and economic value with very minimal or no contact.

Non-invasive techniques provide a fundamental toolkit for achieving an improved understanding and documentation of the physical, chemical and aesthetic properties of

Cultural Heritage. They offer heritage bodies the objective knowledge needed not only to unveil how these objects were produced and preserved over time, but also to ensure their future conservation and exhibition in secure and controlled environments.

While the use of such techniques for general diagnostic purposes has a long history, it is only in quite recent times that technological advancements in sensors and instrumentation have made the characterization and inspection of very precious and vulnerable targets feasible and customizable. Techniques that were initially not exploited for the study of Cultural Heritage, due to their intrinsic technical limitations, have now been proven suitable for this purpose, and are now part of the portfolio of instrumental techniques increasingly used in conservation science. The inclusion of these technologies and methods in conservation curricula, such as historical architecture conservation and archeology, indicates a growing and irreversible trend of integrating modern and objective tools into a standard conservation framework. In many cases, the contribution of geophysical and surveying methods, sometimes jointly with proximal sensing and automation techniques, is significant for the knowledge and documentation of cultural sites or manufacts.

At all scales of implementation, i.e., micro- (manufacts), meso- (sites) and macro-scales (landscapes), the current trend is to integrate different diagnostic techniques, based on the principle that each offers specific capabilities and only their combination can achieve the intended study objectives. This approach applies to different tasks in the lifecycle of Cultural Heritage study and conservation, including data collection, processing, visualization, interpretation, data fusion, scenario reconstruction, virtual fruition and musealization, virtual restoration, hazard reduction, preservation, and repair actions.

This article is part of a solicited editorial project within the Special Issue "*Remote, Proximal Sensing and Geophysics for Cultural Heritage Knowledge and Conservation*" of the "Remote Sensing" journal. It provides an overview of the non-invasive diagnostic methods used for Cultural Heritage assets, covering a range of scales. It briefly discusses the working principles and mechanisms of each "family" of techniques and illustrates these with selected case studies. The goal is not to rank techniques or applications, but to highlight the key advantages and specificities of commonly used diagnostic methods at different scales, as demonstrated by true data from real-world examples.

The present article is the second of a three-part review set, focusing on the following three implementation scales:

- Part I, the micro-scale (manufacts);
- Part II, the meso-scale (sites);
- Part III, the macro-scale (landscapes).

The first article has already been published and investigates the micro-scale, where the targets are small to very small Cultural Heritage items such as individual architectural elements or decorative finishes of historical buildings, paintings, statues, or ancient papers [1]. This second paper focuses on the meso-scale, encompassing historical and archeological sites, monuments, historical buildings, and submerged areas.

2. Materials and Methods

This article presents applications of geophysical and surveying methodologies, preferably used independently to better highlight the features of each, for detecting and characterizing potential archeological features, within sites that are either spatially limited or characterized by the presence of obstacles that prevent the use of most automatic data acquisition systems (typical of the macro-scale/landscapes). Some examples of automation, often involving drones, are provided from experimental cases. In such experimental contexts, the high costs of sophisticated instruments are acceptable, unlike in applicational contexts where the limited investigation areas do not allow for the offsetting of the initial

costs through reduced operational expenses. A section of this manuscript showcases the potential of these methods for diagnostic goals beyond discovering precious artifacts, which has been in any case the first and most diffuse application in the Cultural Heritage sector. This section provides some evidence of their effectiveness in risk management activities for precious sites or buildings, especially focusing on the vulnerability characterization of Cultural Heritage assets.

The paper is organized into three sections:

Section 3.1: Geophysical prospection for archeological sites

3.1.1. Georadar;
3.1.2. Magnetometry;
3.1.3. Electrical Resistivity methods;
3.1.4. Electromagnetic Induction method;
3.1.5. Other techniques.

Section 3.2: Other geophysical applications

3.2.1. Monumental structures;
3.2.2. Submerged archeological areas;
3.2.3. Approaches aiding risk assessment and management.

Section 3.3: Proximal sensing geophysics and geomatics for archeological prospection

Section 3.1 illustrates the first to have become mature application of geophysical methods to Cultural Heritage studies, remaining today the largest part of the scientific and technical literature on these topics. Within this section, case studies are presented to highlight the advantages of each method, often selecting articles with a single or a predominant method to exemplify their own performance in specific contexts and investigation goals. While a single method is rarely the best choice for geophysical diagnostics, synergistic and multi-method investigations are often preferred for more robust information and reconstruction of underground physical properties. Although some presented case studies demonstrate the benefits of multi-methods, this was not our main objective during the compilation of this work. The selection of case studies was not intended to strictly reflect the literature based on parameters like numerosity, originality, impact, or expected impact, though these influenced our choices; these case studies are in fact presented in the paper with the main goal of exemplifying some aspects of the general and potential approaches to the various typologies of applications.

Section 3.2 presents a variety of applications, offering examples from three areas that are more recent than classic archeological geophysics. These examples aim to demonstrate the flexibility and reliability of non-invasive techniques for novel study problems. The first sub-topic involves the investigation of monumental structures, which are a middle ground between the micro-geophysical applications presented in the review Part I [1] and the geophysical methods shown in Section 3.1. A second challenging application is the study of submerged or partially submerged archeological sites, where the customization of data acquisition, processing, and interpretation methods is the main scientific goal. The third main application of this Section provides a partial view of a potentially vast field, addressing the management of risks to Cultural Heritage assets. Although only a few examples are presented, this overview aims to illustrate the effectiveness of non-invasive methods in constructing critical information for Cultural Heritage management.

Section 3.3 presents cross-disciplinary methods and case studies, focusing on the proximal sensing of meso-scale targets using various non-contact sensors, including visible-band cameras, LiDAR, and geophysical tools. These are deployed from platforms that are increasingly aerial, thanks to advancements in drones and their integration with a multitude of sensors.

3. Results: Selected Case Studies and Approaches in the Literature

This section provides an overview of the selected case studies distributed across the three sub-sections, related to the geophysical prospection of archeological sites (Section 3.1), challenging geophysical applications beyond archeological sites (Section 3.2), and proximal sensing geomatics and geophysical applications (Section 3.3).

3.1. Geophysical Prospection of Archeological Sites

The growing interest in geophysical methodologies for the prospection of archeological sites is related to the detection and characterization of numerous locations worldwide [2–4]. Due to their high resolution and the potential for saving time and costs, geophysical prospection techniques have become systematic, especially in the early stages of identifying potential archeological sites and in the enhanced investigation of existing ones.

Ground-Penetrating Radar (GPR) and magnetometric (MAG) surveys are widely used for archeological purposes because of their non-intrusiveness, high resolution, and relatively good depth of investigation. Additionally, other methods, such as electrical resistivity and electromagnetic techniques, can significantly contribute to detecting buried ruins and characterizing historical sites. However, the use of GPR and MAG surveys is limited by sites conditions (i.e., rough surface, conductive soils, and/or the presence of anthropogenic sources of electromagnetic noise, mainly caused by urban and industrialized utilities). Other geophysical methods occasionally used in archeological prospection include seismic (both active and passive) and gravity techniques, while other approaches are rare or potentially emerging (e.g., gamma ray mapping). The essential requirement for the successful application of geophysical methodologies is represented by the presence of a measurable physical property contrast between the researched target, generally hidden, and the surrounding environment. An archeological structure located in the shallow subsoil can typically produce an anomaly in the recorded physical signal. Unfortunately, this is not always the case; sometimes, the structures are made from the same material as the surrounding environment, which can significantly reduce the capability to detect the target. In other circumstances, the specific geophysical method may be ineffective in certain environmental contexts. To try and address and/or mitigate these limitations, the cooperative use of different methodologies can be a valid strategy.

3.1.1. Georadar (GPR)

As concerns the GPR, its use is based on the introduction of an electromagnetic (EM) signal into the ground and the subsequent recording of the reflections due to the dielectric permittivity variations imputable to the presence of buried objects and structures. A crucial role of the GPR application is represented by the antenna frequency, from which the resolution and reachable depth of investigation depend. For archeological applications, the investigations are realized at frequencies ranging between 0.1 and 1 GHz for ensuring a depth of investigation between down to 1 m and 4 m, and with sub-meter and sub-decimeter resolution (even if some applications with frequencies out of that range actually exist).

Usually, GPR data are acquired in reflection mode by exploiting acquisition grids with 2D lines of investigation, equally spaced at a distance that is designed based on the expected dimensions of the underground target bodies, often distributed in two perpendicular directions. The collected data are processed to emphasize the signal due to buried structures and reduce noise and clutter. The results are 2D images, referred to as radargrams (or B-scans), which can be interpolated for the realization of 3D representations able to effectively support the detection of anomalies associable to archeological features. Indeed, if 2D data can give useful insights into morphologically irregular surfaces, 3D data, visualized as three-dimensional blocks or as horizontal (time slices and/or depth slices, C-scans)

or vertical (radargrams or interpolated sections) slices, can provide useful information for detecting horizontal patterning related to anthropogenic/cultural activities. Like all other walking techniques in geophysics, even GPR has benefited from the introduction of geomatic positioning systems, and random planimetric acquisitions are now becoming more frequent than in the past.

GPR has been extensively used to enhance knowledge of historical and archeological sites and to document buried archeological features. Initially, its primary purpose was to support archeologists in developing excavation strategies. More recently, this has been complemented by virtual dissemination of this information to society and scholars.

The high resolution offered by this method and the possibility to derive depth information about the anomalies for the identification of the planimetric and spatial development of the structures, typical of its application to archeological sites, were highlighted by Piro et al. [5] in the detection and reconstruction of Traiano's Villa near Rome. The data shown in the paper were collected, using 500 MHz antenna, by recording parallel profiles equally spaced 0.5 m apart. Thanks to the use of time slice analyses, the ancient structure was reconstructed, allowing for the effective mapping of the ancient rooms of the Villa.

The presence of buried structures characterized by a regular layout represents a favorable condition for achieving optimal results with the GPR [6–10]. At the Aiali site (Grosseto, Italy), a Roman Villa was discovered thanks to the short distance between the profiles (50 cm) and an antenna frequency of 400 MHz [6]. The success of this application was provided by the expected integrity of the structure, as well as its surface location. The results shown in Figure 1, referred to as amplitude or energy (squared amplitude) time slices, clearly provide the location, depth, and shape of the radar reflections most probably associable with the walls of the structures located at depths ranging, approximately, from 15 to 115 cm. In [7], a GPR survey using an antenna frequency of 600 MHz was realized in the archeological area of Saepinum (Italy) in the space between the theater and the *decumanus*, allowing for the imaging of a complex regular pattern of interesting archeological features. Given the articulation of the anomalies and their geometric characteristics being enriched by apsidal environments, it was assumed that they belonged to a thermal complex. Successful results are also presented in [8,9] in unaltered soils at the site of Doclea (Montenegro) and in the deserted town of Corvey (Germany), where several rooms of the ancient buildings (Figure 2) and a Roman Basilica Church (Figure 3a) were, respectively, detected.

The use of 3D representation is also exploited for the detection of archeological features as an improvement on the information obtainable by 2D time slice analyses. Leucci et al. [10] used the means of iso-amplitude surfaces of the complex trace amplitude for highlighting the site of Hierapolis of Phrygia (Turkey)'s possible archeological structures. A similar approach was adopted by Urban et al. [11] at the site of Pantelleria (Italy) for detecting potential curvilinear and linear architectural features. Florit et al. [12] demonstrated the usefulness of the GPR in rural areas when a negligible number of sources of disturbance characterize the investigated site, through the discovery of a Roman Villa in Mallorca (Balearic Islands, Spain).

The scarce attenuation of the EM signal in most of the dry soils makes the use of the GPR particularly promising in arid contexts, where data can be considered reliable for archeological purposes until the depth of 4 m, as discussed by Porcelli et al. [13] at the Valley of the Kings (Luxor, Egypt). The horizontal slices obtained at three different depths highlight the aligned reflective anomalies due to the visitors' path, which covered by natural sediments.

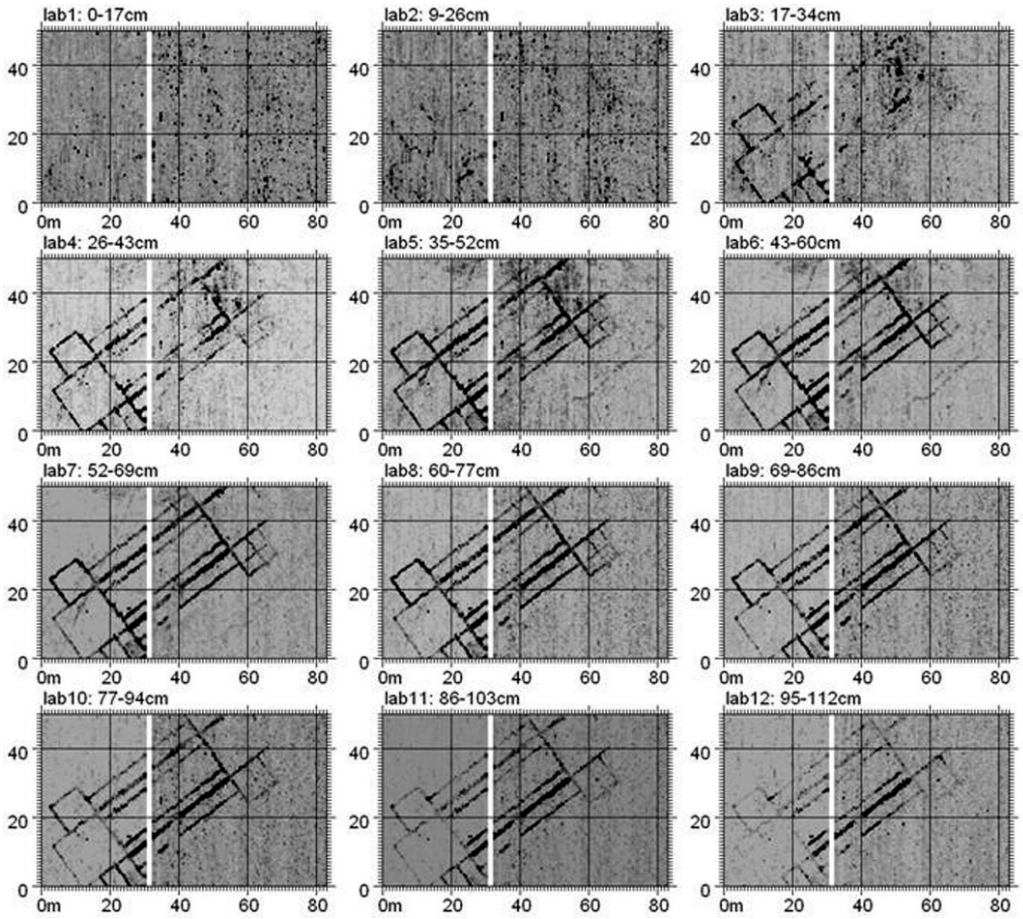


Figure 1. Aiali site (Grosseto, Italy). Depth slices extrapolated by the interpolated and solid 3D volumes of reflections amplitudes [6]. Copyright © John Wiley & Sons, permission obtained.

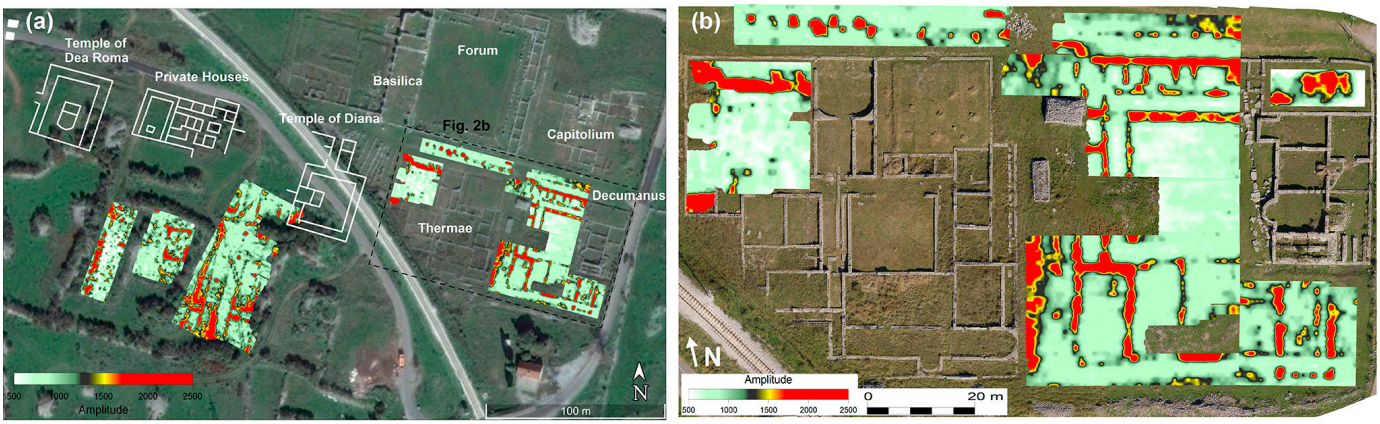
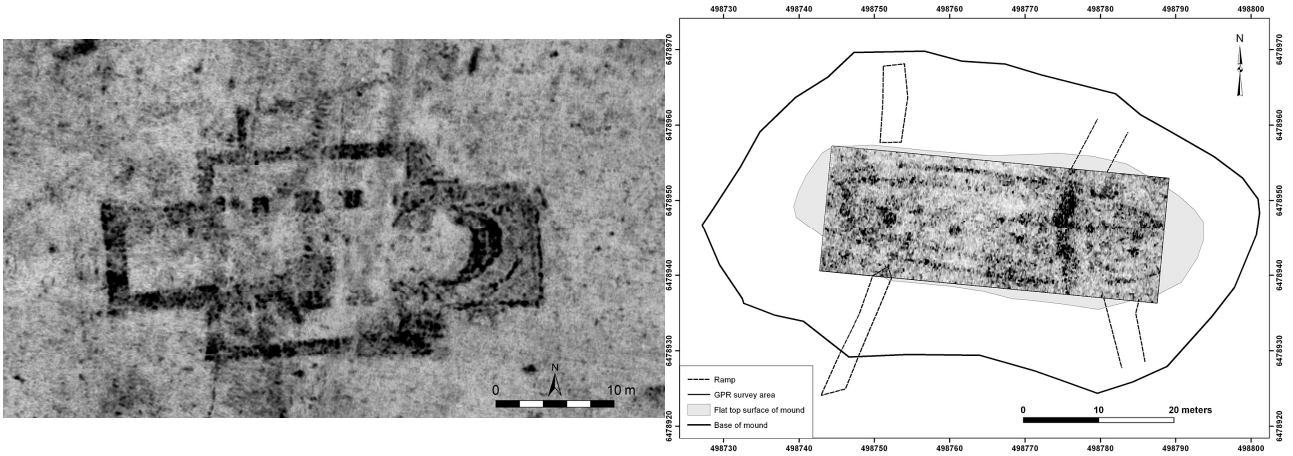


Figure 2. Doclea (Podgorica, Montenegro). GPR time slice relative to the time window 14–18 ns, overlapped on the satellite image of Google Earth™ (**a**) with a focus on the thermae (**b**) [8].



(**a**) (**b**)

Figure 3. Corvey (Germany). Combined GPR depth slice of approx. 70–110 cm below ground surface, showing the foundations of the medieval parish church. Reflective deposits are shown in dark [9], CC BY-NC-ND 4.0 (**a**). Aska (Östergötland, Sweden). GPR depth slice at a depth of 0.8 m shows the layout of a post-borne, three-aisled building with reflections distributed according to a curvilinear path [14]. Copyright © John Wiley & Sons, permission obtained (**b**).

An interesting approach was adopted by Booth et al. [15] for supporting the discovery of archeological features at the South Asasif tomb complex (Luxor, Egypt). The authors highlight how GPR is indirectly able to investigate the structure of an ancient Egyptian tomb placed at depths not reachable by the conventional application by exploiting the capability of observing indirect evidence as to the deflection of sediment horizons in the overburden. Using a deductive method, they assume that the V-shaped reflections are reasonably associable with the presence of a collapsed tomb placed at the remarkable depth of ~4 m, not reachable with the conventional GPR operating frequency.

GPR allows for the obtainment of clear interpretable results, especially when the archeological features are characterized by regular shapes, but its use also provides the ability to reconstruct curvilinear structures, as in the case of the ancient Viking building in Aska (Östergötland, Sweden) imaged by Rundkvist and Viberg [14], which displayed a buried elliptical layout. The resulting reflections shown in Figure 3b allowed them to identify the presence of the main elements constituting the structure, i.e., the ramp, postholes, and hearts. To achieve these results, it was fundamental to adopt a transect spacing of 0.1 m that gave the possibility of identifying the postholes of only 0.2–0.25 m in diameter.

The enhanced complexity regarding the use of many geophysical methodologies in urban context limits their use because of the presence of various sources of electrical and electromagnetic noise and disturbance. However, despite greater difficulty in clearly understanding the results, GPR often represents the only way of detecting the archeological structures present in urban areas.

The feasibility of GPR is demonstrated by [16] for the identification of the archeological remains, due to the presence of an ancient necropolis placed at the historic center of Lecce (Italy). Despite the difficulties imputable to the presence of buildings, paved roads, and tree areas, thanks to the use of archeological data and georeferenced GPR horizontal slices, the authors highlighted the presence of buried and unknown archeological structures.

Another suggestive example concerning the use of GPR in urban contexts was described by Piro et al. [17], who investigated the subsoil of the St. John Lateran Basilica's external areas in Rome (Italy), adopting the frequencies of 400 and 70 MHz for reaching depths of up to 3.4 m and 6.7 m, respectively, and detecting structures belonging to the

medieval and Roman ages. Also, Masini et al. [18] presented an urban prospection with GPR investigations, supported by archeological data that have effectively contributed to the identification of Inca structures under a few decimeters of subsoil in the main square of Cusco (Peru). The achieved results highlight different stratigraphic layers in the center of the city, demonstrating GPR's capability in detecting fundamental archeological features for the comprehension of the evolution of historic cities.

Capozzoli et al. [19] successfully used microwave tomography for better imaging of a buried temple located near the fortification wall of the Greek city of Posedonia (Paestum, Italy). The remains of a small Doric temple backing onto the ancient city's walls were found, also with the support of archeological data and magnetometric analyses, by collecting GPR data according to a grid of parallel lines equally spaced 0.5 m apart in two perpendicular directions, at frequencies of 200 and 600 MHz. The depth slices shown in Figure 4 highlight the foundation system of the temple at different depths, including isolated reflections presumably associable with the other nearest archeological features.

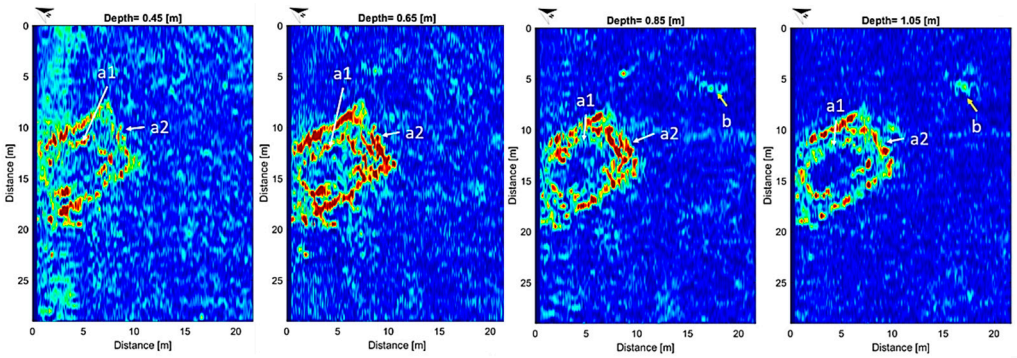


Figure 4. Paestum (Italy). Tomographic images reconstructing the Doric temple structure at a depth ranging between 0.65 and 1.05 m. The high amplitude reflections are due to the foundation system of the buried building (a1,a2) and a possible altar (b) [19].

Zhao et al. [20] investigated the potentialities of GPR attribute analysis for detecting and emphasizing features not easily visible on the usual amplitude data. Data were acquired at the frequency of 250 MHz according to parallel lines at a mutual distance of 0.5–1 m. The authors tested the contributions of the attributes of energy and similarity for detecting possible archeological structures at the archeological site of Aquileia (Italy), and highlighted that the energy can emphasize low or irregular amplitude reflections identifying the most reflective zones, while the similarity allows for the detection of coherently and extended buried structures (Figure 5).

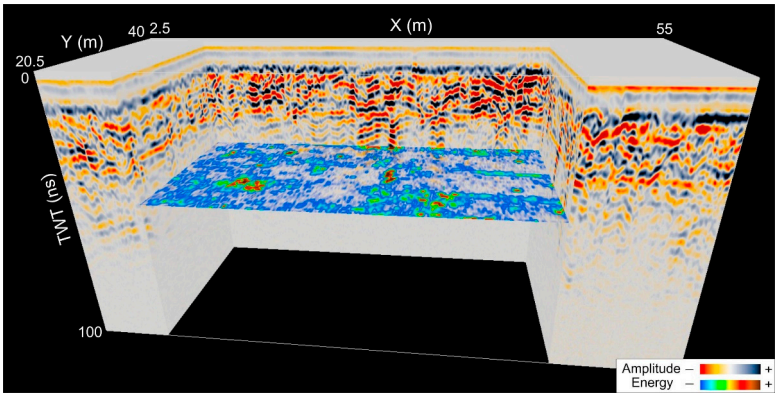


Figure 5. Aquileia (Italy). Joint visualization of 3D GPR volume highlighting high amplitude vertical variations and time slice (at 46 ns), characterized by lateral anomalies with high energy not identifiable with the vertical sections [20], © 2017 Elsevier Ltd., permission obtained.

Recently, Colombero et al. [21] used attribute analyses and 3D reconstruction for supporting the identification of buried linear and localized archeological remains at the archeological site of Augusta Bagiennorum (Bene Vagienna, Italy). GPR data were collected at a frequency of 500 MHz and parallel profiles were acquired, depending on the site, at the mutual distances of 0.3 m and 0.5 m. The authors exploited texture attribute analyses based on the evaluation of the attribute's uniformity, heterogeneity, and dissimilarity, which were finally assembled in 3D data volumes and are represented in values referred to as amplitude of reflection. The computed textural attributes revealed good imaging potential, but only the dissimilarity attribute improved the quality of the obtained information.

3.1.2. Magnetometry (MAG)

Magnetometry investigates the Earth's magnetic anomalies resulting from the magnetic properties of underlying rocks or buried artifacts. Anomalies are generated as a result of the induced and remanent magnetism effects. The first effect is related to the intensity of the magnetic field and magnetic susceptibility of the materials, whilst the second effect, independent of the magnetic field, results principally from thermal and chemical processes characterizing the object itself.

Today, the three most used types of technology for the realization of the magnetometers are fluxgate, proton precession, and optical pumping and, depending on the sensor adopted, the accuracy and speed of the measurements can vary. Measurements are carried out using at least two sensors arranged for performing radiometric analyses that are able to emphasize the response of possible archeological contrasts.

As in the case of the GPR measurements, MAG acquisitions are often carried out using a regular grid, with parallel profiles acquired every 0.5 m or 1.0 m that allow for the continuous recording of the data. In the resulting maps with the distribution of the magnetic field, the recognized anomalies are imputable to the contrast between the magnetic properties of the archeological features and the surrounding environment in terms of magnetic susceptibility.

Depending on the geological context and on the prospection targets, magnetometry is among the most used geophysical methodologies for supporting archeological research, also thanks to very clearly interpretable results. This is the case of the survey of an Iron Age enclosure [22], where the positive anomaly of the ditch was found, accompanied by a fringe of negative data. Similarly, the large pit in the SW corner of the enclosure has a negative halo, most prominently to the north. Under this aspect, the Stonehenge Hidden Landscapes Project (SHLP) represented the successful application of the MAG method in the space surrounding Stonehenge (United Kingdom). Magnetograms of regular and several more irregularly shaped segmented and penannular ditches and pit circles, of various shapes and sizes, are perfectly drawn (Figure 6) [23].

Boschi et al. [24] demonstrated the MAG ability of detecting the main archeological buried structures present at the site of Classe (Italy), where an extensive area of approximately 80 ha was investigated. Different geophysical technologies were applied, but the best results were achieved with the geomagnetic methodology, because of the presence of clayey soils that limited the capability of the GPR. Using cesium and potassium vapor magnetometers, parallel profiles equally spaced 0.5 m apart were acquired, providing impressive information about the ancient city walls, the presence of a huge basilica, and a port. Indeed, despite the problems due to the presence of clay soils and the depth of the archeological structures (2 m), an extensive concentration of ancient buildings was detected, providing new insights to the archeologists for the reconstruction of the ancient urban landscape and understanding the original city planning, also in an urbanized context,

characterized by different sources of magnetic noise, such as railway lines, roads, and buildings placed at a short distance from the surveyed area.

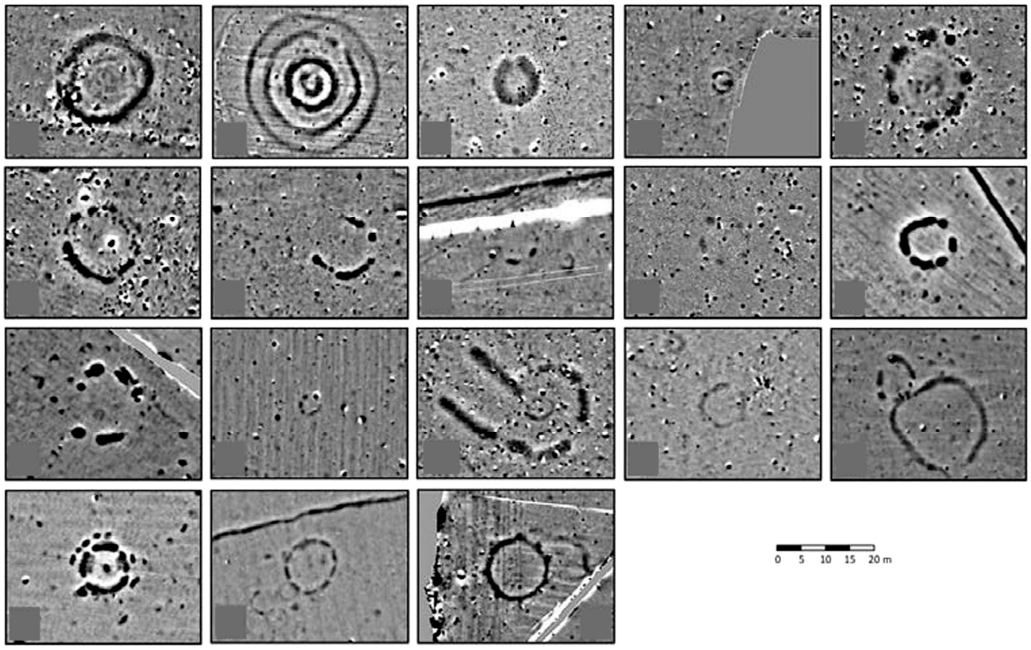
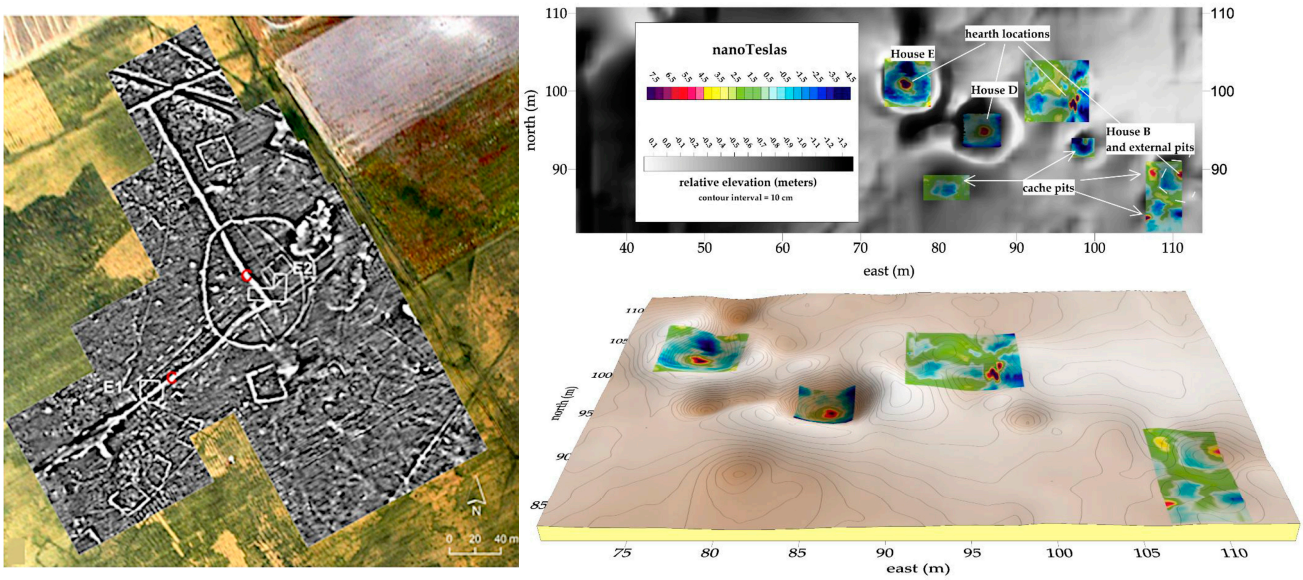


Figure 6. Stonehenge (UK). Magnetograms of eighteen monuments of probable third millennium BC date, mapped within the Stonehenge Hidden Landscapes Project study area. [23] © John Wiley & Sons, permission obtained.

Barta et al. [25] highlighted the possible contribution that MAG surveys can make to archeological investigation in an urban context. Indeed, at Hradcany Square (Prague, Czech Republic), magnetometric measurements supported ERT, GPR, and gravimetric analyses for identifying the medieval trenches going across the square, and some linear and circular anomalies were also detected.

Caldara et al. [26] successfully used the methodology in tandem with aerial observations for investigating the archeological site of Masseria Pantano, located near Foggia, Italy, which has evidence of a long-term human presence dating back to the Neolithic period. An area of 7.6 ha was investigated with parallel profiles equally spaced 0.5 m apart, employing a cesium vapor magnetometer. Results have confirmed the presence of round-shaped marks due to Neolithic ditches, a field system network, and traces of a Roman road and linear and square cropmarks, probably related to the medieval age. Magnetic data have also detected a strong anomaly up to the depth of 3 m below the layer initially considered of interest for the corresponding archeological purposes, as demonstrated by archeological trenches and boreholes of an accommodation work made by the Romans, supposedly a drainage channel (Figure 7a).



(**a**) (**b**)

Figure 7. Masseria Pantano site (Italy). The magnetometric results show the presence of different anomalies imputable to medieval structure, also including a Roman channel characterized by a rectilinear shape and a clear deflection at right angles (C). This structure belongs to the accommodation works before the second half of the thirteenth century AD. Two trial excavations are indicated with E1 and E2. [26] © John Wiley & Sons, permission obtained (**a**). Swift Water Place (Alaska, USA). The integration of magnetometric results overlapped with the DEM of the area clearly highlights the surface depressions hosting the hearth anomalies and four external pits surrounding House B [27], CC BY-NC-ND 4.0 (**b**).

Fitton et al. [28] adopted magnetometry for identifying the putatively ephemeral remains of mobile pastoralists at the Luxmanda site (Tanzania), the largest known settlement documented for the Pastoral Neolithic era in eastern Africa. The authors highlight the contribution of the methodology for recognizing the site's spatial structure, providing information about features (e.g., hearths, livestock pens) and patterns in the structure of refuse deposits fundamental for the comprehension of the settlement dynamics.

The geophysical contrasts can be limited when the target of the investigation has the same magnetic characteristics as its surrounding environment. However, as demonstrated by Lasaponara et al. [29] at the archeological site of Nazca (Peru), magnetic measurements can effectively detect small variations in the soil due to the presence of ceramic materials, linked to tombs and ceremonial offerings.

The successful application of magnetometry is also emphasized by [30], who investigated the Qocho City site in Turpan (China) to detect buried earthen archeological remains. Thanks to the magnetic properties caused by the presence of iron oxides in the mudbrick used for the buildings in the ancient city, the method was able to detect slight magnetic variations (<2 nT) associable with the archeological structures.

The technological advances made in recent decades have allowed for the use of magnetometers with increasing sensitivity. Linford et al. [31] investigated the capability of the cesium magnetometer system in comparison with fluxgate gradiometers to detect weak magnetic anomalies typical of buried archeological features. Through on-field measurements realized at three different sites located in the United Kingdom, the cesium vapor measurements demonstrated a lower level of noise, especially in the presence of deeply buried features overlain by alluvial deposits. Similar results are presented by [32], who evaluated the performance of both the systems on several sites characterized by different archeological structures (ovens, fireplaces, pools, ditches, and stone walls).

As highlighted by [33], magnetic methods provide qualitative information that aids in identifying the presence of archeological structures, but that is unable to accurately reconstruct their real geometries, sizes, and depth. To extract complete 3D information from magnetic data, an inversion strategy is required, and the authors chose to invert vertical-gradient magnetic data, imposing some constraints. The approach was successfully tested at the Unterstammheim archeological site (Switzerland), where an early medieval settlement is present, to recognize the 3D geometries of pit houses, an important form of accommodation during medieval times, as well as ditches.

Argote et al. [34] performed 3D modeling of magnetic data at the archeological site of Teteles de Ocotitla (Mexico) to identify the geometry and depth of buried remains such as tombs, kilns, or walls. The 3D modeling strategy proposed by the authors based on the inversion of the magnetic moments induced by the archeological objects was demonstrated to be accurate for the reconstruction of the shape of heterogeneous underground bodies. Cella and Fedi [35] reviewed the reliability of 3D imaging techniques of potential field data aimed at providing an estimation of the magnetization distribution within the subsurface induced by archeological remains, in order to characterize them in terms of size, shape, and depth. They analyzed the contributions of 3D imaging methods for analyzing the magnetic and electromagnetic data acquired at the Torre Galli archeological site (Italy). In particular, the results were obtained using the enhanced horizontal derivative (EHD) technique and the multiscale analysis of potential fields through the DEXP (depth from extreme points) method. The first method allows for the location of areas where a strong lateral contrast of magnetization occurs, while the DEXP method provides meaningful representations of the source distribution related to archeological structures.

Furthermore, Urban et al. [27] adopted the methodology to investigate archeological sites ranging from the terminal Pleistocene to historic periods located at high latitudes. Figure 7b shows the results obtained at the site of Swift Water Place located in Alaska (USA), where magnetometric measurements integrated with GPR and electromagnetic induction data were performed to identify the locations of hearth anomalies, which were found to be corresponding to the present house depressions.

3.1.3. Electrical Resistivity Methods

The electrical resistivity technique involves injecting an electrical current into the ground using two metal probes and measuring the potential drops via the other two probes. By analyzing the electrical behavior of the soil, it is possible to identify electrical anomalies that may be associated with possible archeological structures. Although the resistivity method has longer acquisition times compared to other methods, it is effective because it provides easily interpretable results, is highly versatile in varying soil conditions, and is ideal for detecting relatively deep structures.

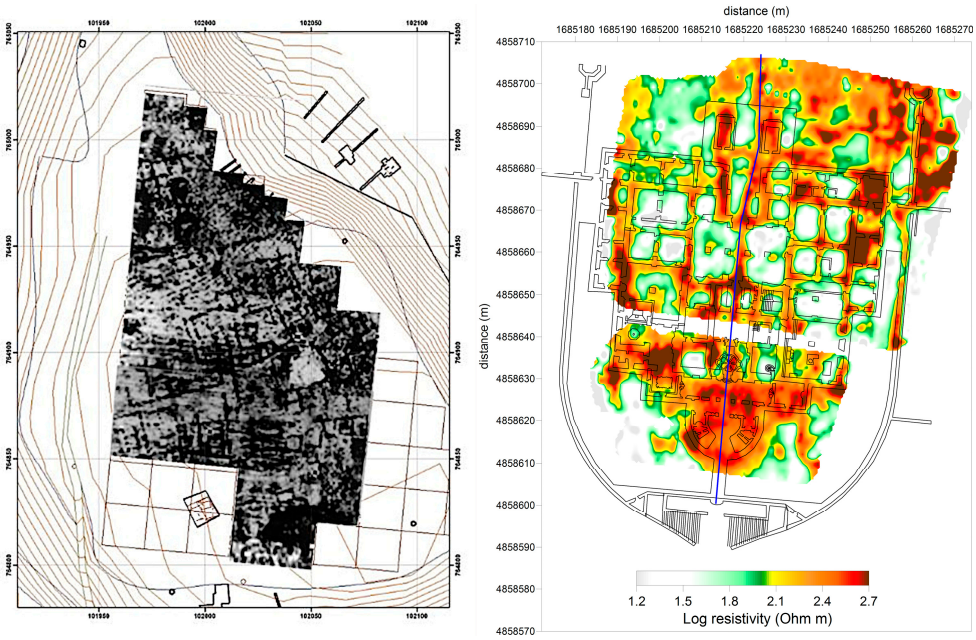
Tsokas et al. [36] demonstrated the potential of the simplest setup of the resistivity method by reconstructing the layout of the urban complex of Europos (Greece) using a twin probe array (this kind of resistivity method is also known as the electrical resistance method). The result was an impressive image of the subsoil in terms of apparent resistivity, which allowed for the identification of both archeological structures and the different phases of the settlement, characterized by two distinct building orientations (Figure 8a). The data were collected by positioning the current electrode and the corresponding potential one in a remote area (>30 times the spacing of the mobile ones) and moving the other current and potential electrode from one measuring position to another. Using a similar approach, Hargrave et al. [37] investigated the site of Fort Riley (Kansas, USA), accurately locating, with high accuracy, the building locations of Army City. Gaffney et al. [38] also performed resistivity measurements for the discovery of the theater of the ancient

city of Sparta (Greece); in this case, the results are combined with the ones obtained by the topographical survey.

Successful examples are also discussed by Cozzolino et al. [39–41], who used the resistivity methods employing a four-electrode array split into two mobile (one for energizing and one for the potentiometric probes) devices for the measurement of a single layer of resistivity values. Apparent resistivity data were processed using the 2D (3D in the case of multiple configurations of the devices' distances, leading to multiple depth maps of raw data) probability-based electrical resistivity tomography inversion (PERTI) algorithm [42]. The results, validated by excavations, identified resistive anomalies associable with the presence of internal divisions with a radial development, such as the theater at Agrigento (Italy) [39], roads and structures at Egnazia (Fasano, Brindisi, Italy) [40], and the ground floor plan of Villa Medici di Pratolino (Vaglia, Firenze, Italy) [41], as shown in Figures 8b and 9.

Electrical resistivity tomography (ERT), similar to other geophysical tomographies, is an imaging method based on the inversion of a typically two-to-four-dimensional raw dataset (in this case, apparent resistivity values) using a priori information, and the reconstruction of the estimated distribution of a real model parameter (in this case, resistivity). This technique is possible due to the collection of apparent resistivity distributions at various depths, and the assumption that each measurement is influenced by the array layout and the distribution of real resistivity around the nominal position of the raw data. The general application of ERT surveys is now quite standard, thanks to instrumental developments over the last decades, which have allowed for automatic and programmable devices as a first step, followed by their more recent evolution of the ability to acquire multiple measurements at a time.

A rich literature testifies a broad use of ERT for different applications in heterogeneous archeological sites and varying geological settings. Masini et al. [43] used ERT for detecting the archeological structures covered by alluvial deposits and the building materials at the site of Kaifeng (China). In this context characterized by clay soils and a great thickness of soil superimposed on the archeological levels, the electromagnetic methodologies do not provide useful information. Conversely, the ERT technique permits the identification of the stratigraphic succession of the site. Five layers characterized by distinct values of resistivity, and presumably associable with the different phases of the site, were detected. Furthermore, strong resistive anomalies are detected at a depth greater than 2.5 m, in correspondence with a small structure characterized by rammed earth walls surrounded by a fence. Vott et al. [44], with a multi-proxy approach, have tried to reconstruct the history and evolution of Ostia's river harbor (Italy). Electrical resistivity tomography surveys, carried out by adopting a Wenner–Schlumberger electrode array and electrode spacings of 0.75 m and 1 m, have contributed to identifying subsurface structures and the local stratigraphy. Furthermore, the data have provided the information needed for planning the vibracoring sites. The joint results have allowed for the identification of the originally vaulted chambers and the *opus reticulatum* walls between them. The interpretation of ERT patterns in terms of potential archeological features is often performed thanks to possible data redundancy, which can come from the synergistic use of multi-method surveys and the acquisition of parallel and crossing ERT lines, in which it is easier to detect and follow spatially coherent signals (Figure 10) [45].



(**a**) (**b**)

Figure 8. Archeological site of Europos (Greece). Resistance map revealing ruins of foundations at the Acropolis of the ancient city [36], © Elsevier B.V., permission obtained (**a**). Villa Medici di Pratolino (Vaglie, Italy). The ground floor plan overlaid by the probability-based electrical resistivity tomography [40], © John Wiley & Sons, permission obtained (**b**).

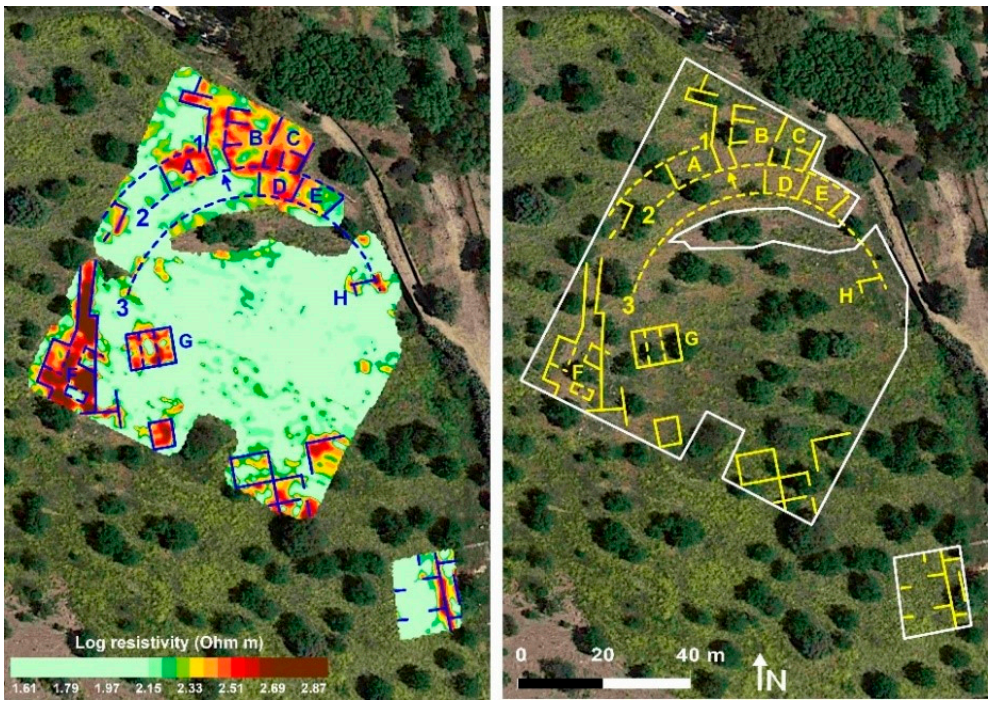


Figure 9. Akragas (Agrigento, Italy). Modeled electrical resistivity map (**left**) and the possible reconstruction of the ancient theater (**right**) [39].

The use of the resistivity methodology is particularly suitable when a strong electrical resistivity contrast occurs between the buried object and the surrounding environment, as in the case of tombs or tumuli placed in the soil. Leucci et al. [46] performed a 3D ERT to investigate the archeological area of Occhiolà (Sicily region, Italy) via the acquisition of ten profiles with electrodes placed every meter, according to the dipole–dipole array. The measurements, realized within the imposing ruins of the Santo Spirito Church, impressively

detected the presence of an elongated resistive anomaly imputable to the presence of a crypt. Orlando [47] presented the results obtained from the integration of GPR and ERT for the detection and characterization of a chamber tomb placed at a Sabine necropolis near Rome (Italy). The problem faced consists of the reduction in the ambiguity present in ERT data inversion using direct observation and GPR data interpretation as constraints of the data inversion. The author noted that there is an ambiguous solution when a void (a resistive anomaly) is placed in a media consisting of two layers (the deeper layer more resistive than the outcropping one). The use of a priori information obtained from GPR data and the dipole–dipole array effectively reduces uncertainties and allows for a better identification of the depth of the buried structure. An exemplary case of the imaging sensitivity filled cavities is given by Compare et al. [48] in a dense (1 m 2D spacing) dipole–dipole survey over a lawn, in correspondence with regular crop marks, where the digs following geophysical characterization confirmed the presence of an ancient *giacciara* (icebox) just where the extremely high resistive values were clustered (Figure 11).

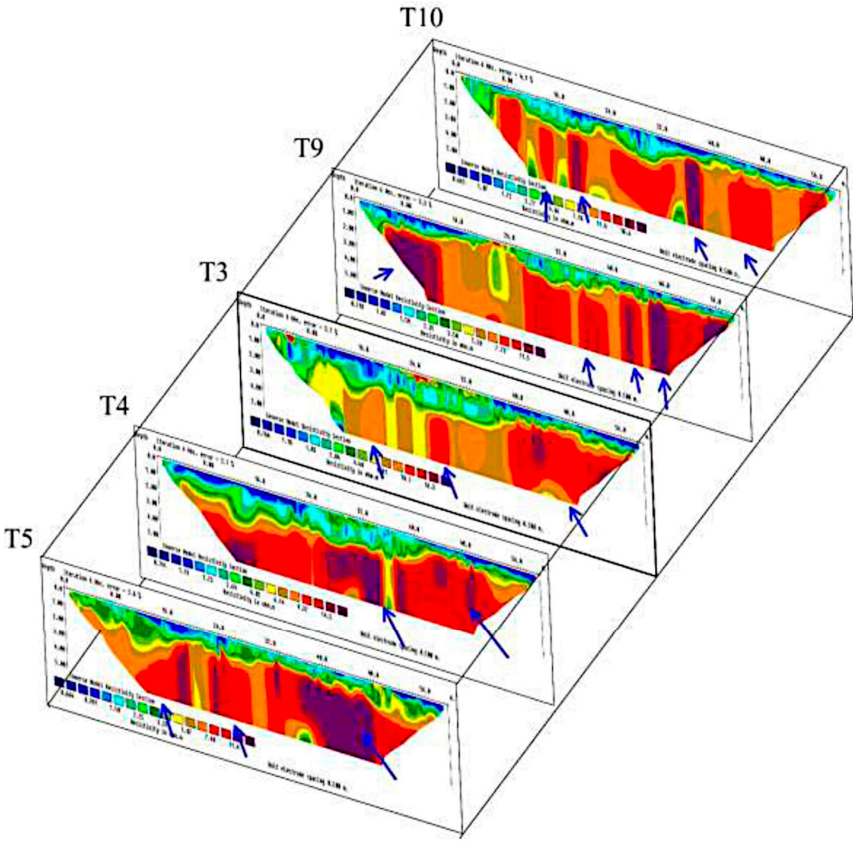


Figure 10. Babylon city (Iraq). Inverse models for selected lines from electrical resistivity tomography to detect archeological walls of Babylonian houses near Ishtar temple. Arrows show subsurface features, which are the brick walls [45], © John Wiley & Sons, permission obtained.

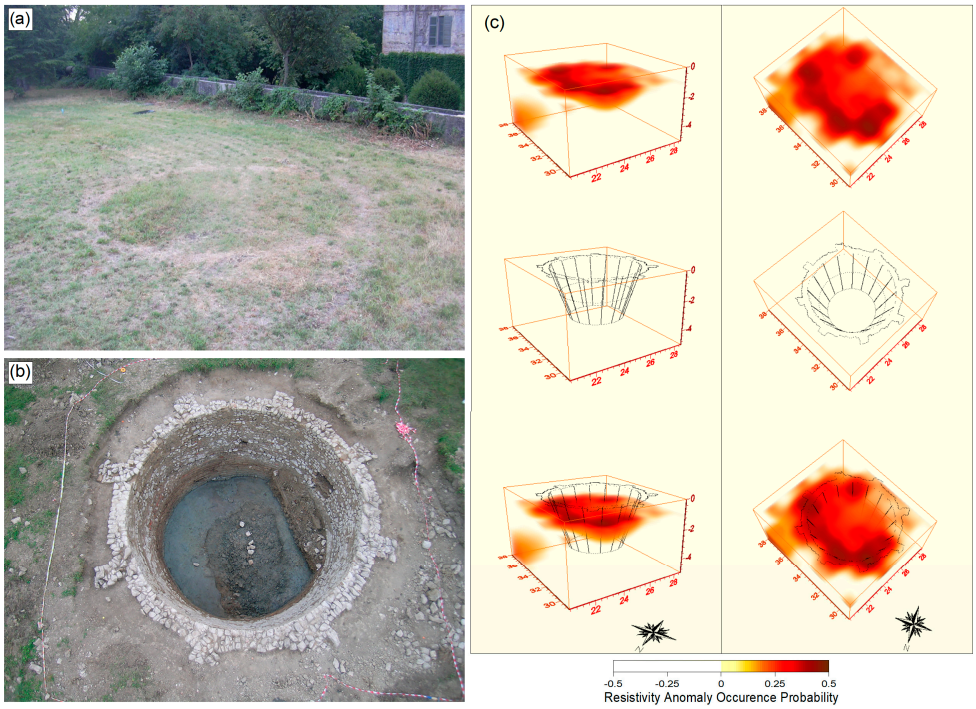


Figure 11. Castle of Zena (Carpeneto Piacentino, Italy). Cropmarks in correspondence with the *giacciara* (**a**), the *giacciara* or icebox found in correspondence with the rounded sequence of nuclei in the probability tomography (**b**), and a sketch of the *giacciara* compared with the particularity of the round sequence of nuclei extracted from the 3D image from a lateral and a top view (**c**) [48], CC BY 2.0.

Different arrays of data acquisition can be used, depending on the research target. In [49], a 3D resistivity inversion algorithm [50] was used to invert synthetic data to reconstruct the subsurface resistivity distribution of two tombs represented by two resistive bodies covered by the tumulus. The dipole–dipole (DD), pole–dipole forward and reverse mode (PD: For and Rev), gradient (GRAD), midpoint-potential-referred (MPR), Schlumberger reciprocal (SCR), and pole–pole (PP) arrays were used for the simulations. The final images exhibit a considerable amount of valuable information, reflecting the advantages and disadvantages of each array. Generally, all tested arrays successfully identified the two different resistivity layers below the tumulus and the increase in resistivity values between the background area and the tumulus material.

However, the DD array is the preferred choice for detecting buried structures. A primary advantage of the DD array is its ease of deployment in the field due to the short wire lengths needed to connect the active and passive dipoles to the measuring ammeter and voltmeter, respectively. Furthermore, it allows for fast data acquisition as it supports multiple receiver channel measurements simultaneously. The DD layout is also more sensitive to lateral resistivity contrasts than other conventional arrays. For this reason, it can be particularly effective in archeological contexts where the goal is often to highlight anthropogenic structures (walls, cisterns, tombs, and trenches, etc.) that cause strong lateral resistivity contrasts at the boundary with the hosting subsoil. Nonetheless, it should be noted that the dipole–dipole array is less sensitive in mapping horizontal structures. Additionally, the main disadvantage of this array is the decrease in signal strength as the distance between the potential dipole pair increases. However, in ERT prospecting for archeology, both the typical small size and closed shape of the target bodies and the modest depths involved largely minimize these drawbacks [51]. To reduce the resolution limits characterizing ERTs, in most of the archeological fields, the distance between the electrodes

does not exceed a meter. The data are acquired by positioning the electrodes along 2D lines or according to unconventional schemes based on 3D acquisitions. As the collection of full 3D resistivity data is extremely time-consuming, the most common geophysical practice is collecting dense, parallel 2D lines [52]. These 2D measurements can be interpreted with 2D algorithms to perform the interpretation of the inverted sections into quasi-3D images or full 3D inversion schemes.

Elwaseif et al. [53] evaluated the performance of the watershed algorithm to enhance the capability of ERT in accurately reconstructing the geometry and distribution of archeological remains. The authors highlight the limitations associated with the regularization of the solution based on the smoothness constraint method, noting that while this approach accurately predicts the center of the targets, it is unable to reliably determine quantitative information about discrete targets, such as their dimensions or depth of burial. The use of the image processing technique based on edge detection effectively supports the reconstruction of buried targets characterized by sharp resistivity contrasts, such as cavities or tombs. Arato et al. [54] utilized GPR reflection and 3D inverted magnetic data as a priori information to guide the 3D inversion of ERT data acquired at the Sabine Necropolis at Colle del Forno (Rome, Italy). Indeed, magnetic data allowed for the detection of the main anomalies present in the subsoil, while GPR data highlighted the tomb roof and the presence of lateral niches. Twenty parallel resistivity profiles were acquired in two main directions using the dipole–dipole array, with an electrode spacing of 0.5 m to carry out the ERTs. The results of the 3D ERT inversion successfully characterized an unexplored chamber tomb preceded by a corridor (dromos), as is typical in the investigated area. Papadopoulos et al. [51] investigated the capabilities of ERT with electrodes placed according to 3D schemes in investigating tumuli through the modeling and inversion of synthetic apparent resistivity data, considering the topography of the structure. The best results were achieved using the pole–dipole array and multiple-gradient array. The numerical tests were positively validated with a 3D ERT performed at the archeological site of Vergina (Greece), where thirty-eight parallel 2D lines were acquired with the pole–dipole array to investigate the tumulus' subsurface properties. Tsourlos et al. [49] evaluated the potential of 3D ERT arrays for investigating tumuli. To select the best array, three different strategies were analyzed, and a pole–dipole array was adopted for all the simulations. A tumulus with a maximum diameter of 14 m and height of 5 m was considered, and a capsized cup model was used for topographic correction. The tumulus was placed in the center of an 18×18 m area to simulate its terrain elevation, and the simulated data were then validated with an in-field survey at the site of Elias–Spilaion (Greece), characterized by the presence of a tumulus with an elevation exceeding 13 m and an average diameter of 56 m. The combined use of radial and regular ERTs produced the best (i.e., netter) results, especially for characterizing the deeper levels (Figure 12).

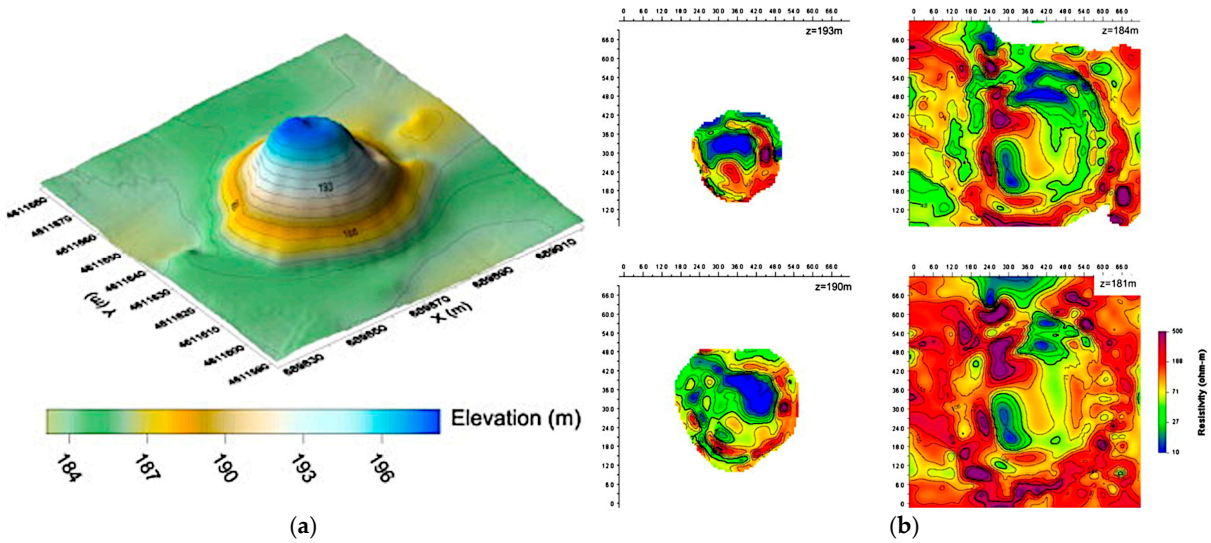


Figure 12. Elias–Spilaion (Greece). Elevation model of the prospected tumulus (**a**), and ERT inversion results of the tumulus area presented in the form of *XY* geoelectrical slices at different elevations (**b**) [49], © 2013 Elsevier B.V., permission obtained.

Different applications deal with the study of historical/archeological sites. Akca et al. [55] conducted 102 DD ERTs with the purpose of answering several questions about the design of a large area near the episcopal site of Side, which dates back to the late antique/early Byzantine times. The 3D geophysical models revealed clear traces of structures characterized by relatively high resistivity, interpreted as buildings originating from the Roman Imperial Period (Figure 13). Al Saadi et al. [56] realized quasi-three-dimensional (3D) ERT measurements in an area of a presumed Roman construction, using a dense electrode network of parallel and orthogonal profiles in a dipole–dipole configuration. The 3D ERT inversion results clearly characterized the main structures of the Roman foundations, imaging most parts of the walls (R1 in Figure 14), pits, and also smaller internal structures of the Roman building (R2, R3). Moreover, excavation ditches that had been refilled prior to the ERT survey are delineated as resistivity heterogeneities (C1, C2) as well.

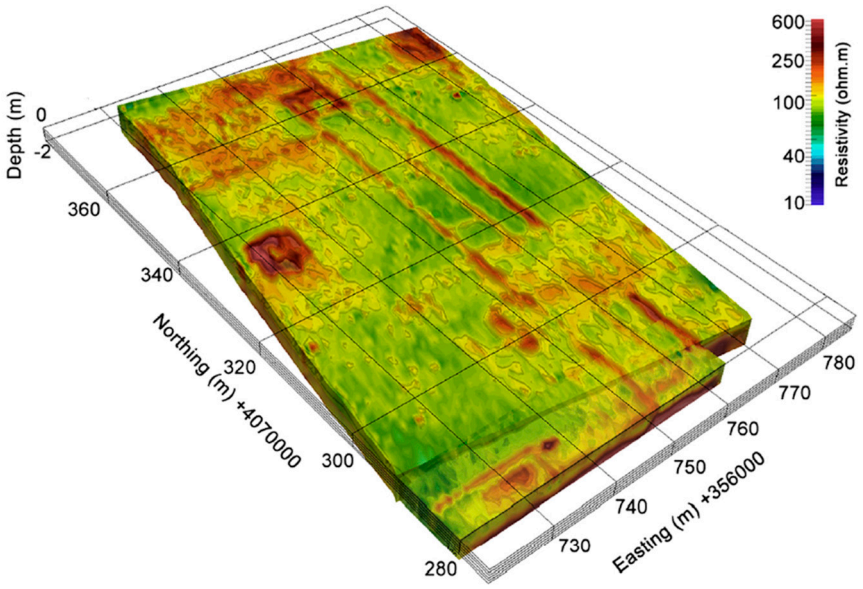


Figure 13. Side (Antalya, Southern Turkey). The three-dimensional resistivity model of the survey area at the episcopal district [55], © 2013 Elsevier B.V., permission obtained.

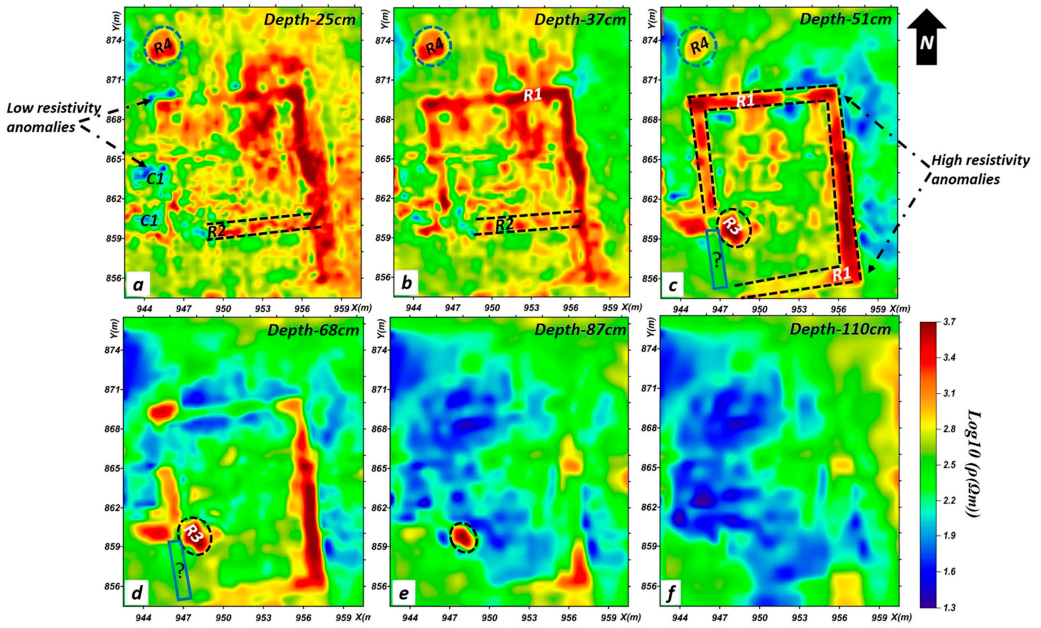


Figure 14. Roman villa near Nonnweiler (Germany). Depth slices from 25 to 110 cm (**a**–**f**) [56], © John Wiley & Sons, permission obtained.

Ullrich et al. [57] performed ERTs at two sites: Tell Jenderes (Syria) and Ain al-Hajar (Morocco). At the first site, the results identified three distinct electro-layers. The more resistive values correspond to the building structures of the Hellenistic-Roman settlement, the intermediate resistive values are associated with a massive mud–brick wall, while the low resistivity values are attributed to the presence of a mud–brick wall surrounding the upper town settlement from the Bronze Age. The second site, a site of ancient metal production, was investigated using a 3D complex resistivity model derived from Induced Polarization (IP) measurements, which clearly defined the contrast between the slag deposit and the bedrock.

Fischanger et al. [58] effectively utilized the development of 3D ERT data inversion to investigate the Tutankhamun tomb (Luxor, Egypt) and detect resistivity anomalies associated with the burial chambers. An extensive survey was carried out adopting ERT lines placed with linear or quasi-linear electrode spreads. The authors exploited the methodology's flexibility, making it particularly suitable for preliminary archeological investigations in topographically complex areas. Given the difficulties, the authors paid great attention to the data quality and presented an estimate of the reliability of the ERT in terms of sensitivity; indeed, higher sensitivity corresponded to greater confidence in the final resistivity model. Pazzi et al. [59] investigated the effects of electrodes' misplacements and topographical errors by performing a geoelectrical survey at the Etruscan site of Poggio (Italy). The results were analyzed using statistical analysis by employing a Monte Carlo simulation to evaluate the influence of the GPS error on the geometric factor and, consequently, on the indirect measurement of the apparent resistivity. The authors highlighted how GPS errors can influence the apparent resistivity values, particularly in the shallowest layers, which often represent the most important levels for archeological applications.

The versatility of ERT was advantageously exploited by Tsokas et al. [60] to enhance the aqueduct system of the Eupalinian Tunnel through the deployment of surface-to-tunnel electrical resistivity tomography. To improve resolution with depth, the authors placed the electrodes both within the tunnel and on its surface. Measurements, performed using the pole–dipole array with a mutual electrode distance of 5 m, demonstrated their usefulness in detecting the presence of the tunnel at a depth ranging between 30 m and 45 m. The

use of 3D ERT is promising and indicative of its high impact for archeological purposes. Its applicability in urban areas is discussed by Bellanova et al. [61], who used a minimally invasive approach to analyze the 3D electrical behavior of the subsoil in the city of Matera (Italy). The results allowed for the detection of a subsurface cistern within the first 3 m of subsoil, supporting the GPR data and reconstructing the stratigraphic succession. Additionally, Rizzo et al. [62] employed 3D ERTs to detect the presence of unknown cellars placed in the subsoil of the historic center of San Benedetto del Tronto (Italy). Cozzolino et al. [63] carried out several ERTs in the urban area of Nicosia (Cyprus) to identify potential archeological risk at Eleftheria Square and Solomon Square, discovering buried archeological constructions from previous historic phases of the city, which supported the shallower results obtained via the other geophysical methodologies (GPR and electromagnetic induction). The contribution of non-conventional systems for ERT acquisition was examined by Capozzoli et al. [64] in an unsaturated and subwater analogue archeological site in a full-scale laboratory test. Using loop–loop shaped ERT, archeological remains were detected, demonstrating the applicability of the method in urban scenarios where the regular disposition of the electrodes is hindered by the constant presence of obstacles.

In a recent paper, Klanica et al. [65] introduced a method for the determination of the volumetric information on architectonic buried ruins based on ERT data. Their analysis is based on the architectural energetics concept, a methodology that translates architectural objects into a quantitative time–labor equivalent, from which information about past societies, labor organizations, or political relations can be inferred. Preliminarily to this, the volume of the architectural structures must be determined, typically by in situ measurements and the computing of volume by mathematical formulae or using UAV-based photogrammetry. Within their work, they were able to apply the same characterization to buried or semi-buried monuments without direct excavation (Figure 15).

Thanks to the recent development of geomatic reconstruction and 3D ERT inversion, innovative applications have been possible for the study of very complex Cultural Heritage sites, such as unexcavated ancient settlements inside caves [66]. In Figure 16, the effectiveness of these joint approaches in the lithological and subsequently archeological sedimentological characterization of the investigated target can be appreciated [67].

3.1.4. Electromagnetic Induction Method (EMI)

The case history of the electromagnetic induction (EMI) methodology is somewhat more limited than the GPR, MAG, and ERT methods for archeological purposes. However, the potential of this method, particularly in contexts where other well-known methodologies face challenges, such as noisy environments or conductive soils, can be particularly interesting. EMI is founded in Faraday's law and the working principle involves the introduction of an alternating magnetic field into the soil using a transmitter coil (primary magnetic field). This magnetic field can induce an electrical field in the ground, which in turn generates a secondary magnetic field recorded by the same transmitter or by a second receiver coil. The intensity of the secondary magnetic field is directly related to the apparent electrical conductivity of the soil. Variations in the magnitude and phase of the field from the primary magnetic field are influenced by soil properties, the spacing orientation of transmitter and receiver coils, and the working frequency (generally variable from some decades of Hz to some decades of kHz). This prevalent (especially in archeological prospection) family of electromagnetic geophysical methods is also known as the Frequency Domain Electromagnetic (FDEM) technique, to distinguish it from the Time Domain Electromagnetic (TDEM) or Transient Electromagnetic (TEM) techniques, which are based on the application of a square-wave EM energization and the recording of

the subsequent response. The latter is quite niche in Cultural Heritage studies, but a few examples will be discussed at the end of this section.

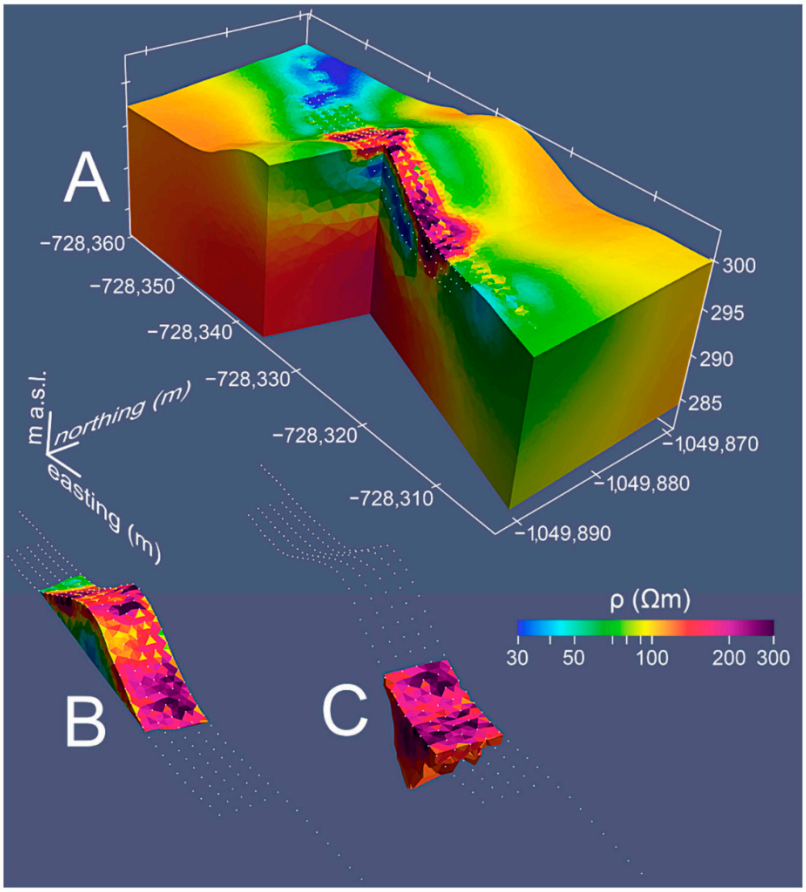


Figure 15. Hillfort Královice (Czech Republic). 3D inversion results. (**A**) Entire 3D model showing the distribution of resistivity. (**B**) Isolated resistivity structure of rampart without any thresholds. (**C**) Resistivity structure of the ditch with a threshold of 126 Ωm was applied. The white dots represent the individual positions of the electrodes. The zero position of the profiles is to the west [65].

Thanks to the great sensitivity of the EMI methods to variations in soil humidity content, they can effectively support archeological research by providing fundamental information for reconstructing paleo-environments and identifying shallow hydrogeological structures, which are often of archeological interest.

Measurements can be taken by carrying the instrument in a normal position (horizontally oriented planes of the loops, vertical dipole mode) and horizontal position (vertically oriented planes of the loops, horizontal dipole mode). The relative influence of the material at different depths to the secondary magnetic field is different for each mode: in vertical mode, the material near the surface has very little influence, whereas in the horizontal mode, it is at maximum. In the vertical mode, the contribution of material at a depth of around 1.5 m (order of value for the most common configurations for shallow and detailed prospections) is maximal, whereas for the horizontal mode, the response falls off monotonically with increasing depth. By turning the instrument face-up (normal position) and on its side, it is possible to determine whether the earth is layered or not.

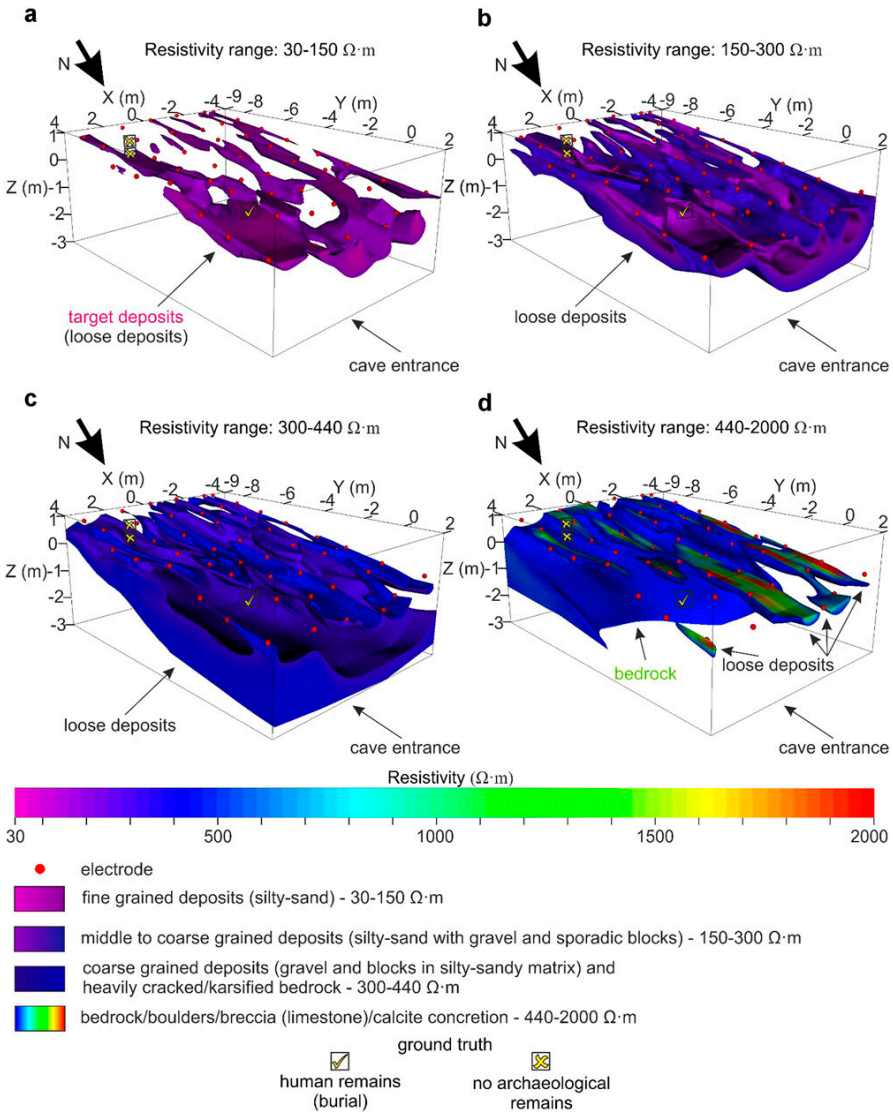


Figure 16. Arma Veirana cave (northern Italy). A perspective view from above showing different resistivity range extractions from the 3D inverse resistivity model ((**a**) 30–150 Ωm; (**b**) 150–300 Ωm; (**c**) 300–440 Ωm; (**d**) 440–200 Ωm), along with the lithological interpretation of the resistivity ranges [67], © John Wiley & Sons, permission obtained.

Despite the low resolution, Gugler and Gex [68] applied the method for investigating a Celtic tumulus in the Canton of Fribourg (Switzerland), identifying a circular zone of high conductivity presumably induced by a refilled ditch surrounding the tomb. The authors highlighted the strong influence of the topography on the results and showed an empirical method for correcting the topography-related conductivity. Furthermore, despite the good results obtainable via the analyses of two-dimensional maps, able to show the spatial distribution of conductivity anomalies, the authors emphasize the importance of the profiles that can host archeological clues. In this case, the necessity of removing the shifts occurring during the survey induced by electronic instabilities, as well as temperature and soil moisture variations, is evident.

The great sensibility of the method for reconstructing past environments has been exploited by various authors to identify the geomorphological processes and anthropogenic soil changes that have influenced settlement dynamics. Conyers et al. [69] carried out electromagnetic conductivity measurements to identify possible archeological sites in meandering river floodplains in different sites located in the USA. The results show the possible contribution of the methodology in supporting archeologists in areas where

agricultural leveling and ploughing activities and the presence of thick layers of flood sediments strongly reduce the capabilities of other geophysical methodologies. Simpson et al. [70] used EMI for investigating 8 ha of soil with an EM38DD sensor equipped with a differential GPS with a 2 × 2 m resolution at a medieval manor, which was a lost dependency of the Benedictine St. Peters Abbey of Gent (Belgium) in the Dutch polders. The site was buried by flooded sediments. They analyzed the complementary contributions of both the apparent electrical conductivity (ECa) and magnetic susceptibility (MS) in providing complementary information valuable for archeological prospection, concluding that the nest results were obtained by measuring the ECa measured in vertical dipole orientation and the MS in horizontal dipole orientation. The ECa map, able to delineate the natural and artificial soil anomalies, showed the location of the moated site, including the ditch system, whilst MS was only sensible to the archeological traces of the moated site.

Furthermore, as observed in [71], EMI, measuring apparent magnetic susceptibility, is able to detect some anomalies due to magnetic susceptible materials such as magnetometric gradiometers. The authors presented results from the simultaneous use of electromagnetic induction and fluxgate gradiometer measurements to detect buried remains of a 17th-century castle in Vinkem, Belgium. These findings confirmed the method's capability for detecting archeological structures, although the resolution was lower than that of magnetic measurements alone. De Smedt et al. [72] acquired a 90 ha surface with a motorized multi-receiver EMI device; the ECa maps showed a large variety of signs and patterns, both of natural and anthropogenic origin. The fine resolution and continuous peculiarity of the experimental dataset allowed them to trace the lateral extent of many continuous features, such as a paleo-river system and the network of linear man-made ditch systems. By modeling the EC of three non-overlapping soil layers, i.e., 0–0.5 m (Slice 1), 0.5–1.0 m (Slice 2), and >1.0 m (Slice 3) beneath the soil surface (Figure 17), the authors better recognized and characterized some features, in particular their vertical extent.

Di Maio et al. [73] carried out an integrated geophysical survey at the site of Phaistos (Greece) and EMI measurements have allowed for the identification of a marked contrast between the physical properties of soils induced by the presence or not of anthropic artifacts. Indeed, low conductivity values were detected where archeological structures are present. These results also improved thanks to the high magnetic contrasts recorded in the same area. On the contrary, relatively high conductivity values were measured in a marshy environment, where no structures are expected. Tang et al. [74] showed the potentialities of the method in the identification of small archeological structures in sandy loess and sandy loam soil by deploying a multi-frequency EMI instrument at the two Chinese archeological sites of Han Hangu Pass and Xishan Yang. Results permitted the identification of EM anomalies at considerable depths greater than 3 m, associable with the archeological structures (kilns and roads), as confirmed by the excavation activities.

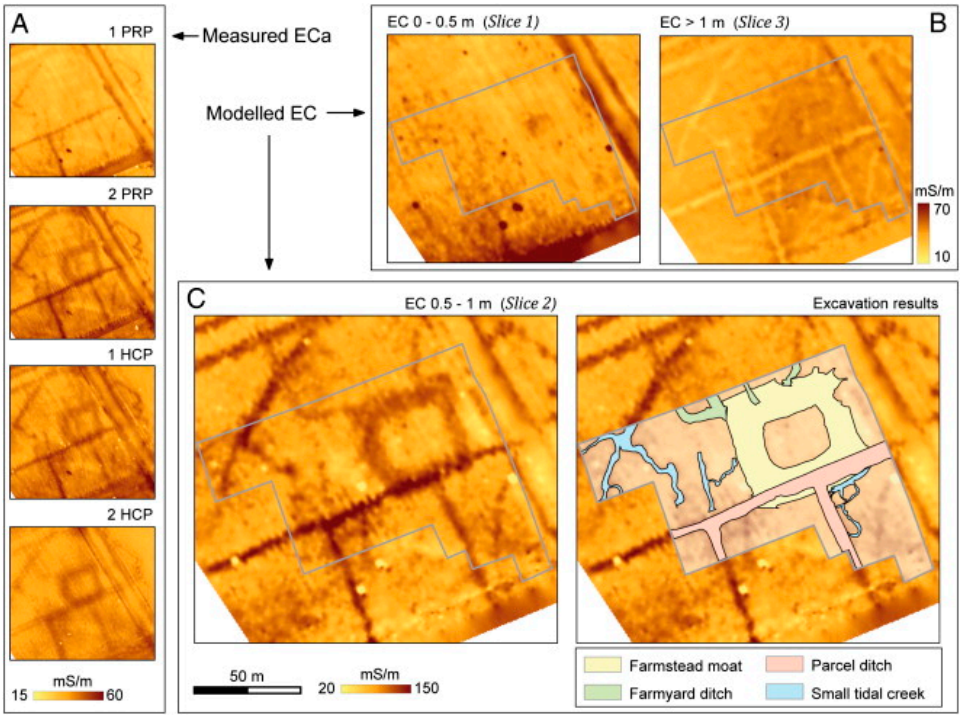


Figure 17. Koksijde (Belgium). Dualem ECa measurements from site 1 (**A**), with modeled EC for topsoil (Slice 1) and substrate (Slice 3) soil volumes (**B**), and the modeled EC of the soil volume between 0.5 and 1 m (Slice 2) below the sensor, with and without excavation results (**C**) [72] (ECa: apparent electrical conductivity, EC: electrical conductivity, PRP: perpendicular geometry, and HCP: horizontal co-planar geometry). © 2013 Elsevier B.V., permission obtained.

Deiana et al. [75] used EMI in tandem with ERT and aerial/satellite images for characterizing the Late Bronze Age Terramara settlement of Fondo Paviani (Italy), providing useful information about the stratigraphic/sedimentation relationships of the older river systems. The FDEM data showed a resistivity pattern compatible with the presence of the paleo-system visible from the satellite image and the integration with ERT, providing the necessary information for reconstructing the lateral extension and total depth of the buried geomorphological paleo-structures hosting the ancient settlement, surrounded by ditches and palisades. Multi-frequency and multi-coil electromagnetic measurements were used in [76] for detecting buried archeological features at the Nuraghe S'Urachi site (Italy) placed inside the monument and its immediate surroundings. The authors exploited the capability of FDEM measurements to map the subsoil conductivity at several depths over a large area, improving the results of some ERTs performed to delineate the lateral and vertical distribution of the electrical anomalies. The application of EMI was also necessary due to the scarcity of contributions obtained from the previous surveys realized with GPR and MAG, which were strongly influenced by the presence of volcanic stone material and metallic waste, as well as collapsed material and garbage. Despite FDEM measurements being ineffective for the analysis of the deeper buried structure of the Nuraghe, interesting results were obtained when investigating the remains of the habitation area at the base of the structure, as shown in Figure 18.

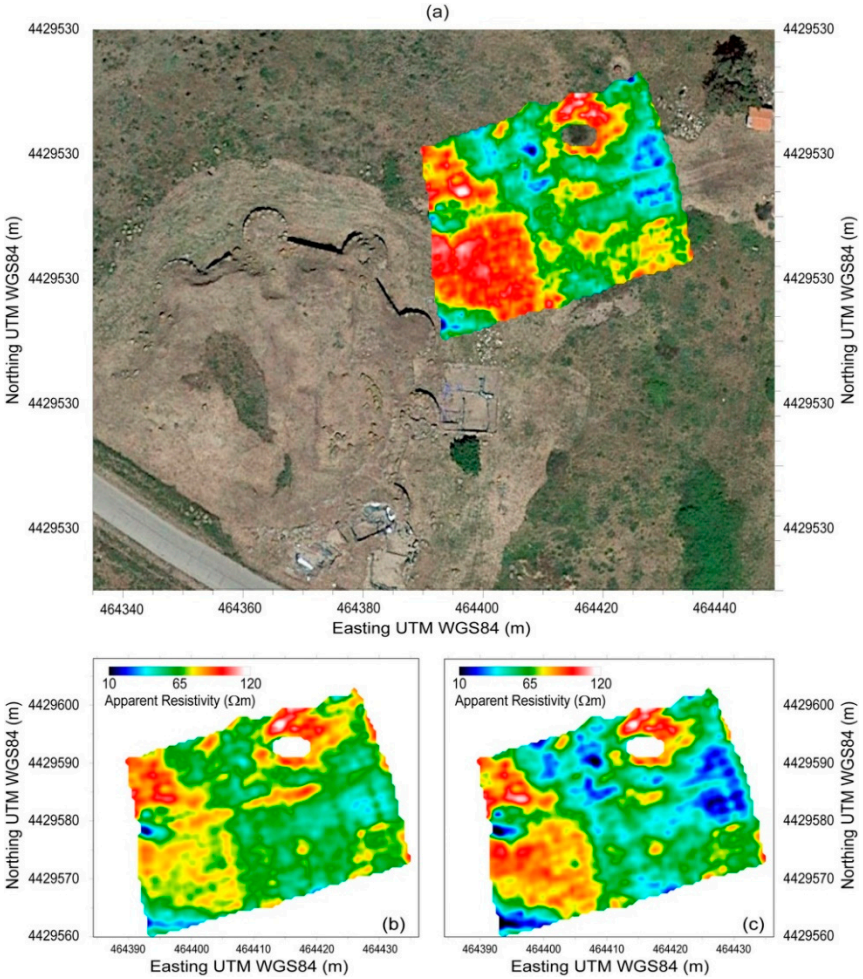


Figure 18. Nuraghe S'Urachi, San Vero Milis (Italy). Apparent resistivity of the quadrature component of the EM signal at the foot of the Nuraghe (**a**) frequency 16,725 Hz, (**b**) frequency 28,725 Hz, and (**c**) frequency 47,025 Hz collected in 2019 with GEM 2 in HCP configuration. The data show the presence of an alternation of relatively more conductive and resistive soils imputable to the presence of the ditch [76] CC BY 4.0.

Time Domain Electromagnetic (TDEM) prospection is rare in archeological prospection, but a few cases exist. A first, predominantly theoretical application was given by Tabbagh and Dabas [77], who proposed the use of a new magnetic parameter—the magnetic viscosity—to allow for the distinction between anthropogenic and natural effects (anthropogenic activity results in an increase in magnetic susceptibility) in the topsoil of the ground. Given that this parameter can be measured by either time-domain instruments (TDEM) or quadrature susceptibility in the frequency domain, they analyzed the scientific literature, concluding that also in the time domain, a decay law is observed for the viscosity response, which depends only on pulse duration for most of the soils. Furthermore, they studied the processing and calibration steps to retrieve the magnetic viscosity in situ with a TDEM apparatus.

Ranieri et al. [78,79] illustrated some archeological applications of TDEM measurements, with a particular emphasis on the study of disturbances at the early-stage samples (4 μs) of the decay curve, recorded by the instrument in response to shallow voids and archeological structures (both with significantly greater electrical resistivity in comparison to the surrounding soils).

Trogu et al. [80] studied a joint protocol for the detection of deep buried voids by applying ERT, TDEM, and Very Low Frequency (VLF) methods. The VLF method is

another geophysical technique based on the EM response of the investigated targets to the EM waves generated at large distances by military stations all around the world at selected wavelengths. By applying these three methods to the industrial site of Elmas (Sardinia, Italy) with the partially known presence of the Karales Roman Aqueduct gallery (80 × 120 cm section) at around 10 m depth in a high conductive environment (clays), they studied the best parameters to collect and process the data. In Figure 19, some of their results are presented. Further investigations with the very rare use of the VLF method in CH studies are provided by [81,82] for two archeological sites in Turkey.

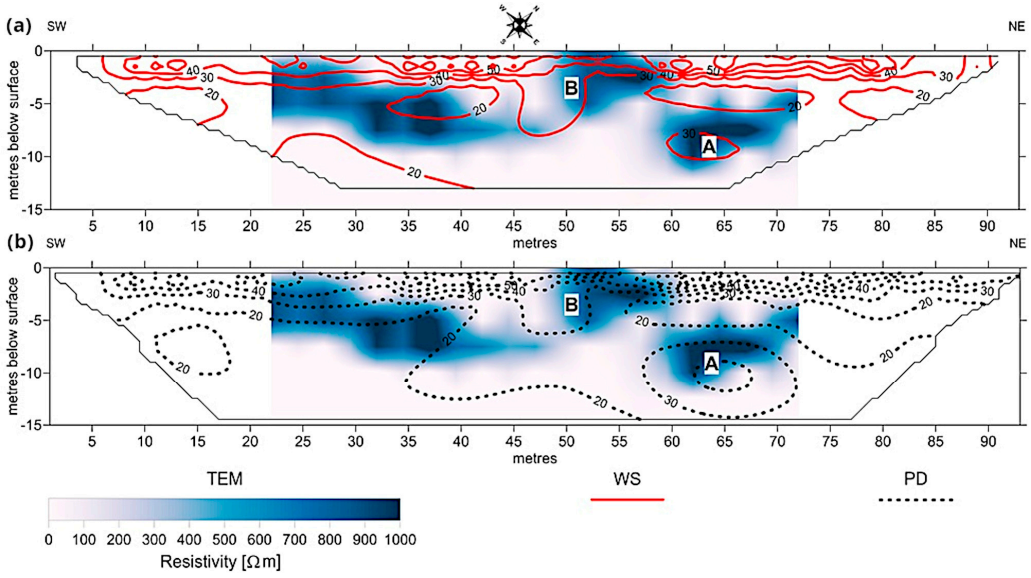


Figure 19. Karales aqueduct (Italy). Comparison between TEM 1 sounding and ERT 9 Wenner– Schlumberger profile (**a**). Comparison between TEM 1 sounding and ERT 10 pole–dipole profile (**b**). Resistivity contours in Ω m. (A) Aqueduct, (B) anomaly probably related to the construction of the aqueduct or to the lateral effect of the nearby open pit [80], © John Wiley & Sons, permission obtained.

3.1.5. Other Methods

In this sub-section, we present some very rare applications that surveyors run less frequently compared to the previous cases, especially when encountering different kinds of difficulties related to specific physical and logistic site conditions.

In essence, the family of seismic imaging methods is used to probe the elastic properties of the subsurface, primarily allowing their reconstruction in terms of wave velocities. This group of techniques includes seismic refraction, seismic reflection, and passive seismic methods, among others. To our knowledge, the seismic reflection method, despite sharing many theoretical principles with GPR, has not been applied in archeology due to strict constraints on horizontal and vertical resolutions, which are required to gain useful information about the very shallow subsurface characteristics. Both horizontal and vertical resolutions depend on signal frequency and velocity, which indeed control the wavelength of the seismic signals (e.g., for a depth of 6 m and a seismic velocity of 800 m/s, vertical resolution could be on the order of a few meters, with horizontal resolution typically measuring more than double that (approximately equal to the product of vertical resolution and the square root of the depth [83])). While some pioneering papers have explored the use of very high-resolution signals in very shallow seismic reflection site investigations [84], these have primarily focused on engineering applications, where there is a high elastic impedance contrast between anomalies and the surrounding soil. Such methods have limited applicability in archeology, being primarily restricted to characterizing the local

geology beneath archeological sites [85] and searching for large-scale buried historical infrastructure, as exemplified by the King Xerxes Canal in Greece [83,86].

Another seismic method, which is much more common in geology than in archeology, is the Horizontal-to-Vertical Spectral Ratio (HVSR) method [87,88]. Belonging to the passive seismic techniques, the HVSR is based on the spectral analysis of natural ambient seismic noise consisting of wide-period, small-amplitude oscillations ($<10^{-2}$ mm) of ground materials. The frequency of these vibrations ranges between <1 Hz and ~100 Hz and originates from several different natural sources such as wind, oceanic waves, and meteorological conditions (i.e., microseisms), and those of an anthropogenic origin, such as traffic and industrial activities (i.e., microtremors [89–91]).

In the HVSR method, each discontinuity in the subsurface, characterized by a contrast in elastic impedance (the product of velocity and density), can manifest as a frequency peak in the H/V spectral curve. The amplitude of this peak is related to the magnitude of the elastic impedance contrast, while the frequency of the peak provides information about the depth of the discontinuity. Among these applications, we can mention Castellaro et al. [92], who used the method together with GPR to investigate the shallow subsurface of a Roman Amphitheater in the urban context of Catania (Italy). HVSR and GPR techniques were also used by Bottari et al. [93] to locate an ancient Greek-Roman buried harbor (Tindari, NE Sicily). Similarly, Wilken et al. [94] used HVSR to retrieve very shallow archeological information on the location of buried houses made of bricks with a marked elastic impedance contrast against the filling soil (Viking-age village, Föhr island, N. Germany).

Recently, Abu Zeid et al. [95] successfully applied the HVSR method both in single station and 2D array modalities to detect and map the existence of paleo-surfaces of the Bronze Age in the archeological site of Pilastri Terramare (Italy). As confirmed by the archeological digs, paleo-surfaces are represented by thin layers of hardened clay (Figure 20) that were not detected with GPR and ERT surveys; their spatial continuity was imaged thanks to the use of an array of 4.5 Hz tri-axial geophones (noise antennas). In Figure 20a, an example of a 2D vertical section is reported that shows HVSR amplitude distribution as a function of frequency across the sensors' horizontal distance. It is possible to distinguish the following two frequency horizons (i.e., peaks): the 20 Hz continuous one and the 75–85 Hz feature that clearly appears beneath the left side of the section. Previous and purposedly conducted excavations (red rectangles) have proven the validity of the method used. As noted previously, peak frequencies in the HVSR spectral curve can be converted into approximate depths of elastic discontinuities, assuming the knowledge of the shear wave velocity of the surface materials and a power law model to describe how velocity increases with depth. The power law model is characterized by an exponent, which can be determined locally for specific sites. In Figure 20b,c, we report a HVSR section along a profile intersecting the southern boundary of the Terramara habitat. The sections show, respectively, the distribution of the H/V amplitude values as a function of frequency and depth. This latter representation (i.e., with depth) was considered more easily interpretable by archeologists. Two significant features, labeled A and B in Figure 20b,c, were identified. Event A was attributed to the natural level of the site, which corresponds to the habitat border. Event B was interpreted as a seismic discontinuity located at an approximately 1 m depth, representing the compacted paleo-surface (potentially the more recent living level of this ancient site). Between these two events, H/V amplitudes were less than 1, indicating the presence of sediments with a low shear wave velocity (Vs). Conversely, H/V ratios greater than 2 suggested amplifications due to an elastic discontinuity characterized by a significant contrast in elastic impedance. Such discontinuities might correspond to archeological features like footfall levels or geological structures.

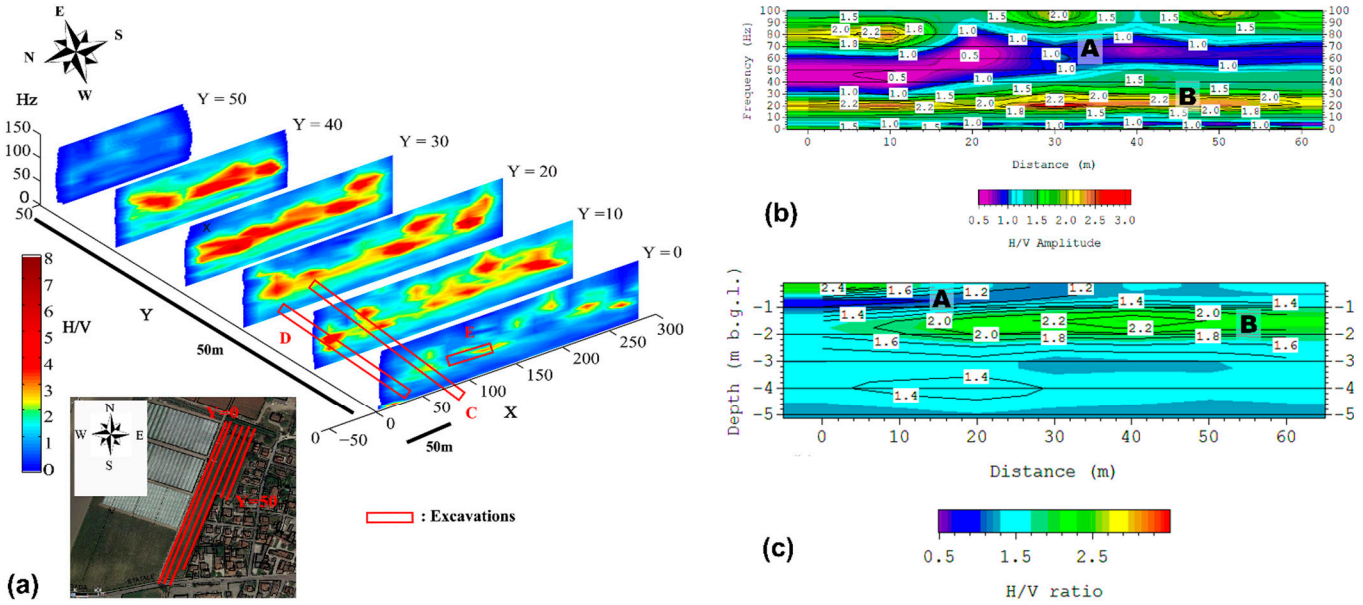


Figure 20. (**a**) Pseudo-2D H/V amplitude ratio sections along the eastern border of the Pilastri Terramara Bronze Age site, NE Italy. The sections, shown in orthographic projection, and the interpolated H/V amplitudes as a function of space and frequency (see insert for the location). The Y-axis is oriented from west to east. Sections are spaced 10 m. The red rectangles highlight the elastic impedance contrast anomalies related to discontinuities produced by previous excavations and their successive filling (C, D, and E). Trench C, re-opened in 2015, confirmed the presence of archeological findings [95], © John Wiley & Sons, permission obtained. (**b**,**c**) HVSR section along a profile intersecting the southern border of the Pilastri Terramara site, N. Italy. The H/V ratio is represented as a function of frequency (**b**) and approximate depth (**c**). A and B indicate, respectively, the most recent paleo-archeological surface (depth of nearly 1 m) and a lithostratigraphic contact (depth of about 1.5 m).

Seismic refraction is a physical phenomenon that is quite often exploited in a very specific archeological context, the tumuli studies. There, thanks to the possibility of deploying sensors all around the investigation targets, it is possible to reconstruct the seismic properties of the discretized medium with tomographic inversions of travel times or amplitude attenuations acquired in transmission/transillumination setups to search for chambers or other 3D bodies inside the tumulus. Tsoksas et al. [96] used the seismic refraction technique to detect monumental tombs buried in three tumuli in Greece, analyzing and modeling the experimental travel times with radial and circular deployments of geophones and shots; differently from most recent applications, archeological evaluations and physical simulations were performed on raw data without tomographic inversion, not directly searching for the rooms but, instead, looking for delays in travel time caused by the variations in compaction of the natural soils during the realization of the chambers. Another application of the refraction technique was also conducted, to an archeological problem physically similar to tumuli, to image the Nuragic infrastructure of the "Cuccuru Nuraxi" well in a small hill in the village of Settimo San Pietro (Italy) [97]; the circular layouts of the geophones all around the well location, and the 3D paths of the seismic waves, allowed the author to reconstruct the velocity in three horizontal sections of the hill. Forte and Pipan (1998) produced a detailed 3D reconstruction and interpretation of artificial features and small, localized discontinuities within a Bronze Age burial mound in northern Italy [98]. Their work also included a comparison with subsequent archeological excavations and documentation. This was carried out by analyzing radial GPR profiles synergically with refraction tomography acquired with a (double) circular layout of seismic sources and receivers, together with an accurate 3D reconstruction of the tumulus shape. Polymenakos

and Tweeton [99,100] also exploited the circular acquisition layout all around a burial mound to reconstruct, in 3D, the P-wave velocity and attenuation tomographic images to non-invasively assess the soil *mass*, or *bulk*, quality of a tumulus, and discriminate areas of differing quality (and possibly lithology) that are of importance for the understanding of the tumulus soil structure and engineering state (Figure 21).

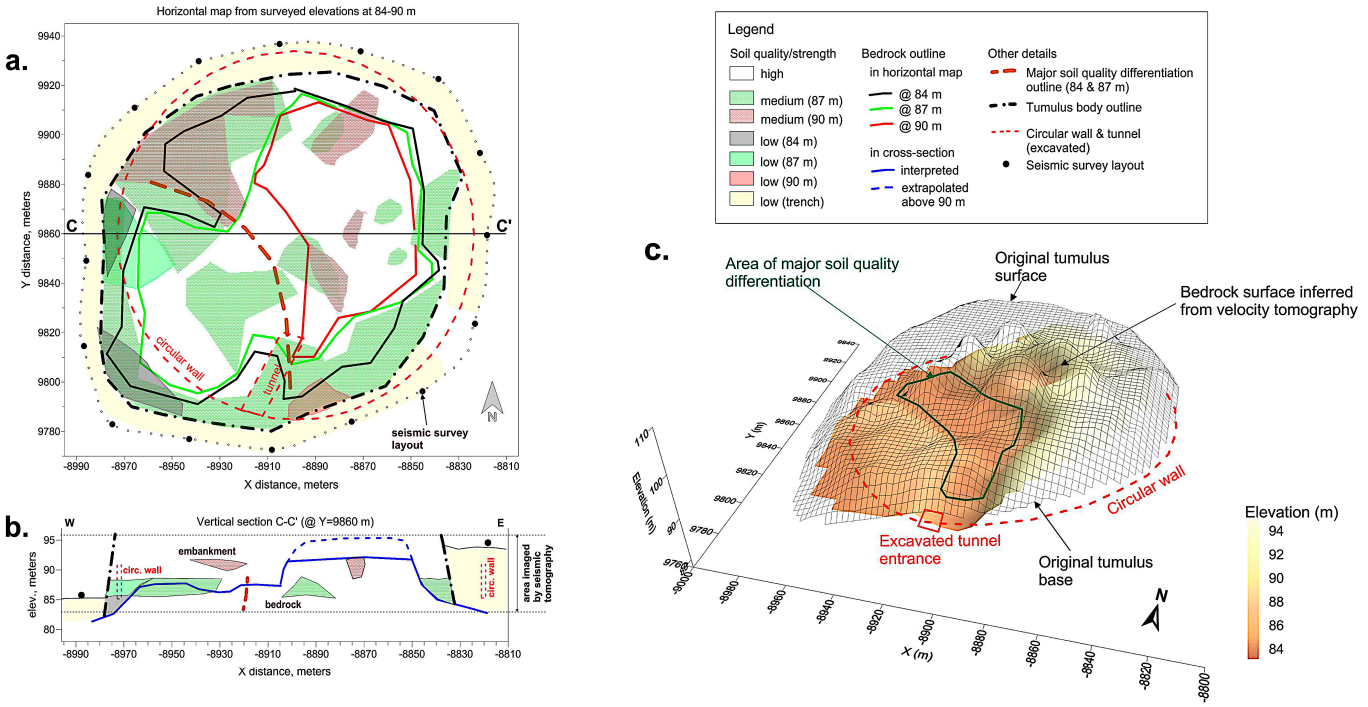


Figure 21. Kastas site in Amphipolis (northern Greece). Combined interpretation of P-wave velocity and attenuation tomography. Horizontal map, based on field data from surveyed elevations from 84 to 90 m (**a**). Cross-section C-C′ in the E–W direction (**b**). 3D surface map of the bedrock produced from velocity tomography. The area of interpreted major soil quality is also shown (**c**) [100], © Elsevier, permission obtained.

Another geophysical approach for the discovery and mapping of buried voids consists of the collection and analysis of gravity data. In this method, the measurements of the Earth's gravitational field on a generic surface (typically the ground surface) are first reduced and corrected to compensate for (typically bigger) site-dependent components of the gravity acceleration. Then, they are spatially decomposed into a regional and a local anomaly field (separation that is carried out parametrically based on the searched targets to image) and, finally, they can be inverted to estimate the 3D distribution of subsurface density contrast values. Gołębiowski et al. [101] presented the gravimetric study in the village of Wiślica, which, between the fourteenth and sixteenth centuries, was one of the administrative capitals of Poland, an important commercial center, and one of the most important centers of salt trade in the country. The microgravimetric study, jointly with GPR and ERT surveys, was performed on the hypothesis that the underground chambers that previously existed in Wiślica were dedicated to salt storing. In particular, ERT and microgravity measurements, validated with boreholes, were applied for the detection of chambers or their remains located at depths of up to about a dozen meters. It is likely that two or three anomalies indicated the locations of remains of medieval underground salt chambers. Even Rabbel et al. [102] proposed an integrated (ERT, magnetic, GPR, and microgravity) geophysical prospection of an archeological site for the discovery of a Byzantine Church in Iznik/Nicaea (Turkey). At the investigation site, the soil appeared homogeneous, compacted, and was dried out from the hot climate.

The magnetic results did not show any evidence of buried construction, whereas the GPR ones provided clear evidence of a spatially coherent structure underneath. ERT and gravity analyses, in correspondence with a small region inside the regular pattern reconstructed by GPR (and interpreted jointly with the GPR sections), suggested a low-density zone at about a 1 m depth that could be interpreted as a grave filled with loose sediment.

Some promising and very recent results are coming from the on-field spectrometric mapping of gamma-ray emissions from investigated archeological sites [103–105]. Radiation surveys look to measure subtle variations in the concentrations of naturally occurring radioactivity present in potential targets and the surrounding soil, using portable modern spectrometers. Of particular interest in the field of archeology is the historic use of imported construction materials and the concentration of radioactivity in these materials [104]. Throughout history, construction materials have often been transported over significant distances to a desired location or settlement. There are multiple mechanisms that can cause measurable differences in the concentrations of radioactivity within targets, as summarized in Figure 22.

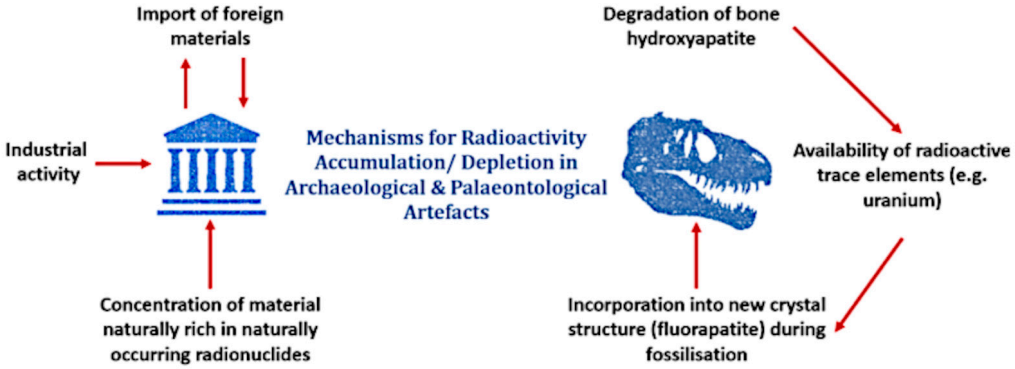


Figure 22. Mechanisms for the accumulation/depletion of naturally occurring radioactivity in buried archeological and paleontological artifacts [104]. Creative Commons BY-NC-ND.

Extremely rarely, another non-invasive technology can be applied to the recognition of shallow anomalous bodies buried in archeological sites. This is the case of muon tomography, which is a particular technique based on the tomographic imaging of studied volumes, localizing one or more receiving stations underground to record the cosmic muon flux coming from the sky down to the deepest layers of the Earth [106,107]. The need for a transparency/transmission functioning scheme implies very peculiar site conditions for application; in the Etruscan necropolis known as Palazzone near Perugia, Italy, the data were collected from galleries and underground rooms looking toward an upstanding hill, and tomographies revealed the presence of unknown voids probably attributable to tombs [106].

3.2. Other Geophysical Applications

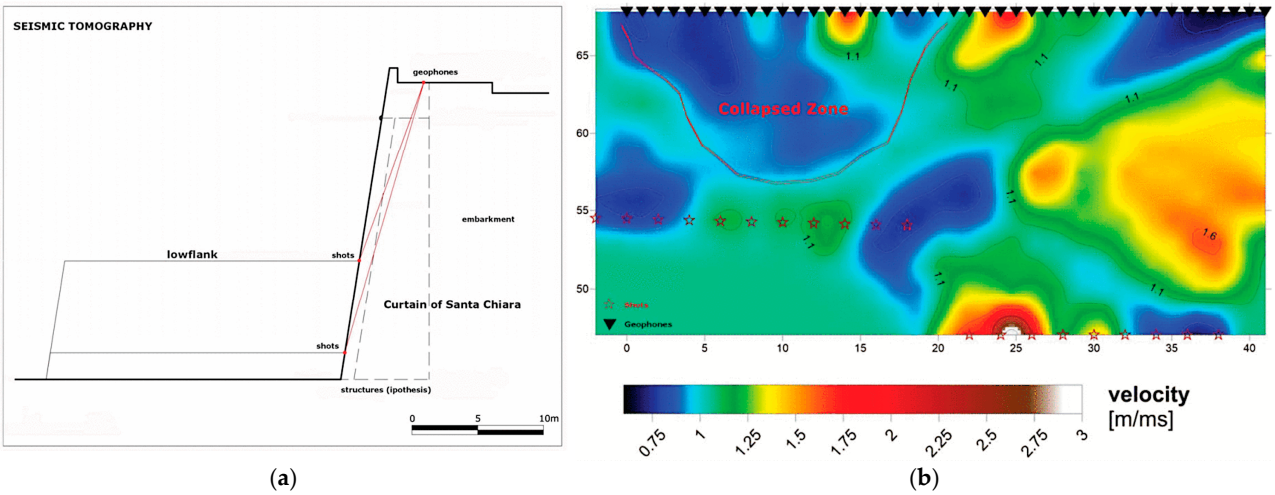
3.2.1. Monumental Structure Geophysics

Geophysical surveys provide both qualitative information and quantitative data for the adoption of the correct conservation activities and suitable restoration procedures of monumental structures. The study of the physical state of historical structures and building materials supports specific technical solutions through the definition of a complete diagnostic framework for the state of inaccessible environments and the inspection of structural elements. Historical churches, ancient amphitheaters, and colossal statues are the main subjects of numerous studies. The surveys mainly include the inspection of structural foundations and the discovery of previously underground structures, the identification of the causes at the base of several kinds of geotechnical problems, the prevention of

collapse and subsidence phenomena of the foundation soils, non-destructive analyses of pillars, vaults, arches, and other structural elements, and even the mapping of the degraded volumes of the construction materials. Some miniaturized applications have already been presented in *Part I, the micro-scale (manufacts)* [1], section *Micro-Geophysics*, where we focus on applications at a slightly larger scale without the need for instrumental miniaturization, but still maintaining many of the technical difficulties of those surveys.

Tsourlos and Tsokas [108] performed a fully non-destructive ERT imaging survey to assess the conditions of the south walls of the Acropolis of Athens. The investigation faced several technical difficulties and required the design of special measuring arrangements and software modifications. Climbers mounted the cable on the wall, and bentonite electrodes substituted spike electrodes. ERTs were acquired in both ground-to-external-wall and cross-wall configurations and allowed for the detection of some moisture paths that could put the Acropolis wall at risk of damage. Angelis et al. [109] studied the moisture levels and patterns of a sector of the wall structure at the Heptapyrgion fortress (Thessaloniki, Greece) with ERT and GPR, and interpreted their results against synthetic datasets simulating that condition.

The monumental walls of the Bastion of the Holy Cross in Cagliari (Italy) were investigated with surface and borehole-to-wall seismic refraction tomography techniques [110]. The borehole-to-wall seismic tomographies were acquired in four sections of the Renaissance curtain wall, moving the energy source in the boreholes and fixing the geophones on the wall vertical surface through adhesive strips at a relative distance of one meter, applied by climber operators. The results clearly imaged several structural elements like the preexisting medieval walls, the soft fillings typical of Renaissance defensive structures against artillery fire, the external curtain, and the foundations of buildings. The same bastion, in a different sector, has been studied with a quasi-vertical cross-wall seismic tomography, providing evidence of a large volume with a low P-wave velocity, which was interpreted as an ancient collapse of the wall thanks to historical sources [111] (Figure 23). Beyond historical and archeological interests, the techniques proposed here provide direct information on the elastic characteristics of the materials involved and therefore also useful information for safeguarding, consolidating, and restoring, which is difficult to obtain in a direct way with other non-invasive techniques.



(**a**) (**b**)

Figure 23. Bastion of the Holy Cross (Cagliari, Italy). Section of the investigated defensive wall with the indication of the positions of shots (bottom and middle of the section) and geophones (top of the section), and simplified rectilinear seismic rays paths in red (**a**), and seismic tomography along the best fitting rays flat surface, with the indication of shots, geophones, and the low velocity volumes interpreted as a sign of a previous collapse (**b**) [111], © IEEE, permission obtained.

The Cathedral of Mallorca (Spain) was the subject of an integrated diagnostic study based on Ground-Penetrating Radar investigations, electrical surveys, and passive seismic surveys (Refraction Microtremor) [112]. The geophysical investigations discussed by the authors were part of a deeper multi-disciplinary study aimed at identifying the structural and experimental dynamic behavior of the ancient church. Electrical surveys were performed through the capacitively coupled resistivity method. This diagnostic technique was utilized to derive several two-dimensional images of the underground medium. The multi-method approach allowed for the definition of a complex model of the ground, which represents the fundamental base for the implementation of more advanced soil–structure numerical models of the building for the structural dynamic analysis. The GPR surveys made the detection of several shallow underground archeological structures and other superficial buried features possible. Electrical tomographies and seismic data supported the geological interpretations, specifically the complementary use of direct stratigraphic profiles, enabling the constraining of the geophysical models and allowed for the obtainment of a detailed model of the site.

The occurrence of potential archeological remains from the Roman age under the paves of the Cathedral of Tarragona (Catalonia, Spain) was verified through integrated geophysical surveys carried out by Casas et al. [113]. Both ERT and GPR prospections were planned for the inspection of the subsurface volumes inside the church. The authors performed 3D ERT acquisitions with a method based on the Maximum Yield Grid (MYG) approach [114], which has been developed to reduce the number of current electrodes of the acquisition grid during the active electrical surveys for the injection of the electrical current. Different types of electrodes were utilized for the measurements: small steel electrodes for the injection of the electrical current and foam Ag/AgCl electrodes for the measurements of the electrical potential, utilized to perform electrocardiogram (ECG) clinical exams and previously tested and analyzed by the same authors in other studies [114,115]. The geophysical investigations revealed the presence of several buried structures and allowed for the definition of the most promising sectors for selective excavations. Direct diggings confirmed the archeological nature of the underground objects as the basement of the Roman Temple that headed the Provincial Forum of the ancient Roman town of Tarraco, the seat of the Concilium of Hispania Citerior Province.

Three-dimensional GPR and seismic investigations were carried out for a structural restoration project of the Great Church of St. Sophia of Istanbul (Turkey) [116,117]. The experimental campaign for diagnostic analysis of this monument, historically significant to both Christian and Islamic cults, included geophysical surveys to map the geometry of the foundations and identify the buried remains of earlier structures. The study delineated the perimeter of a large cistern previously discovered through 2D GPR surveys conducted at the site.

To explore the GPR performance in reconstructing useful information for the historical stratification of monuments, an experimental survey on the pavement of the nave of the Romanic church of San Leonardo de Siete Fuentes in Santu Lussurgiu (Italy) was conducted [118]. Joint analysis of B- and C-scans revealed significant patterns in the subsurface, allowing for the identification of a primary church foundation based on signal characteristics. Three-dimensional signal attribute analysis, horizon detection, and visualization were used to define volumes with consistent signal behavior (Figure 24a–c), providing insights into past events that have affected the shallow subsurface. Furthermore, to provide more robust and insightful information, the GPR results were interpreted and analyzed in conjunction with a thermal infrared survey and a historical–artistic analysis of the monument. Based on the integrated geophysical and historical analysis of the monument, the ancient

layout of the church was reconstructed, and other potential archeological features were identified (Figure 24d).

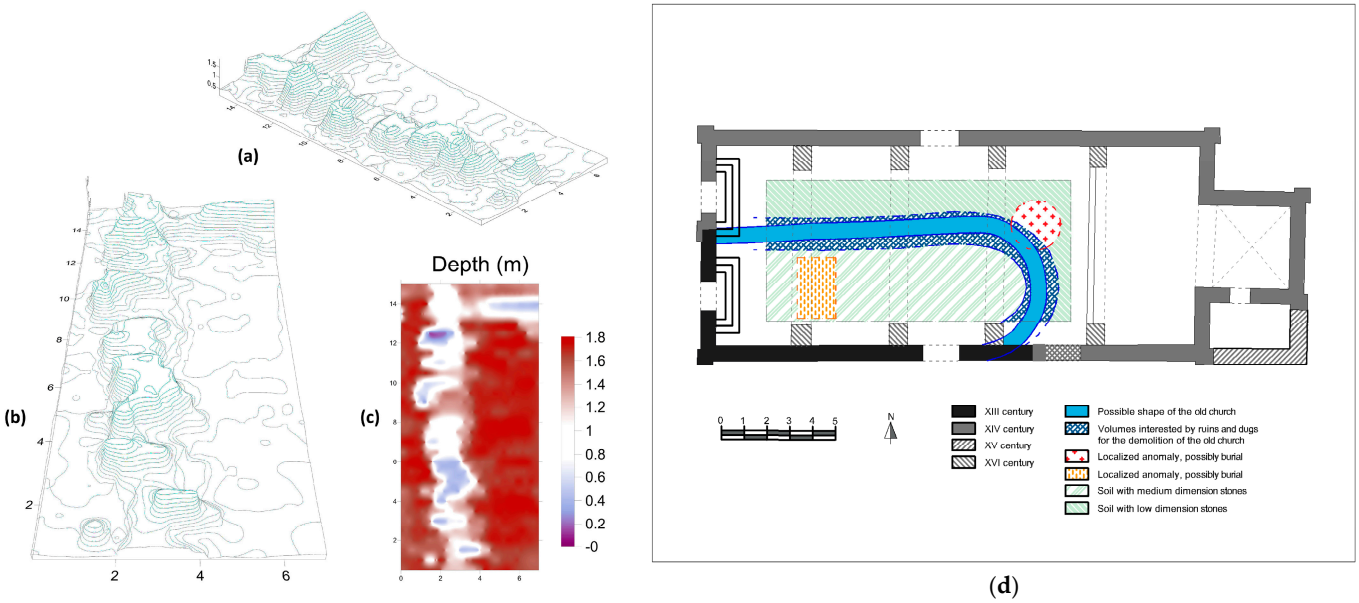


Figure 24. Church of San Leonardo de Siete Fuentes (Italy). 3D manual recognition of possible archeological features by interpolating GPR horizons picked from transversal radargrams. Three-dimensional visualization of the recognized horizon surface belonging to the envelope of anomalies B and C, which appear fused inside a unique pattern (**a**,**b**); map with the depth from the floor surface of the reconstructed volumes (larger depth values for deeper targets) (**c**); and archeological interpretation based on stylistic, historic, and geophysical analyses (**d**) [118].

GPR surveys were also performed to improve the knowledge of the construction techniques and building materials of the world-famous Amphitheater Flavium of Rome (Italy), with the purpose of collecting information and data for assessing the seismic vulnerability of the structure [119]. The GPR measurements were carried out on the floor and on the walls of the so-called Passage of Commodus by using a set of radar antennas with different central frequencies. Thanks to the surveys, the authors identified three equally spaced GPR anomalies related to old utilities parallel to the passageway at a depth of about 1 m below the surface. The high-resolution GPR measurements allowed for the evaluation of the thickness of the concrete covering the foundation and the localization of the edges of buried structural elements. The results of the multi-scale GPR survey highlight the usefulness of this method in providing concrete answers to numerous technical problems and historical questions.

Argote-Espino et al. [120] presented a new 3D ERT methodology involving different conventional electrodes for studying the archeological site of El Pahñú (Mexico). Here, two important structures were studied, the Main Pyramid and the Tecpan. The L-Corner (LC), Equatorial (Eq), and Minimum Coupling (MC) were adopted for reconstructing the electrical behavior of the subsoil. The first monument was investigated with 33 electrodes placed around the structure, for the second one 44 electrodes surrounded the structure, and other electrodes were placed within the structure for performing a traditional 3D ERT. The results provided useful information at a depth not reachable with other geophysical methodologies about the presence of archeological features, such as a collapsed tunnel and temple foundations (Figure 25).

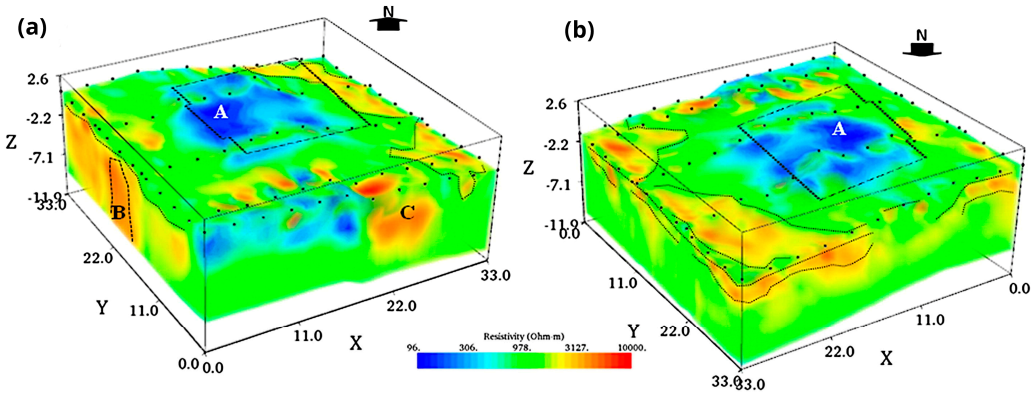


Figure 25. El Pahñú site (Mexico). Three-dimensional ERT acquired inside the Tecpan in two different views, South view, (**a**), and North view, (**b**). Resistive anomalies B and C can be associated with an entrance of a cave and a consolidated tuff, while the conductive anomaly A is interpreted as a buried room or a foundation structure [120], © Elsevier, permission obtained.

Chavez et al. [121] employed unconventional and non-invasive geoelectric arrays for investigating two Maya Pyramids located at the archeological site of Chichen Itza (Mexico) without disturbing the archeological context. Three-dimensional ERTs were carried out by deploying non-intrusive flat-base copper electrodes placed around the base of the temples, and some resistive anomalies, likely due to the presence of cavities, were detected (Figure 26). A fundamental question is related to the sensitivity of the approach used for the analyses (that are limited to the middle of the investigated area), which is maximum near the edges. Indeed, the authors observed that the obtained information allows for a good estimation of lateral distribution, but the vertical resolution was limited, as shown by the synthetic models computed for the research.

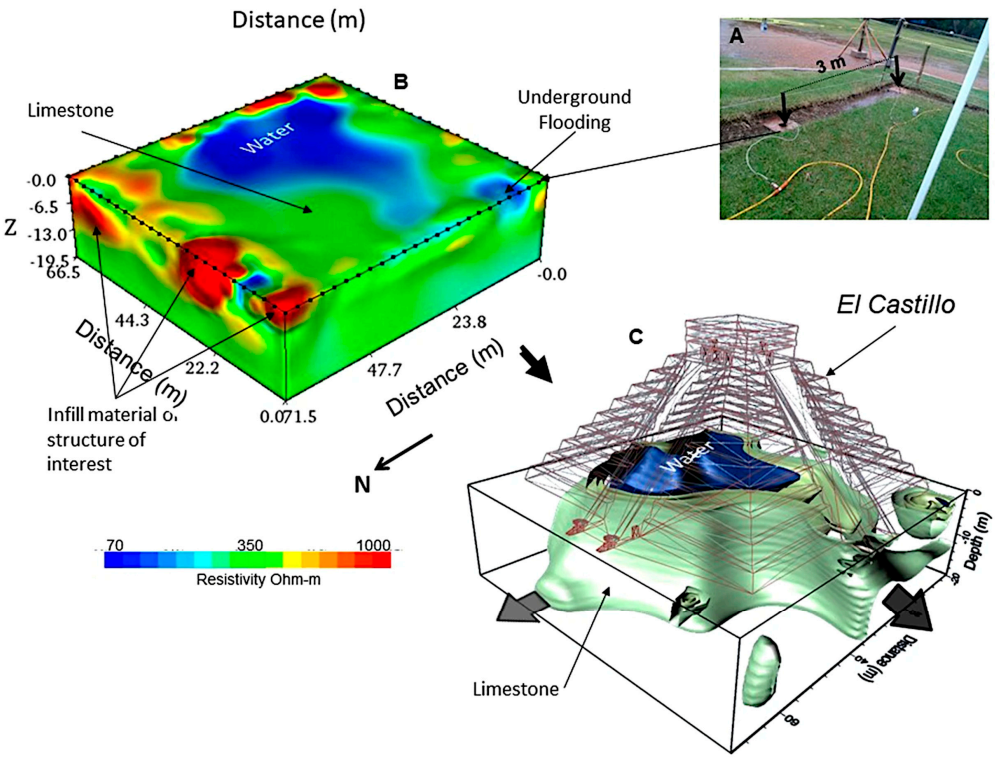


Figure 26. Chichen Itza (Mexico). 3D ERT performed around the base of the Pyramid El Castillo by adopting flat non-invasive electrodes (**A**). The model (**B**) shows a conductive anomaly imputable to the presence of a water-saturated zone and a resistive body due to a cavity partially filled with water (**C**) [121] CC BY 4.0.

Pazzi et al. [122] adopted an electric and electromagnetic geophysical approach for the subsurface investigation of an urban anthropogenic mound in the English Cemetery of Florence, Italy. To overcome the logistic issues linked to the presence of the monumental cemetery and to the surrounding urban environment, the authors investigated the site with a quite dense, eighty-two-VLF profile grid homogeneously distributed across the cemetery, and five ERTs located in the few free-from-obstacles areas. The high resistive anomalies observed in the VLF results were attributed to remnants of an ancient perimeter wall buried along the southern side of the mound. While no apparent correlation was found between the causes of tomb and ground movements for which the survey was carried out, the crack pattern map supplemented the overall structural assessment, and the northern portion of the remaining wall was classed with the highest hazard rate.

Microgravimetric studies inside monumental buildings are quite rare. Still, some interesting results are present in the scientific literature. Their common element, which differentiates them from many outdoor gravimetric surveys, is the necessity of a careful and detailed topographic correction to compensate for the gravity (upward) attraction of massive walls and elements toward the close stations where microgravity measurements are gathered. Pašteka et al. [123] presented a collection of selected case studies on the discovery of crypts and tombs under the pavements of historical buildings (mainly churches). It is worth pointing out that, during data acquisition, it was very important to precisely measure the position of measurement points and to avoid their close proximity to any walls (not closer than 15–20 cm). In the processing stage, the lightening contribution of walls and columns was estimated point by point using the forward modeling approach. Padín et al. [124] studied the don church in Valencia, Spain, detecting a large negative anomaly on the Bouguer map after all corrections and reductions. This microgravimetric signature was compared with synthetic data to estimate the dimensions and position of a known but unlocated crypt. Fais et al. [125] proposed the same workflow to study tombs and other shallow and small cavities inside a paleo-Christian church and across its closest surroundings.

As already introduced in Section 2, "*Geophysical prospection of archeological sites*", the muon tomography has scant applications, even in the study of monumental structures, thanks to its trait of needing a transillumination setup with the target volumes located in-between the sensor and the free environment. The first applications date back to the early 1970s, with the search for hidden chambers in the Second Pyramid of Giza by cosmic-ray absorption [126]. Recently, this family of techniques has been the object of many studies on ancient buildings, mines of historical prominence, pyramids, and other massive targets, with the possibility of installing the required equipment in appropriate rooms [127–130]. Technological and economic constraints still limit this technique to a few, mostly academic, implementations.

For inspecting large and massive historical objects, satellite techniques have recently been proposed. For example, the Great Pyramid of Giza was recently studied using synthetic aperture radar Doppler tomography, revealing possible internal void configurations based on their influence on surface vibrations [131].

To conclude this sub-section, it is valuable to remember that monumental statues are constantly exposed to atmospheric agents, chemical attacks, weathering phenomena, seasonal environmental cycles, and thermal variations. Over time, all these factors determine the alterations in the construction materials and can progressively reduce mechanical resistance. In addition, both chemical and physical alteration phenomena can be responsible for the opening of cracks, failures, and shallow defects. Such defects and degraded volumes generally exhibit different physical properties and different responses at the acoustic, electrical, or electromagnetic sources. Thus, the non-destructive techniques contribute to the

identification of the anomalous sectors and volumes of the media. Famous statues of Moai on Easter Island were studied by [132]. The authors described a wide and accurate study performed with different geophysical methods and through geodetic surveying activities to derive 3D high-resolution numerical models of the statues. The interdisciplinary study proposed the integration of laser scanner surveys, geomechanical tests on rock samples, seismic tomographies, and Ground-Penetrating Radar investigations. The combined use of two imaging techniques allowed for the overcoming of some ambiguities related to the argillification and unsaturated condition of rock. The joint interpretation of the geophysical data removed this factor, providing a useful tool to plan possible conservation projects and other specific interventions.

3.2.2. Submerged Archeological Areas

Numerous archeological sites include underwater and submerged areas. Both natural phenomena (e.g., environmental climate changes, eustatic and isostatic sea level variations, subsidence, and geological and seismological effects) and human historical events (shipwrecks, naval battles, and wars) are the main causes of the presence of underwater archeological structures located along the coastlines, and artifacts and manmade objects lost in submerged environments over the past centuries. Many outstanding archeological discoveries were made in submerged areas [133–136]. In this context, underwater archeological surveys have included a wide range of geophysical methods: acoustic methods and electrical resistivity techniques; magnetometry; and Ground-Penetrating Radar investigations. In addition, several underwater systems, like Autonomous Underwater Vehicles (AUVs) and Remotely Operated Vehicles (ROVs), have been widely utilized to identify candidate archeological targets and to remotely explore the submerged seabed and inaccessible landscapes.

Acoustic methods, which are commonly used to study submerged and buried media, employ various technological systems based on the propagation of acoustic waves. These methods are mainly utilized to define geometric features of the underground geological units (seismic stratigraphic methods like 4D, 3D, and 2D seismic reflection techniques and Sub-bottom profiler analyses), or are applied to map the seabed topography or identify geological outcrops and partially buried artificial bodies or shallow irregularities and sunken wrecks (Side-scan sonar). In particular, the Side-scan sonar and the Sub-bottom profiler are two types of equipment utilized to perform submarine and underwater explorations. A Side-scan sonar is a tool effectively employed to map the topographic surface of the seafloor. The system provides 3D surface images of the seabed through the processing of backscattered acoustic signals. Conversely, a Sub-bottom profiler is a measurement system based on the detection of 3D volumes of contrasts of acoustic impedance between geological horizons with different elastic properties. In fact, while the Side-scan sonar technology works using only the first arrivals of backscattered acoustic waves, the Sub-bottom profiler technology employs all the backscattered and reflected signals, acquiring the full wave train, typically producing vertical sections of the investigated volumes. Sub-bottom profiler systems generate acoustic signals through an internal transducer and collect the reflected echoes coming from the buried mechanical interfaces between different geological materials. The combined use of both types of equipment has allowed for the identification of the geomorphological features of the seafloor and the definition of geological models of the investigated volumes for shallow depths [137].

Several authors have accurately described the results of geophysical investigations using acoustic methods to exactly locate the spatial position of historical shipwrecks [137]. In addition, to provide more detailed information for archeological interpretation, these authors often propose an integrated approach using different prospecting methods. Both

acoustic and magnetic methods were utilized to identify the spatial coordinates of the sunken remains of two vessels partially buried within soft sediments in the area of the Gulf of Naples (Italy) [138].

Other authors [139] faced the integration of archeological, geological, and geophysical surveys to study the submerged structures of ancient harbors and to map the archeological remains found along the coastline in southern Turkey. The authors employed seismic surveys to identify the geological features that may have caused the subsidence phenomena of the area of study over the past centuries.

The electrical resistivity tomography method is considered a suitable technical solution to explore submerged areas, especially in environmental systems with very shallow water (shores, lagoons, and saltworks). The contribution of non-conventional systems to ERT acquisition was examined by Capozzoli et al. [140] in an unsaturated and subwater analog archeological site in a full-scale laboratory test. Using loop–loop shaped ERT, the archeological remains were detected, and the applicability of the method in urban scenarios where the regular disposition of the electrodes is not fully achievable for the constant presence of obstacles is demonstrated.

In the case of submerged targets, the direct measurement of the electrical conductivity of the water samples represents a piece of important information to improve the results of the analyses and to constrain the inversion procedures of the experimental data of apparent electrical resistivity. Numerous authors have proposed ERT surveys to explore underwater archeological systems and to identify submerged and buried remains and structures [141–143]. ERT, gradiometric magnetic, and Ground-Penetrating Radar investigations have been tested to reveal antiquities and buried archeological remains in different shallow coastal environments by [143]. Specific technical solutions have been found to perform 3D ERT measurements with a set of floating electrodes. This methodological approach was utilized to provide a three-dimensional electrical model of the site and to better resolve the sizes and shapes of the geophysical anomalies. The experimental results obtained from the integrated geophysical surveys contributed to defining the superficial extension of the archeological sites and demonstrated that non-invasive methods are an effective technical solution for resolving underground anomalies, even in the presence of high-conductivity shallow layers, such as the water table along the coastlines. In Figure 27, a few images document this integrated geophysical approach to characterizing the experimental site, featuring two pictures from the data collection phases (ERT data in the top-left corner and GPR in the middle-left side). Additionally, some imaging results from the data processing are illustrated, with screenshots from the electrical resistivity model of the investigated volumes (top-right), the GPR amplitude maps (bottom-left), and the magnetic map over the seashore (bottom-right). Mobile streamers dragged along the sea bottom below the sea surface were utilized to perform archeological investigations at a submerged archeological site in central Greece [142]. Three-dimensional ERT data were processed through a new approach based on a fast technique that optimizes the calculation of the Jacobian matrix values, allowing for the derivation of the inversion model with a significant reduction in computer time and memory required to solve the least-squares optimization equation [144].

Magnetic prospection, quite often, has been utilized for underwater archeological surveys. High-resolution magnetic gradiometric and bathymetric surveys were carried out to identify the geometric distribution of candidate archeological targets and ancient remains from both the Roman and pre-Roman periods at an offshore archeological site in southern Italy [145]. The authors analyzed the pattern distribution of the anomalies of the horizontal gradient magnitude derived from marine magnetic investigations and identified alignments of magnetic sources, consistent with buried and submerged harbor structures.

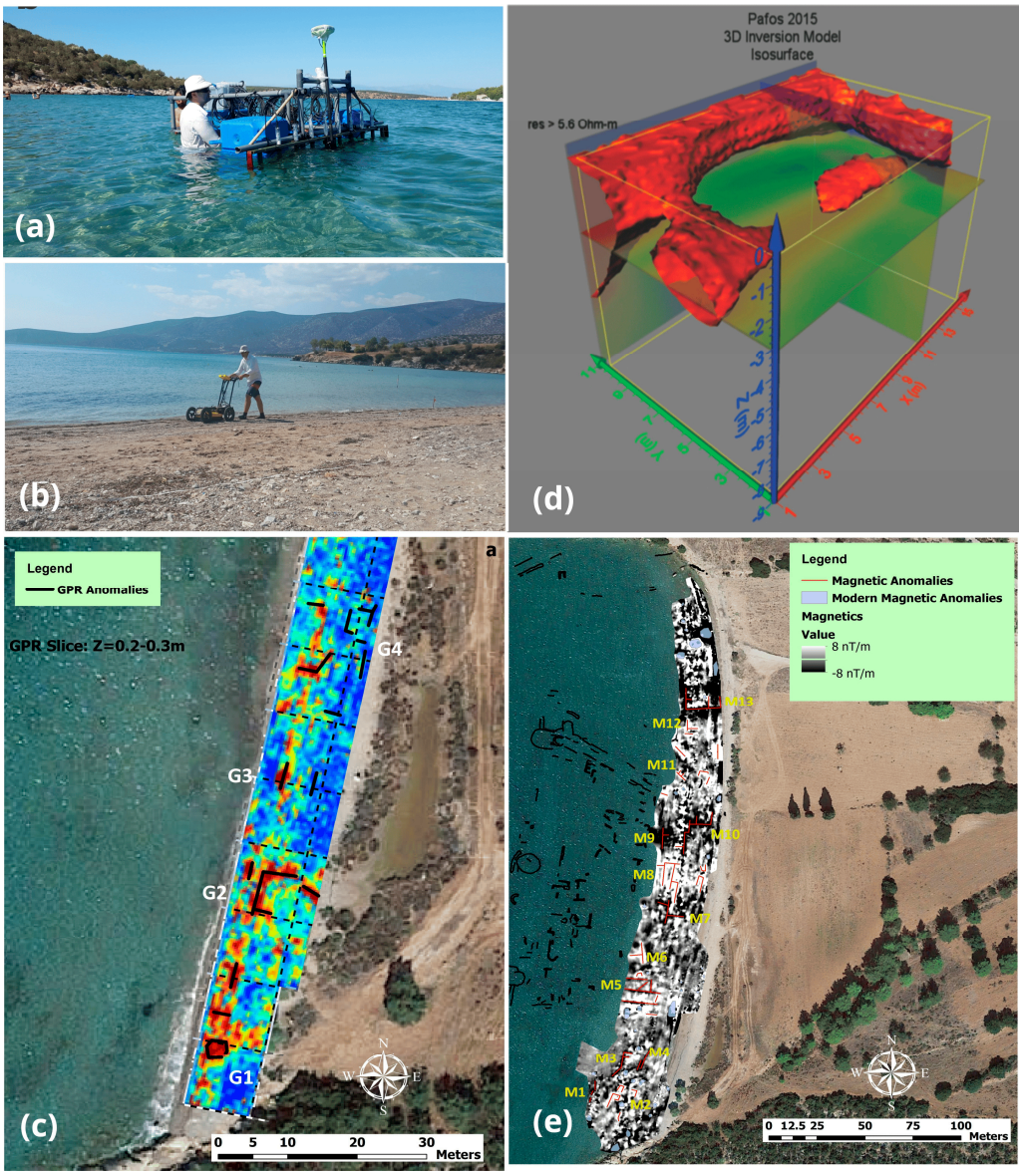


Figure 27. Eastern Mediterranean (Greece). Shallow offshore geophysical prospection of archeological sites; on the left, an acquisition scheme of offshore ERT (**a**), onshore GPR survey (**b**), and GPR time-slice in the same condition (**c**); on the right, an example of a retrieved 3D resistivity model under the seabed (**d**), and a map of the magnetic anomalies in an onshore configuration (**e**). G1–G4 and M1–M4 indicate the GPR and magnetometric anomalies respectively detected by the two geophysical surveys over the shore [143].

Data processing is a fundamental step for the identification of archeological features, and the development of strategies to enhance GPR data is a key research area. Ludeno et al. [146] exploited the microwave tomography approach for detecting and imaging underwater objects by utilizing a spatially variable equivalent permittivity in the inverse scattering model. The research, performed in laboratory conditions, demonstrated the usefulness of the adopted algorithm for retrieving the exact position and size of archeological structures realized at a real scale, as depicted in Figure 28.

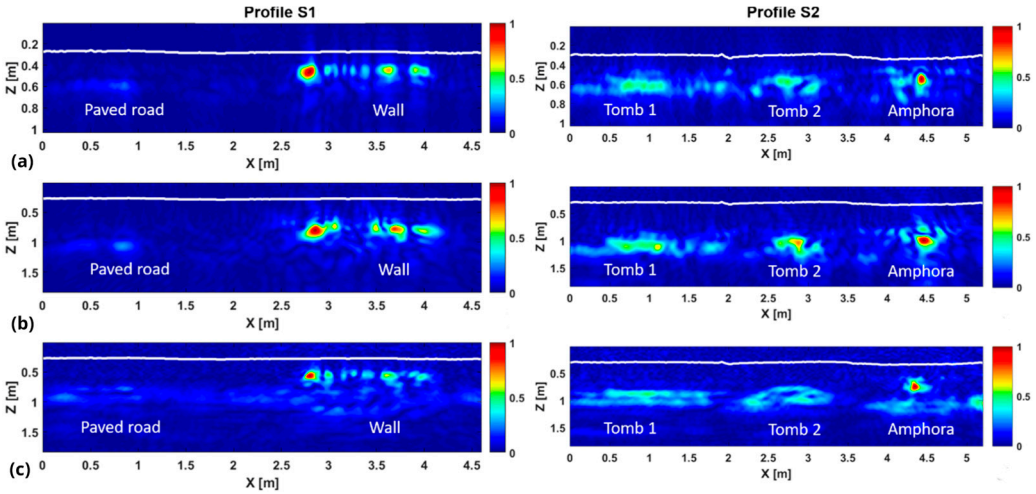


Figure 28. Hydrogeosite Laboratory (research infrastructure of CNR-IMAA) (Italy). Tomographic inversion of GPR data recorded along two different lines (**S1** and **S2**) for the detection of archeological targets artificially placed in the subsoil, adopted for the reconstruction of the permittivity of the freshwater (tomographies (**a**) for both **S1** and **S2** profiles, the wet sand (**b**), and the equivalent one (**c**), respectively). The tomographic images show the normalized intensity of the retrieved contrast. The acquisitions were performed in the presence of a water column equal to 0.3 m (approximately) and the white lines identify the bathymetry of the investigated site [146].

3.2.3. Approaches Aiding Risk Assessment and Management

The protection and conservation of cultural and architectural heritage are key global challenges that require the collaboration of various disciplines. Additionally, the growing demand for safety necessitates an evolution in the knowledge and assessment processes of heritage structures under both natural and exceptional loads. This sub-section provides an overview of the usefulness of contact and remotely operating geophysical techniques in defining, preventing, and managing potential risk-related issues. In the context of risk management, the focus is on vulnerability topics as a significant component of accurate risk evaluation and assessment.

Over the past decades, numerous destructive earthquakes and extreme events worldwide have caused extensive damage to historical buildings and Cultural Heritage sites. Consequently, assessing vulnerability is crucial for urban disaster management. It has been suggested that simple and low-cost early warning equipment should be designed, implemented, and used to manage and prepare for disasters, particularly in sustainable development efforts. Therefore, evaluating the vulnerability of historical buildings and Cultural Heritage sites is vital. Historical buildings can be vulnerable to seismic activity due to factors such as age, construction materials, and design. Common vulnerability factors include a lack of seismic retrofitting, brittle materials, weak connections between different parts, and foundational problems. To mitigate these vulnerabilities, seismic retrofitting can be undertaken to strengthen the building and enhance its resilience to earthquakes. This may involve reinforcing walls, upgrading connections between different parts of the building, or strengthening the foundations. Various sources of excitation generate vibrations in the structural and non-structural components of structures [147,148]. These sources can be classified based on their position either inside or outside the structure. Different classes are associated with serviceability conditions, but severe performance issues can arise from earthquakes or extreme wind events. Several studies in the literature [149,150] focus on the effects of vibrations on buildings, and specific codes and guidelines establish limits for vibration duration and exposure.

Experimental measurements of historic buildings necessitate non-invasive investigation methods to preserve the integrity of the monuments [151,152]. In this regard, dynamic identification, coupled with appropriately tuned numerical models, is considered a powerful and effective approach for investigating the health status of ancient buildings. Geophysical techniques offer a non-invasive and cost-effective means to provide unbiased information on the main frequencies and modal shape, which can be directly related to the assessment of structural damage [153–159]. In this context, numerical modeling plays a crucial role in assessing the seismic vulnerability of structures, especially historical buildings. Through computer simulations, it is possible to predict a structure's behavior under seismic loads, evaluate the effectiveness of retrofitting strategies, and develop appropriate seismic design standards. One key application of numerical modeling in seismic vulnerability assessment is the development of finite element models. These models use mathematical equations to simulate the behavior of a structure under different seismic loads, such as ground motions of varying intensity and direction. The results of these simulations can identify the areas of the building most susceptible to damage or collapse during an earthquake, and develop retrofitting strategies targeting those specific areas. Numerical modeling also allows for conducting sensitivity analyses to evaluate the impact of various design and retrofitting strategies on the behavior of a structure under seismic loads. This information can be used to optimize retrofitting strategies and develop cost-effective solutions for improving the seismic performance of historical buildings. Bartoli et al. [160] report methodologies and numerical approaches evaluating the seismic risk of historic masonry towers, discussing expeditious experimental techniques that can estimate the data needed for subsequent structural analyses. This is particularly important in countries like Italy [161,162], considering the high density of masonry historical buildings, which are highly vulnerable and can be easily exposed to significant damage from earthquakes and other extreme events.

In recent times, various satellite and remote sensing systems have been miniaturized to create compact radar equipment suitable for performing non-contact measurements of displacement time series for several kinds of terrestrial targets. Real and Synthetic Aperture Radar (RAR and SAR, respectively) systems enable the acquisition of one-dimensional and two-dimensional images of the displacements of multiple targets within the radar scenario. Ground-based Radar Interferometry (GB-SAR or GB-RAR) systems implement the interferometric technique to derive the displacements from the phase analysis of the microwave signals. The electromagnetic signals return to the radar antenna after being backscattered or reflected by natural and man-made elements or specific corner reflectors. The phase difference between two signals received by the radar antenna allows for the derivation of the target's displacement, measured along the Line-of-Sight of the radar sensor. In these radar systems, both the transmitter and receiver are located in the same physical unit and consist of two polarized antennas that generate signals in different frequency bands. The most utilized wavelengths of the microwave signals are usually within the frequency range from 8 GHz to 18 GHz (X band and Ku band). These features of the radar signals allow for the detection of vibrations with an accuracy of up to tens of micrometers. The radar equipment transmits microwave pulses generated with the Stepped-Frequency Continuous-Wave technique (SF-CW). The most diffuse systems allow for a spatial resolution of 0.75 m along the radar scenario.

Terrestrial remote sensing surveys can provide crucial information to find effective technical solutions for numerous environmental and engineering problems requiring the displacement data of natural and artificial targets. Numerous opportunities from the acquisition of synchronous time series of displacements related to several back-scatterers have suggested the use of terrestrial radar systems to carry out experimental dynamic and

static surveys of engineering structures. In the field of Cultural Heritage, experimental vibration analyses have been widely utilized to identify the main dynamic properties of historical and monumental structures. The vibration surveys provide fundamental data to predict the effects of earthquakes on structures and to prevent structural damages by identifying the anomalous mechanical behaviors of the buildings. The natural frequencies, damping ratios, and experimental modal shapes of the structures are usually derived from experimental tests based on the measurement of both random vibration (e.g., volcanic microtremor, micro-seismic noise, atmospheric storms, oceanic wave motion, mechanical vibrations induced by winds and vehicular traffic, etc.) and different known artificial input sources (e.g., vibrodynes, dynamic shakers, and direct impact of heavy bodies) distributed in well-identified structural elements of the buildings. Numerous studies have described experimental vibration analyses carried out using terrestrial microwave systems. This approach allows for the acquisition of synchronous time series of displacement from different positions of the monitored structures. The experimental dynamic behavior of tall ancient structures (such as historical civic towers and ancient bell towers) was derived using terrestrial radar interferometry data by several authors [163–171]. The radar surveys were carried out by means of coherent radar systems installed on the ground surface with a simple tripod to support the sensor unit. Generally, more radar stations should be used to overcome possible ambiguities in the Power Radar Profiles and to compare the displacement data measured from different perspective views of the sensor. The risk and vulnerability mitigation of historical structures is fundamental for planning effective conservation and preservation strategies of tangible Cultural Heritage. In this framework, several studies have proposed the application of proximal radar sensing techniques to study the dynamic response of ancient structures with different states of damage [164,172]. In fact, the structural health state significantly affects the dynamic properties of the buildings, modifying both the natural frequencies and modal shapes of the structures. The dynamic behavior may provide quantitative data to evaluate the risk exposure of people and technicians during the restoration works. Several studies are based on the integrated use of different pieces of experimental equipment and methods (topographical surveys, photogrammetric analyses, accelerometers, and triaxial velocity sensors, etc.) and numerical modeling techniques to derive the operational dynamic response of Cultural Heritage structures [165,166,168,173]. In addition, although indoor radar surveys are conditioned by different technical issues, several authors proposed the use of Ground-based Radar Interferometry for the vibration monitoring of the internal surfaces of ancient structures (internal sides of domes and vaults) [174,175]. In [175], Piroddi and Calcina integrated non-destructive sensing methods to retrieve the experimental vibration properties of a historical dome by means of environmental microtremor measurements. The approach involved using both contact and remote sensors to acquire ambient vibration data. The measurements were carried out with a high-sensitivity tri-axial seismometer and a coherent RAR interferometer. Both seismic time series and microwave signals were processed to derive the experimental vibration properties of the structure, mainly concerning the dynamic behavior of the circular dome. Additionally, to evaluate the capabilities of the radar system in the indoor configuration, a finite element model of the structure was built, and the experimental results were compared to the numerical outputs, showing good agreement between the experimental and numerical techniques. Some representative images are given in Figure 29.

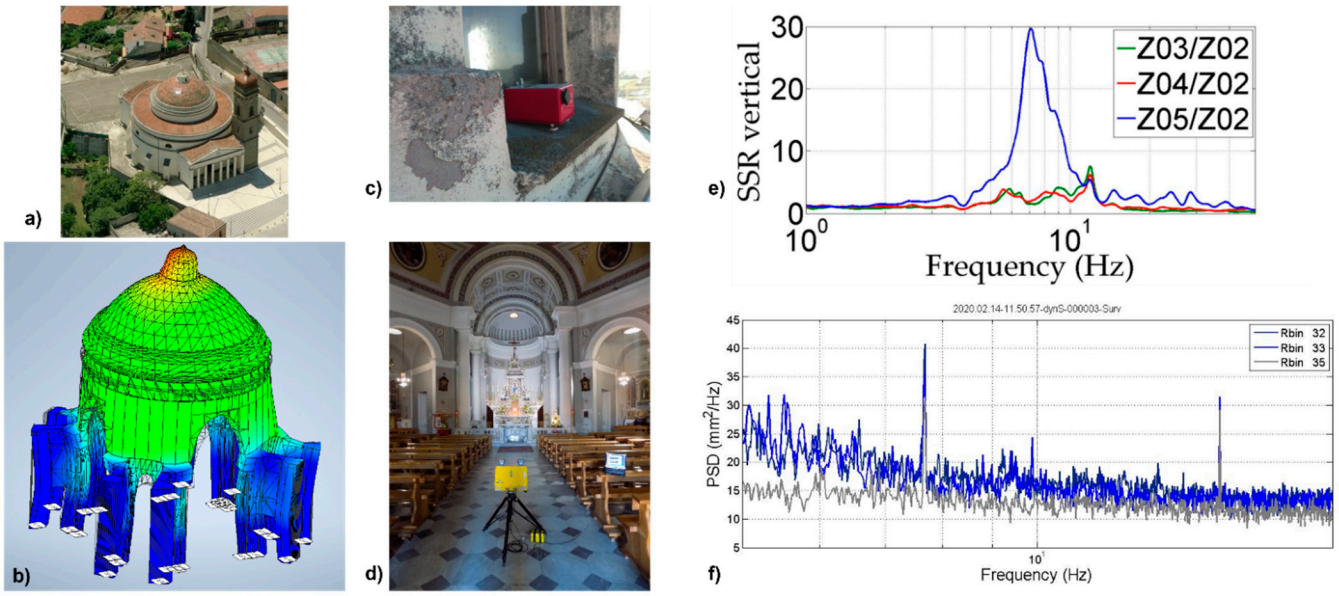


Figure 29. Church of Beata Vergine Assunta in Guasila (Italy). Integrated vibration analysis for historical dome structures: aerial view (**a**), finite element model of the central body of the church with the first modal deformation (**b**), contact measurements with a 3D-component tromometer (**c**), close-range vibration measurements with a RAR interferometer (**d**), Standard Spectral Ratios (SSRs) diagram for the evaluation of the dynamic amplification against a reference station of environmental noise (**e**), and Power Spectral Density functions derived from the range bins 32, 33, and 35, selected from a radar scenario corresponding to a specific interferometric acquisition station (**f**) [175], © Springer Nature Switzerland AG, permission obtained.

Remote and proximal geophysical techniques are also effective in studying different scenarios of instability, from urban or archeological settlements to site-specific subsoil diagnostics. SAR systems allow operators to illuminate two-dimensional radar scenarios, and are effective in performing continuous monitoring of surfaces and large-scale targets, providing suitable solutions for a wide gamma of environmental, engineering, and architectural problems (e.g., slope deformations, dam inspection, quarry and mine monitoring, detachments, and subsidence phenomena of structures, etc.) [176,177]. Historical towns and archeological settlements are often affected by instability phenomena, like collapses of ancient walls, deformation processes of rocky ridges and unstable cliffs and Acropolises, subsidence phenomena associated with natural voids or artificial underground tunnels, and past excavation activities. In this framework, Ground-based Synthetic Aperture Radar Interferometry (GBInSAR) has been successfully applied to support early-warning procedures thanks to the real-time evaluation of the rate of deterioration and deformation processes, which involve ancient structures and historical towns [178]. The monitoring systems usually consist of different tools and are based on a multi-methodological approach combining complementary data collected through the integration of terrestrial laser scanners (TLSs) and Spaceborne and Ground-based Radar Interferometry techniques [179]. The earliest demonstration that GBInSAR deformation rates can be effectively integrated with TLS point clouds for the real-time structural monitoring of complex archeological monuments and scenarios was achieved in the Roman Forum in Rome (Italy) [180]. The so-called 3D interferometric radar point clouds provide an example of multi-sensor data fusion products aiming to facilitate the spatial interpretation of the detected deformation, and thus make GBInSAR monitoring outputs more intelligible to non-expert users (Figure 30).

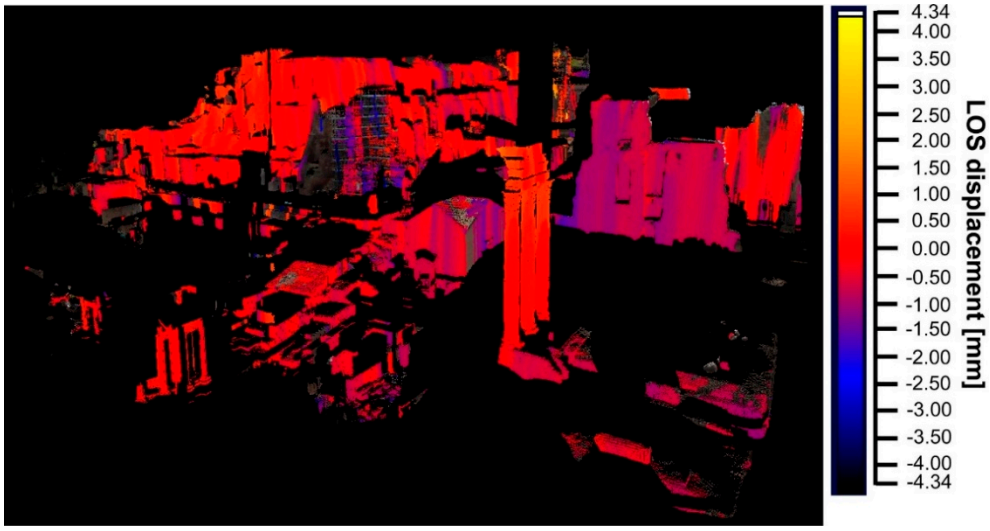


Figure 30. Domus Tiberiana and the surrounding monuments of the Roman Forum (Italy). Three-dimensional interferometric radar point cloud showing cumulative LOS displacements measured in the period 18 April–3 June 2009. The blue–violet colors in correspondence with the restoration scaffoldings are an artifact due to the disturbance created by the metallic materials of the scaffoldings themselves and the ongoing restoration activities [180], CC BY-NC-ND 3.0.

Since the above earliest experiments in Cultural Heritage, RAR and SAR technologies have further developed, and nowadays, there is a clear understanding of the pros and cons of the various techniques for the various Cultural Heritage applications. A comparative analysis, also encompassing an outlook on commercial and operational applications, is provided in [181].

Moscatelli et al. [182] characterized the anthropic layer of the Palatine Hill and Roman Forum (Rome, Italy) by means of the joint use of boreholes and ERT, which have provided detailed information about the geometry and thickness of the anthropic cover of the Palatine hill and surrounding areas. Twenty-four ERTs were performed with forty-eight electrodes, arranged according to the Wenner–Schlumberger array and placed at a constant spacing ranging from 1 to 10 m. The results obtained and integrated with GPR prospecting (at the frequency of 35 MHz) were addressed to assess the local seismic hazard and to define a detailed map of the basal surface of the anthropic layer. Indeed, ERTs have allowed for the identification of dominant masonry ($\rho > 160$ Ωm) and dominant infill ($60 < \rho < 160$ Ωm) zones, which play a crucial role local seismic amplification. Technological advances in geophysical equipment have recently enabled the use of multichannel systems with a large number of electrodes, thus improving the achievable resolution. The depth of investigation reachable by the ERT provides fundamental information for understanding the geological context and evolution of ancient settlements. In this context, Capozzoli et al. [183] adopted ERTs for identifying the presence of a landslide (Figure 31) at the archeological site of Pietragalla (Potenza, Italy) responsible for the abandonment of the site. Shallow resistive layers (>80 Ωm, a1 in Figure 31b,c) were detected in proximity of the southern edge of the line and the northern one (the Acropolis), and similar resistivity patterns were found between 75 and 85 m in the ERT3, at the location of an old archeological dump of excavated materials. In the deeper part of the ERT3, two relatively conductive zones were detected (a2 and a3) where the electrical values were less than 20 and 80 Ωm, respectively, which were interpreted as evidence of the landslide characterizing the area.

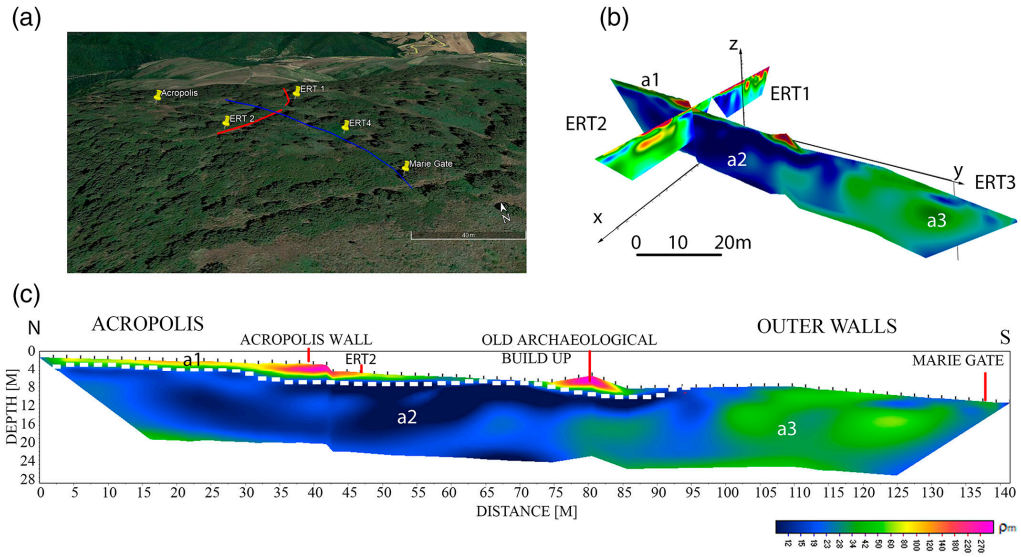


Figure 31. Pietragalla (Italy). Location of the ERT lines (**a**); joint 3D visualization of the inverted ERT1, ERT2, and ERT3 (**b**); and ERT3 (**c**). The lowest values of electrical resistivity have permitted the supposition of the presence of a landslide under the Acropolis [183], © John Wiley & Sons, permission obtained. Resistive patterns of potential cultural interests are identified as a1, while some relatively conductive volumes, a2 and a3, are interpreted in terms of potential stability issues of the site.

3.3. Proximal Sensing Geophysics and Geomatics for Archeological Prospection

Over time, low-altitude aerial photography and ground-based geomatic methods have been largely used in archeological studies for a combination of different goals, which can be divided into two branches: documentation through the survey and 3D modeling of archeological sites, and, secondly, the knowledge, identification, and prediction of unknown parts of archeological heritage.

The documentation of archeological sites is typically undertaken through active and passive ground sensing (laser scanners and terrestrial photography) and passive close-range sensing (aerial photography using unmanned devices such as balloons, drones, kites, model aircrafts, blimps, and poles).

In the last decade, the use of these methods has permitted the expansion of the scope of the geometric survey process, allowing for the production of high-resolution, reality-based digital models. They greatly enhanced the quality of the conventional, bi-dimensional, hand-made survey, which resulted in timesaving in document processing and gaining knowledge for the archeologists. Nowadays, the extraordinary development of camera sensors, the manufacturing of the lenses, and the more accurate algorithms for the recognition of homologous points on images allow for the complete reconstruction of the investigated object. Ground sensing is performed using image-based methods such as terrestrial photogrammetry (passive method), range-based methods such as laser scanners (active method), or an integration of both techniques.

Image-based data acquisition requires the acquisition of sets of photographs/images using terrestrial cameras that collect at least two images framing the same scene with an overlap of at least 60–80%. For archeological documentation, RGB (Red, Green, Blue) cameras are the most frequently employed sensors, capturing images in visible wavelengths (400–700 nm). The reconstruction of the point clouds can be obtained through digital stereoscopy with planar photo triplets [184,185], spherical photogrammetry applied on panoramic images [186], and dense image matching using frame images through Structure from Motion (SfM) algorithms [187]. Nowadays, thanks to the development of very effective algorithms and software, SfM is the most used algorithm in 3D modeling. The quality of the

results can be linked to one or more factors, such as the type of sensor (camera and lenses), calibration of the camera, data acquisition mode (parallel or convergent), characteristics and complexity of the object, use of markers and ground control points (GCPs) measured with topographic equipment (total stations, GPS), and direct measurements of known points on the object and processing algorithms.

Range-based data acquisition is carried out by using terrestrial laser scanners that mainly use two different principles for distance measurement between the sensor system and its target. The first principle is based on the time-of-flight (TOF): a short laser pulse is emitted toward the target and reflected back from its surface and a portion of the energy then returns to the scanner's detector, where the sending and arrival times are measured. The second principle is based on the phase shift (PS), in which the distance is determined by the phase difference between the sent and received waveforms. The accuracy of the range data can be dependent on the scanner mechanism precision (mirror center offset or rotation mechanism aberrations), properties of the scanned surface (roughness, reflectivity, or color), environment conditions (ambient light, humidity, or temperature), and scanning geometry (incidence angle on the surface or range differences) [188].

Even if image-based and range-based methods are based on different geometric principles, their output is similar, i.e., point clouds. Based on completely different geometric principles, the two techniques are mainly focused on short-range object modeling. Image-based data acquisition provides good metric accuracy and true colored information on the point cloud (i.e., the assignment of an RGB value to each scan coordinate) and is cost-effective and time-efficient; range-based data allow for high accuracy (the reflectance image has a very high resolution in grayscale), but the acquisition process is time-consuming. A good balance between geometric resolution, costs, and time can be achieved by integrating the two techniques, considering the specific necessities of each diagnostic study.

In [189], TOF laser scanning and image-based modeling were applied for a 3D analysis of a "nuraghe", a typical megalithic monument built only in Sardinia (Italy) during the Bronze Age. The research highlighted interesting details in construction techniques in order to perform volumetric reconstruction and map some structural issues of the monument, like cracks or disruptions in the stones and masonry. The same technique was implemented to create geometric models of the masonry and mosaic floors of the churches at Umm ar-Rasas (Jordan), allowing for an in-depth analysis to understand the evolution of the iconographic repertoire [190,191]. In refs. [192,193], the remaining ancient Byzantine city walls of the archeological site of Aquileia in Friuli Venezia Giulia (Italy), and the medieval walled enclosure surrounding the historic city center of Pontevedra (Spain), were documented. Three-dimensional data were used to create maps, orthophotos, and sections providing information such as the investigation of architectural construction techniques or construction phases. Karsent et al. [194] described the 3D modeling of Pinchango Alto (Peru) based on a combination of image and range data with the aim of conducting spatial archeological analyses at different scales. Several other authors reported similar applications [195–197], while in other cases, the two techniques were applied individually or integrated with non-destructive diagnostic methods [198–200]. Regarding built Cultural Heritage, many authors reported applications of indirect surveys to identify phenomena of degradation triggered over time, such as the cracking of walls and columns, presence of humidity, and the irregularity of the structure in plan and height [201–205]. Angelini et al. [206] studied the route and characterization of a stretch of the ancient Via Salaria, an ancient Roman consular road, which connected Rome with Porto d'Ascoli (Italy) on the Adriatic Sea. Three-dimensional laser scanner and digital photogrammetric surveys of the structures were carried out and supplemented with a campaign of radar surveys. Figure 32

shows an aerial view of the high-resolution point cloud of the Via Salaria, assessing the capability of these techniques.



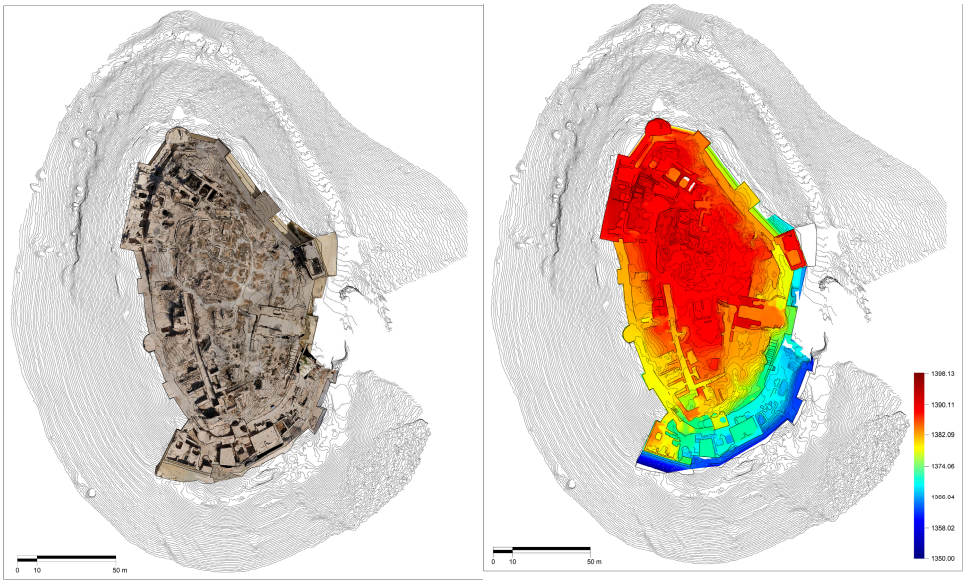
Figure 32. Via Salaria (Cittaducale, Italy). High-resolution point cloud of road (about 30 m long by 5 m wide) [206], © Springer Nature Switzerland AG, permission obtained.

Close-range aerial photography using platforms operating at low altitude is dated to the late nineteenth and early twentieth centuries [207]. A comprehensive overview has been published by Verhoeven [208], while in [209], a summary of the available platforms, along with their main merits and disadvantages, is proposed. However, masts, poles, booms, towers, kites, balloons, and blimps seem to have been less intensively used in recent years [210–216]. In [191], a stereoscopic photogrammetry hardware with three cameras was adapted to fly on a helium balloon at a 50 m altitude. Each image could simultaneously capture coordinate points over an area of 3000 m^2. This system was used in different archeological sites in Jordan: at the Shawbak Crusader castle (Figure 33) to map the visible area and to study the geomorphology of the terrain within the walls, and at Petra on the Palace Tomb, to draw the architectural façade and investigate the pathologies of the surface deterioration (Figure 34).

Recently, the development of UAVs has shown considerable progress in the field of aerial photography for documenting archeological excavations [197,209,217–220], three-dimensional surveys of monuments and historic buildings [221–225], and the survey of archeological sites and landscapes [226–229]. In addition, different researchers report the integration of terrestrial laser scanning and terrestrial and unmanned aerial vehicle digital photogrammetry for different purposes [194,230–237].

The knowledge, identification, and prediction of unknown parts of tangible heritage, especially archeological built heritage, can be acquired through techniques of active and passive close-range sensing and geophysical prospections. They can give visibility to buried archeological heritage, in some cases providing high-resolution drawings of it, even at different depths, which facilitate an overall interpretation of the site. In recent years, these applications have grown impressively in terms of instrumentation, information handling, representation strategies, as well as processing and combined systems. They require min-

imal intrusive effort (they allow fast prospecting and mapping at multiple scales, rapid analysis, and the dynamic monitoring of archeological sites and their surrounding environments investigating the presence of crop marks (differential growth of vegetation due to moisture content), parch marks (sharp chromatic contrast due to the lack of humidity), and shadow marks (unevenness of the ground) [238].



(**a**) (**b**)

Figure 33. Shawbak castle (Jordan). Orthophoto overlaid with contour lines generated by the numerical model (**a**) and DEM overlaid with contour lines (**b**) [191].

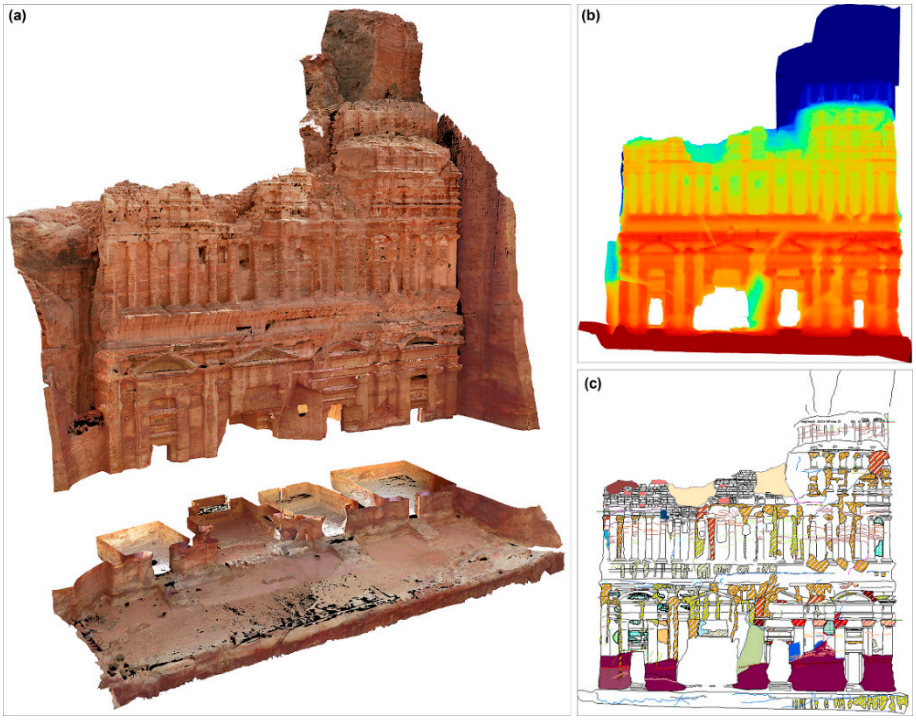


Figure 34. Palace Tomb (Jordan). Numerical model (**a**), DEM with a chromatic scale ranging between blue (deep layers) and dark red (shallow layers) (**b**), and degradation map (**c**) [191].

In a recent comprehensive literature review [239], the technological developments in UAVs and in lightweight sensors operating with visible (VIS), near-infrared (NIR), thermal-infrared (TIR), multi-spectral (MS), and hyperspectral (HS) cameras and laser and radar

sensors are analyzed. Specific applications in archeological sites across the world, with primary clusters of activity in Europe and North America, mainly deal with prospection studies, with the interpretation of visible spectrum orthophotos and digital surface models (DSMs) considering the contrast between the buried remains and the surrounding matrix. Products are mainly realized using SfM and multiple-view-stereo (MVS) techniques, typically by using shape reconstruction and GIS software platforms. The data are commonly analyzed toward the manual identification of traces. Several studies report the use of the Principal Component Analysis (PCA) [240–242], the normalized difference vegetation index (NDVI) [240–259] or, in a few cases, multiple soil indices [240,246,253,256,258,259]. Regarding the utilization of sensors, RGB cameras are often combined with other sensors and, in general, studies report the implementation of multiple devices [240–245,251,256,258–266].

Thermographic imaging is frequently exploited in archeological surveys [267–273]. Piga et al. [273] studied a Punic site in Sardinia (Italy) with ground-based GPR and aerial thermography, installing a thermal camera suspended under an aerostatic balloon. By acquiring the thermal infrared data in a time-lapse fashion during the initial hours after the sunset (for a total of about 2 h and 40 min), and with a rate of acquisition of one image per minute, they were able to compensate the balloon and sensor oscillations (due to winds at 50 m height) allowing for the recording of a significantly larger area than the fixed sensor geometry, with a sufficient thermal data (per pixel) repetition (across time) to produce derivative thermal maps summarizing the cooling behavior of the exposed surfaced. The ntercept temperature and night thermal G=gradient are shown in Figure 35.

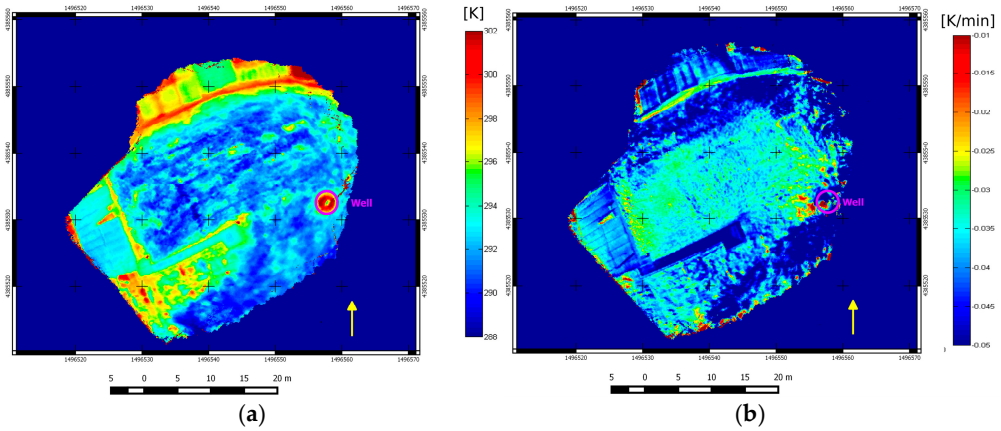


Figure 35. Punic site of Villamar (Italy). The thermal map of apparent intercept temperature (in Kelvin) (**a**), and the night thermal gradient (NTG) index (in Kelvin/minute, negative values), resulting from the merging of many thermograms and processing temperature over time, (**b**) [273].

In [274], a method for the collection and processing of high-resolution thermal imagery using an UAV is presented. The results, tested at the Chaco-period Blue J community in northwestern New Mexico, allowed for the ready mapping of most habitation sites, revealing previously undocumented architectural features. Barazzetti et al. [275] implemented new algorithms for registering thermal images with the geometrical survey from RGB data. The georeferenced images (thermal orthophotos) were then used to inspect the ground and discover buried features.

Single applications rely on the use of active NIR [276,277], IR [254,278], and LiDAR sensors [279–282]. The latter ones are emerging given their capability to penetrate the foliage, directly measuring the effects that buried remains have on the topography.

Regarding aerial GPR, only a few recent studies have reported GPR experiments, while other electromagnetic sensors and magnetometers have been used fewer times as systems on-board a UAV for archeological and Cultural Heritage applications [283].

In [284], several GPR aspects such as speed, cost, security, and ability to detect both metallic and dielectric targets were improved. In particular, the problem of generation of a high-resolution radar image by using Synthetic Aperture Radar (SAR) algorithms and the detection of small objects was discussed. In [285], the overall radar imaging system in terms of device hardware and data processing was described, and a measurement campaign demonstrated the ability to provide focused images in controlled conditions. Reference [286] demonstrated that an antenna with a central frequency of 80 MHz could have been effectively used to detect many relevant archeological features in the Roman forum of Cambodunum (Germany). Testing the efficiency of passive sensors on UAVs opens up new branches of research aimed at optimizing acquisition time compared to geophysical applications, and the resolution of the results in comparison to remote sensing outputs [283]. Accomando and Florio [287] implemented a magnetic vertical gradiometer UAV system in an archeological area of Metaponto (Southern Italy). To reduce the magnetic and electromagnetic noise caused by the aircraft, the magnetometer was suspended 3 m below the drone using ropes. This noise was then eliminated with a low-pass filter, and the resulting drone-borne vertical gradient data compared with ground-based magnetic measurements was collected in the same area and taken as a control dataset (Figure 36).

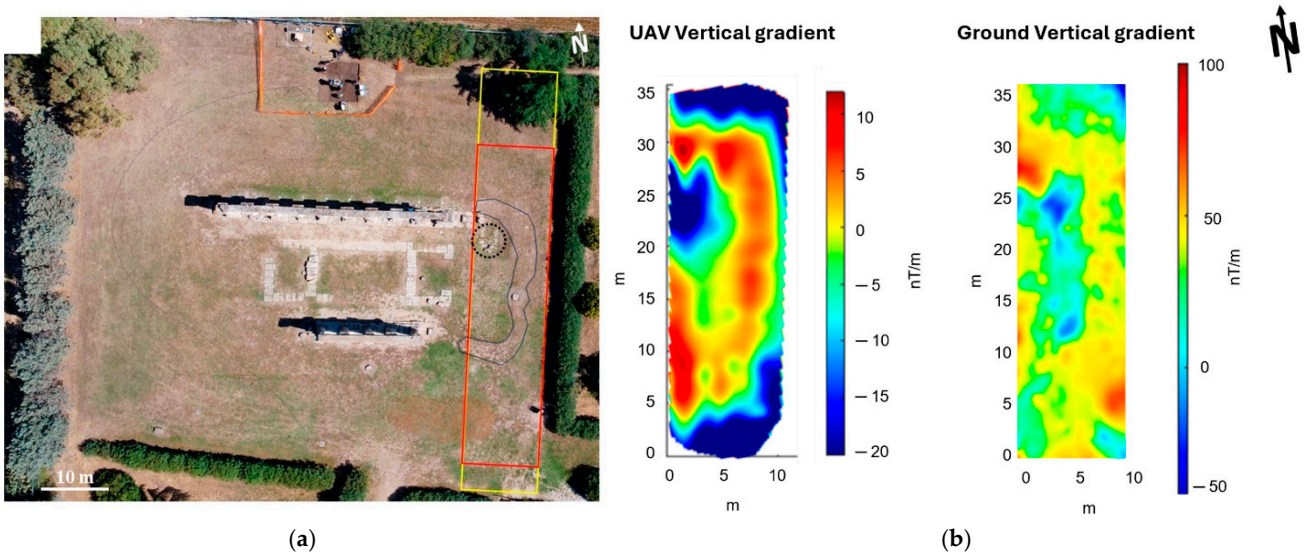


Figure 36. Archeological site of Metaponto (Italy). Aerial image of the Hera temple with the yellow and red box indicating, respectively, the areas covered by ground-based and UAV magnetic datasets. The dotted circle highlights an outcropping calcarenite structure forming a relic at the base of the eastern temple side. The blue line encloses an area corresponding to a subtle change in vegetation (**a**) and side-by-side comparison of the vertical gradient maps obtained from drone-borne (on the left) and ground-based (on the right) datasets (**b**) [287].

4. Discussion

At the meso-scale, the analyzed non-invasive imaging applications for heritage sites were primarily based on geophysical methods or other techniques/specializations often acting as support, and occasionally taking a primary role, which falls outside our overview.

The first mature application of geophysical methods to Cultural Heritage studies consists of the survey of archeological sites for inferring a probable distribution of buried archeological features in terms of tridimensional (typically, but not exclusively architectonic) bodies or even stratification of cultural layers, signs of anthropic uses and natural events that occurred at specific sites. A variety of contexts and diagnostic goals have been presented in Section 3.1 to exemplify the effectiveness of individual geophysical techniques in real-world case studies. It is important to emphasize that a single technical method

is rarely, if ever, the best choice for geophysical diagnostics in archeological prospection. Given the non-unique nature of the results from reconstruction problems, which are generally ill posed and implicitly probabilistic, synergistic and multi-method investigations are often the preferred experimental approach to obtain more robust technical information about the distribution of underground physical properties. It is also crucial to underline the significant role that researchers/practitioners play in all stages, from the design and meta-design of the diagnostic goals to the choice of the technological and methodological tools for the acquisition, processing, and interpretation steps. In a modern approach to the knowledge building process, this is possible thanks to multi- and cross-disciplinary cultural instruments, including methods and competencies from a wide variety of specializations involved in the discovery, characterization, and management of Cultural Heritage goods and sites.

Non-invasive and non-destructive applications of geophysical methods can be highly effective in studying CH meso-scale assets, as evidenced by the case studies shown in the sub-sections related to the investigation of monumental structures, submerged archeological sites, and the risk assessment and management of precious structures/sites. In such contexts, the examples proposed clearly highlight the flexibility and reliability of non-invasive techniques across many challenging study problems, provided they are (at least due to their novelty) appropriately designed and managed to construct crucial information for CH managers, decision-makers, and the preservation of institutions.

Among the successful strategies of utilizing multiple non-invasive methods to study meso-scale precious elements and sites, a recent trend involves integrating modern geomatics, geophysics, and robotics technologies to produce digital documentation with varying levels of integration, up to more or less detailed digital twins [288–292]. Since the Malta Convention [293], excavations have not been recommended, but the rapid development of non-invasive methods makes it possible to attempt to study/solve research problems about the past without interfering with strata systems. This concept is generally applicable to many contexts described in the text, including sites where a large excavation campaign could be too expensive or too slow for cultural exploitation, sites with multiple cultural layers where excavations imply the destruction or relocation of the shallowest ones, or sites with difficult accessibility, such as submerged sites or areas behind building elements of precious monuments. The joint historical/diagnostic documentation of delicate and valuable CH sites is now possible in relatively short terms through explorable and/or hypertextual virtual digital models [66,294–297].

It is useful to underline that the process of information building is an expression of the mutual interaction among various complementary and often overlapping disciplines and specializations. The present overview is primarily intended to document some potentialities that have emerged from the application of a subset of possible investigation techniques, as evidenced by the literature. This three-paper project is expected to contribute to the general debates related to the characterization of precious assets. Clear limitations in expecting a unique and objective answer from the acquisition of diagnostic data are implicit in their application. In fact, they are generally based on an iterative process of information building, effective only through a multi-/trans-disciplinary approach that considers probabilistic scenarios in all stages of processing and interpretation to constrain and lead to the most probable and best-fitting solution. This process is subject to the cultural profiles of the researchers involved and the natural evolution of the critical disciplinary debate.

Even if not primarily oriented to reconstruct a best-practice manual in the sense of a generalization of the presented investigation protocols, for which many text books exist and are suggested for a quick but rigorous introduction [2–4,298–301], the overview within Section 3 of case studies, both supported by images and not, can be a valuable contribution

to addressing many inhomogeneous but important issues faced by researchers studying meso-scale Cultural Heritage sites.

5. Conclusions

At the meso-scale, the analyzed prospecting applications for heritage sites were mostly based on geophysical methods, with other techniques and specializations mainly acting as support, though sometimes taking a primary role. The first type of targets investigated in the literature are archeological sites, both from the temporal and quantitative points of view. Archeological sites are not the original focus of applied geophysics, which initially targeted mineral exploration and later environmental fields, but they share many practical problems and solutions related to basic on-field activities and processing. The majority of the scientific and technical literature for the non-invasive and non-destructive investigation of Cultural Heritage at the intermediate scale focuses on the geophysical prospection of archeological sites, primarily aimed at discovering buried structures. Another important application, briefly introduced in this review for coherence, is the documentation of excavations or the preexisting surface and over-surface conditions, where geomatic techniques are predominant.

Other non-invasive investigations are gaining relevance in the study of Cultural Heritage sites. We have grouped them into a common section entitled "Other geophysical applications", which includes at least three classes based on our literature review: the study of monumental structures, the study of submerged archeological areas, and various aspects where non-invasive techniques are particularly effective in managing Cultural Heritage assets and sites exposed to natural and artificial risks. These applications of geophysical techniques began as niche areas and are now rapidly developing specific approaches and tools with notable innovation.

Finally, we have identified a third major group of non-invasive approaches to heritage sites, involving proximal sensing applications of geophysical or geomatic techniques. This section of the manuscript introduces supporting techniques for collecting surface information, as well as innovative installations of geophysical instruments on drones and balloons for studying underground archeological structures in difficult and inaccessible areas. These futuristic applications and the growing role of positioning and automation techniques in archeological prospections pave the way for precise and cost-effective investigations, where the expected industrialization of processes will allow for the quick, delicate, and cost-effective inspection of large, inaccessible, or delicate targets.

Compared to the first review, which was dedicated to the small scale (manufacts) [1], at the meso-scale, the study of sites has encouraged and driven research toward more efficient and cost-effective solutions, while specific topics of distinction and in-depth analyses remain present across the three groups of non-invasive and non-destructive applications that we have identified. This trend is likely to continue at the macro-scale (landscapes), the topic of the next review. For meso-scale applications, as with micro-scale applications, it is important to emphasize the probabilistic nature of most modern diagnostic approaches. In this context, convergence toward a probable or possible solution scenario is primarily achieved through joint protocols, involving the synthesis of contributions from different disciplines and methods.

Author Contributions: Conceptualization, L.P. and M.C.; writing—original draft preparation, L.P., N.A.Z., S.V.C., L.C., M.C., S.D. and D.T.; writing—review and editing, L.P., N.A.Z., S.V.C., P.C., L.C., I.C., M.C., S.D., R.L. and D.T.; supervision, L.P. All authors have read and agreed to the published version of the manuscript.

Funding: This research received no external funding.

Conflicts of Interest: N.A.Z. is employed by the TeamGeofisica.CEG geophysical data analysis company. The remaining authors declare that the research was conducted in the absence of any commercial or financial relationships that could be construed as a potential conflict of interest.

References

1. Piroddi, L.; Abu Zeid, N.; Calcina, S.V.; Capizzi, P.; Capozzoli, L.; Catapano, I.; Cozzolino, M.; D'Amico, S.; Lasaponara, R.; Tapete, D. Imaging Cultural Heritage at Different Scales: Part I, the Micro-Scale (Manufacts). *Remote Sens.* **2023**, *15*, 2586. [CrossRef]
2. Oswin, J. *A Field Guide to Geophysics in Archaeology*; Springer Science & Business Media: Berlin, Germany, 2009.
3. Witten, A. *Handbook of Geophysics and Archaeology*; Routledge: London, UK, 2017.
4. Schmidt, A. *Geophysical Data in Archaeology: A Guide to Good Practice*; Oxbow Books: Oxford, UK, 2013. [CrossRef]
5. Piro, S.; Goodman, D.; Nishimura, Y. The study and characterization of Emperor Traiano's Villa (Altopiani di Arcinazzo, Roma) using high-resolution integrated geophysical surveys. *Archaeol. Prospect.* **2003**, *10*, 1–25. [CrossRef]
6. Piro, S.; Campana, S. GPR investigation in different archaeological sites in Tuscany (Italy). Analysis and comparison of the obtained results. *Near Surf. Geophys.* **2012**, *10*, 47–56. [CrossRef]
7. Cozzolino, M.; Gentile, V.; Giordano, C.; Mauriello, P. Imaging Buried Archaeological Features through Ground Penetrating Radar: The Case of the Ancient Saepinum (Campobasso, Italy). *Geosciences* **2020**, *10*, 225. [CrossRef]
8. Cozzolino, M.; Baković, M.; Borovinić, N.; Galli, G.; Gentile, V.; Jabučanin, M.; Mauriello, P.; Merola, P.; Živanović, M. The Contribution of Geophysics to the Knowledge of the Hidden Archaeological Heritage of Montenegro. *Geosciences* **2020**, *10*, 187. [CrossRef]
9. Coolen, J.; Wallner, M.; Trausmuth, T.; König, A. New Insights into a Romanesque Basilica Church in the Deserted Town of Corvey, Germany, Based on a High-Resolution GPR Survey. *ArcheoSciences* **2021**, *45*, 35–38. [CrossRef]
10. Leucci, G.; Di Giacomo, G.; Ditaranto, I.; Miccoli, I.; Scardozzi, G. Integrated Ground-penetrating Radar and Archaeological Surveys in the Ancient City of Hierapolis of Phrygia (Turkey). *Archaeol. Prospect.* **2013**, *20*, 285–301. [CrossRef]
11. Urban, T.M.; Murray, C.A.; Vella, C.; Lahikainen, A. Ground-penetrating radar survey on the island of Pantelleria (Italy) reveals an ancient architectural complex with likely Punic and Roman components. *J. Appl. Geophys.* **2015**, *123*, 164–169. [CrossRef]
12. Florit, C.M.; Ontiveros, M.Á.C.; Goossens, L.; Meyer, C.; Sala, R.; Ortiz, H. Geophysical survey of two rural sites in Mallorca (Balearic Islands, Spain): Unveiling Roman villae. *J. Appl. Geophys.* **2018**, *150*, 101–117. [CrossRef]
13. Porcelli, F.; Sambuelli, L.; Comina, C.; Spanò, A.; Lingua, A.; Calantropio, A.; Catanzariti, G.; Chiabrando, F.; Fischanger, F.; Maschio, P.; et al. Integrated Geophysics and Geomatics Surveys in the Valley of the Kings. *Sensors* **2020**, *20*, 1552. [CrossRef] [PubMed]
14. Rundkvist, M.; Viberg, A. Geophysical investigations on the Viking period platform mound at Aska in Hagebyhöga parish, Sweden. *Archaeol. Prospect.* **2015**, *22*, 131–138. [CrossRef]
15. Booth, A.D.; Szpakowska, K.; Pischikova, E.; Griffin, K. Structure of an ancient Egyptian tomb inferred from ground-penetrating radar imaging of deflected overburden horizons. *Archaeol. Prospect.* **2015**, *22*, 33–44. [CrossRef]
16. Leucci, G.; De Giorgi, L.; Di Giacomo, G.; Ditaranto, I.; Miccoli, I.; Scardozzi, G. 3D GPR survey for the archaeological characterization of the ancient Messapian necropolis in Lecce, South Italy. *J. Archaeol. Sci. Rep.* **2016**, *7*, 290–302. [CrossRef]
17. Piro, S.; Haynes, I.; Liverani, P.; Zamuner, D. GPR investigation to map the subsoil of the St. John Lateran Basilica (Rome, Italy). *Boll. Geofis. Teor. Appl.* **2017**, *58*, 431–444.
18. Masini, N.; Leucci, G.; Vera, D.; Sileo, M.; Pecci, A.; Garcia, S.; López, R.; Holguín, H.; Lasaponara, R. Towards Urban Archaeo-Geophysics in Peru. The Case Study of Plaza de Armas in Cusco. *Sensors* **2020**, *20*, 2869. [CrossRef] [PubMed]
19. Capozzoli, L.; Catapano, I.; De Martino, G.; Gennarelli, G.; Ludeno, G.; Rizzo, E.; Soldovieri, F.; Uliano Scelza, F.; Zuchtriegel, G. The Discovery of a Buried Temple in Paestum: The Advantages of the Geophysical Multi-Sensor Application. *Remote Sens.* **2020**, *12*, 2711. [CrossRef]
20. Zhao, W.; Forte, E.; Fontana, F.; Pipan, M.; Tian, G. GPR imaging and characterization of ancient Roman ruins in the Aquileia Archaeological Park, NE Italy. *Measurement* **2018**, *113*, 161–171. [CrossRef]
21. Colombero, C.; Comina, C.; Rocchietti, D.; Garbarino, G.B.; Sambuelli, L. Ground penetrating radar surveys in the archaeological area of Augusta Bagiennorum: Comparisons between geophysical and archaeological campaigns. *Archaeol. Prospect.* **2021**, *29*, 451–464. [CrossRef]
22. Schmidt, A. Electrical and magnetic methods in archaeological prospection. In *Seeing the Unseen. Geophysics and Landscape Archaeology*; Campana, S., Piro, S., Eds.; Taylor & Francis Group: London, UK, 2009; pp. 67–81.
23. Gaffney, V.; Neubauer, W.; Garwood, P.; Gaffney, C.; Löcker, K.; Bates, R.; De Smedt, P.; Baldwin, E.; Chapman, H.; Hinterleitner, A.; et al. Durrington walls and the Stonehenge Hidden Landscape Project 2010–2016. *Archaeol. Prospect.* **2018**, *25*, 255–269. [CrossRef]
24. Boschi, F. Magnetic Prospecting for the Archaeology of Classe, Archaeological Prospection. *Archaeol. Prospect.* **2012**, *19*, 219–227. [CrossRef]

25. Bárta, J.; Belov, T.; Frolík, J.; Jirků, J. Applications of Geophysical Surveys for Archaeological Studies in Urban and Rural Areas in Czech Republic and Armenia. *Geosciences* **2020**, *10*, 356. [CrossRef]
26. Caldara, M.; Ciminale, M.; De Santis, V.; Noviello, M. A Multidisciplinary Approach to Reveal and Interpret 'Missing' Archaeological Features at the Masseria Pantano Site in Apulia. *Archaeol. Prospect.* **2014**, *21*, 301–309. [CrossRef]
27. Urban, T.M.; Rasic, J.T.; Alix, C.; Anderson, D.D.; Chisholm, L.; Jacob, R.W.; Manning, S.W.; Mason, O.K.; Tremayne, A.H.; Vinson, D. Magnetic detection of archaeological hearths in Alaska: A tool for investigating the full span of human presence at the gateway to North America. *Quat. Sci. Rev.* **2019**, *211*, 73–92. [CrossRef]
28. Fitton, T.; Contreras, D.A.; Gidna, A.O.; Mabulla, A.Z.; Prendergast, M.E.; Grillo, K.M. Detecting and mapping the 'ephemeral': Magnetometric survey of a Pastoral Neolithic settlement at Luxmanda, Tanzania. *Antiquity* **2022**, *96*, 298–318. [CrossRef]
29. Lasaponara, R.; Masini, N.; Rizzo, E.; Orefici, G. New discoveries in the Piramide Naranjada in Cahuachi (Peru) using satellite, Ground Probing Radar and magnetic investigations. *J. Archaeol. Sci.* **2011**, *38*, 2031–2039. [CrossRef]
30. Shi, Z.; Tian, G.; Hobbs, R.W.; Wo, H.; Lin, J.; Wu, L.; Liu, H. Magnetic gradient and ground penetrating radar prospecting of buried earthen archaeological remains at the Qocho City site in Turpan, China. *Near Surf. Geophys.* **2015**, *13*, 477–485. [CrossRef]
31. Linford, N.; Linford, P.; Martin, L.; Payne, A. Recent Results from the English Heritage Caesium Magnetometer Systemin Comparison with Recent Fluxgate Gradiometers. *Archaeol. Prospect.* **2007**, *14*, 151–166. [CrossRef]
32. Mathé, V.; Leveque, F.; Mathé, P.-E.; Chevallier, C.; Pons, Y. Soil anomaly mapping using a caesium magnetometer: Limits in the low magnetic amplitude case. *J. Appl. Geophys.* **2006**, *58*, 202–217. [CrossRef]
33. Herwanger, J.; Maurer, H.; Green, A.J.; Leckebusch, J. 3-D inversions of magnetic gradiometer data in archaeological prospecting: Possibilities and limitations. *Geophysics* **2020**, *65*, 3–849.
34. Argote, D.L.; Tejero, A.; Chavez, R.E.; Lopez, P.A.; Bravo, R. 3D modelling of magnetic data from an archaeological site in north-western Tlaxcala state, Mexico. *J. Archaeol. Sci.* **2009**, *36*, 1661–1671. [CrossRef]
35. Cella, F.; Fedi, M. High-resolution geophysical 3D imaging for archaeology by magnetic and EM data: The case of the iron age settlement of Torre Galli, Southern Italy. *Surv. Geophys.* **2015**, *36*, 831–850. [CrossRef]
36. Tsokas, G.N.; Giannopoulos, A.; Tsourlos, P.; Vargemezis, G.; Tealby, J.M.; Sarris, A.; Papazachos, C.B.; Savopoulou, T. A large scale geophysical survey in the archaeological site of Europos. *J. Appl. Geophys.* **1994**, *32*, 85–98. [CrossRef]
37. Hargrave, M.L.; Somers, L.E.; Larson, T.K.; Shields, R.; Dendy, J. The Role of Resistivity Survey in Historic Site Assessment and Management: An Example from Fort Riley, Kansas. *Hist. Archaeol.* **2002**, *36*, 89–110. [CrossRef]
38. Gaffney, C.; Goodchild, H.; Harrison, S. *Geophysical and Topographical Survey of the Theatre at Ancient Sparta*; Birmingham Archaeology Report, PN 1643; Birmingham Archaeology: Birmingham, UK, 2007.
39. Cozzolino, M.; Caliò, L.M.; Gentile, V.; Mauriello, P.; Di Meo, A. The Discovery of the Theater of Akragas (Valley of Temples, Agrigento, Italy): An Archaeological Confirmation of the Supposed Buried Structures from a Geophysical Survey. *Geosciences* **2020**, *10*, 161. [CrossRef]
40. Cozzolino, M.; Di Giovanni, E.; Mauriello, P.; Vanni Desideri, A.; Patella, D. Resistivity tomography in the park of Pratolino at Vaglia (Florence, Italy). *Archaeol. Prospect.* **2012**, *19*, 253–260. [CrossRef]
41. Cozzolino, M.; Di Giovanni, E.; Mauriello, P.; Piro, S.; Zamuner, D. *Geophysical Methods for Cultural Heritage Management*; Springer: Cham, Switzerland, 2018; p. 211.
42. Mauriello, P.; Patella, D. A data-adaptive probability-based fast ERT inversion method. *Prog. Electromagn. Res.* **2009**, *97*, 275–290. [CrossRef]
43. Masini, N.; Capozzoli, L.; Chen, P.; Chen, F.; Romano, G.; Lu, P.; Tang, P.; Sileo, M.; Ge, Q.; Lasaponara, R. Towards an Operational Use of Geophysics for Archaeology in Henan (China): Methodological Approach and Results in Kaifeng. *Remote Sens.* **2017**, *9*, 809. [CrossRef]
44. Vött, A.; Willershäuser, T.; Hadler, H.; Obrocki, L.; Fischer, P.; Heinzelmann, M. Geoarchaeological evidence of Ostia's river harbour operating until the fourth century AD. *Archaeol. Anthropol. Sci.* **2020**, *12*, 88. [CrossRef]
45. AL-Hameedawi, M.M.; Thabit, J.M.; AL-Menshed, F.H. Electrical resistivity tomography and ground-penetrating radar methods to detect archaeological walls of Babylonian houses near Ishtar temple, ancient Babylon city, Iraq. *Geophys. Prospect.* **2022**, *71*, 1792–1806. [CrossRef]
46. Leucci, G.; Greco, F. 3D ERT Survey to Reconstruct Archaeological Features in the Subsoil of the "Spirito Santo" Church Ruins at the Site of Occhiolà (Sicily, Italy). *Archaeology* **2012**, *1*, 1–6.
47. Orlando, L. GPR to constrain ERT data inversion in cavity searching: Theoretical and practical applications in archaeology. *J. Appl. Geophys.* **2013**, *89*, 35–47. [CrossRef]
48. Compare, V.; Cozzolino, M.; Mauriello, P.; Patella, D. Resistivity probability tomography at the Castle of Zena (Italy). *Eurasip. J. Image Video* **2009**, *2009*, 693274. [CrossRef]
49. Tsourlos, P.; Papadopoulos, N.; Yi, M.J.; Kim, J.H.; Tsokas, G. Comparison of measuring strategies for the 3-D electrical resistivity imaging of tumuli. *J. Appl. Geophys.* **2014**, *101*, 77–85. [CrossRef]

50. Yi, M.J.; Kim, J.H.; Song, Y.; Cho, S.J.; Chung, S.H.; Suh, J.H. Three-dimensional imaging of subsurface structures using resistivity data. *Geophys. Prospect.* **2001**, *49*, 483–497. [CrossRef]
51. Papadopoulos, N.G.; Yi, M.J.; Kim, J.H.; Tsourlos, P.; Tsokas, G.N. Geophysical investigation of tumuli by means of surface 3D Electrical Resistivity Tomography. *J. Appl. Geophys.* **2010**, *70*, 192–205. [CrossRef]
52. Cozzolino, M.; Mauriello, P.; Patella, D. The Extended data-adaptive Probability-based Electrical Resistivity Tomography Inversion Method (E-PERTI) for the characterization of the buried ditch of the ancient Egnazia (Puglia, Italy). *Appl. Sci.* **2022**, *12*, 2690. [CrossRef]
53. Elwaseif, M.; Slater, L. Quantifying tomb geometries in resistivity images using watershed algorithms. *J. Archaeol. Sci.* **2010**, *37*, 1424–1436. [CrossRef]
54. Arato, A.; Piro, S.; Sambuelli, L. 3D inversion of ERT data on an archaeological site using GPR reflection and 3D inverted magnetic data as a priori information. *Near Surf. Geophys.* **2015**, *13*, 545–556. [CrossRef]
55. Akca, İ.; Balkaya, Ç.; Pülz, A.; Alanyalı, H.S.; Kaya, M.A. Integrated geophysical investigations to reconstruct the archaeological features in the episcopal district of Side (Antalya, Southern Turkey). *J. Appl. Geophys.* **2019**, *163*, 22–30. [CrossRef]
56. Al-Saadi, O.S.; Schmidt, V.; Becken, M.; Fritsch, T. Very-high-resolution electrical resistivity imaging of buried foundations of a Roman villa near Nonnweiler, Germany. *Archaeol. Prospect.* **2018**, *25*, 209–218. [CrossRef]
57. Ullrich, B.; Günther, T.; Rücker, C. Electrical resistivity tomography methods for archaeological prospection. Conference: Layers of perception. In Proceedings of the 35th International Conference on Computer Applications and Quantitative Methods in Archaeology (CAA), Berlin, Germany, 2–6 April 2007.
58. Fischanger, F.; Catanzariti, G.; Comina, C.; Sambuelli, L.; Morelli, G.; Barsuglia, F.; Ellaithy, A.; Porcelli, F. Geophysical anomalies detected by electrical resistivity tomography in the area surrounding Tutankhamun's tomb. *J. Cult. Herit.* **2019**, *36*, 63–71. [CrossRef]
59. Pazzi, V.; Ceccatelli, M.; Ciani, L.; Patrizi, G.; Guidi, G.; Cappuccini, L.; Casagli, N.; Catelani, M. Analysis of the Influence of the GPS Errors Occurred While Collecting Electrode Coordinates on the Electrical Resistivity of Tumuli. *Sensors* **2020**, *20*, 2966. [CrossRef]
60. Tsokas, G.N.; Tsourlos, P.I.; Kim, J.H.; Papazachos, C.B.; Vargemezis, G.; Bogiatzis, P. Assessing the Condition of the Rock Mass over the Tunnel of Eupalinus in Samos (Greece) using both Conventional Geophysical Methods and Surface to Tunnel Electrical Resistivity Tomography. *Archaeol. Prospect.* **2014**, *21*, 277–291. [CrossRef]
61. Bellanova, J.; Calamita, G.; Catapano, I.; Ciucci, A.; Cornacchia, C.; Gennarelli, G.; Giocoli, A.; Fisangher, F.; Ludeno, G.; Morelli, G.; et al. GPR and ERT Investigations in Urban Areas: The Case-Study of Matera (Southern Italy). *Remote Sens.* **2020**, *12*, 1879. [CrossRef]
62. Rizzo, E.; Capozzoli, L.; De Martino, G.; Grimaldi, S. Urban geophysical approach to characterize the subsoil of the main square in San Benedetto del Tronto town (Italy). *Eng. Geol.* **2019**, *257*, 105133. [CrossRef]
63. Cozzolino, M.; Gentile, V.; Mauriello, P.; Peditrou, A. Non-Destructive Techniques for Building Evaluation in Urban Areas: The Case Study of the Redesigning Project of Eleftheria Square (Nicosia, Cyprus). *Appl. Sci.* **2020**, *10*, 4296. [CrossRef]
64. Capozzoli, L.; Fornasari, G.; Giampaolo, V.; De Martino, G.; Rizzo, E. Multi-Sensors Geophysical Monitoring for Reinforced Concrete Engineering Structures: A Laboratory Test. *Sensors* **2021**, *21*, 5565. [CrossRef]
65. Klanica, R.; Grison, H.; Šteffl, J.; Beránek, R. Assessing the Volume of Defensive Structures for Architectural Energetics Analysis Using 3D Electrical Resistivity Tomography. *Remote Sens.* **2022**, *14*, 2652. [CrossRef]
66. Zeid, N.A.; Bignardi, S.; Russo, P.; Peresani, M. Deep in a Paleolithic archive: Integrated geophysical investigations and laser-scanner reconstruction at Fumane Cave, Italy. *J. Archaeol. Sci. Rep.* **2019**, *27*, 101976.
67. Torrese, P.; Zucca, F.; Martini, S.; Benazzi, S.; Drohobytsky, D.; Gravel-Miguel, C.; Hodgkins, J.; Meyer, D.; Miller, C.; Peresani, M.; et al. NegrinoGround truth validated 3D electrical resistivity imaging of the archaeological deposits at Arma Veirana cave (northern Italy). *J. Quat. Sci.* **2022**, *37*, 1112–1132. [CrossRef]
68. Frfhlich Gugler, I.M.; Gex, P. Electromagnetic survey of a Celtic tumulus. *J. Appl. Geophys.* **1996**, *35*, 15–25. [CrossRef]
69. Conyers, L.B.; Ernenwein, E.G.; Grealy, M.; Lowe, K.M. Electromagnetic Conductivity Mapping for Site Prediction in Meandering River Floodplains. *Archaeol. Prospect.* **2008**, *15*, 81–91. [CrossRef]
70. Simpson, D.; Lehouck, A.; Van Meirvenne, M.; Bourgeois, J.; Thoen, E.; Vervloet, J. Geoarchaeological prospection of a medieval manor in the Dutch Polders using an electromagnetic induction sensor in combination with soil augerings. *Geoarchaeology* **2008**, *23*, 305–319. [CrossRef]
71. Simpson, D.; Lehouck, A.; Verdonck, L.; Vermeersch, H.; Van Meirvenne, M.; Bourgeois, J.; Thoen, E.; Docter, R. Comparison between electromagnetic induction and fluxgate gradiometer measurements on the buried remains of a 17th century castle. *J. Appl. Geophys.* **2009**, *68*, 294–300. [CrossRef]
72. De Smedt, P.; Saey, T.; Lehouck, A.; Stichelbaut, B.; Meerschman, E.; Islam, M.M.; Van De Vijver, E.; Van Meirvenne, M. Exploring the potential of multi-receiver EMI survey for geoarchaeological prospection: A 90 ha dataset. *Geoderma* **2013**, *199*, 30–36. [CrossRef]

73. Di Maio, R.; La Manna, M.; Piegari, E.; Mancini, C.; Achilli, V.; Fabris, M. Multi-methodological Geophysical Exploration for the Interpretation of the Ancient Landscape of Phaistos (Greece). *Archaeol. Prospect.* **2016**, *23*, 287–299. [CrossRef]
74. Tang, P.; Chen, F.; Jiang, A.; Zhou, W.; Wang, H.; Leucci, G.; Sileo, M.; Luo, R.; Lasaponara, R.; Masini, N. Multi-frequency electromagnetic induction survey for archaeological prospection: Approach and results in Han Hangu Pass and Xishan Yang in China. *Surv. Geophys.* **2018**, *39*, 1285–1302. [CrossRef]
75. Deiana, R.; Vicenzutto, D.; Deidda, G.P.; Boaga, J.; Cupitò, M. Remote Sensing, Archaeological, and Geophysical Data to Study the Terramare Settlements: The Case Study of Fondo Paviani (Northern Italy). *Remote Sens.* **2020**, *12*, 2617. [CrossRef]
76. Deiana, R.; Deidda, G.P.; Cusí, E.D.; van Dommelen, P.; Stiglitz, A. FDEM and ERT measurements for archaeological prospections at Nuraghe S'Urachi (West-Central Sardinia). *Archaeol. Prospect.* **2022**, *29*, 69–86. [CrossRef]
77. Tabbagh, A.; Dabas, M. Absolute magnetic viscosity determination using time-domain electromagnetic devices. *Archaeol. Prospect.* **1996**, *3*, 199–208. [CrossRef]
78. Ranieri, G.; Deiana, R.; Deidda, G.P.; Haile, T.; Erriu, S.; Nuvoli, M. Tem-fast shallow soundings for archaeological investigations. In Proceedings of the 9th EAGE/EEGS Meeting, Prague, Czech Republic, 31 August–4 September 2003; European Association of Geoscientists & Engineers: Bunnik, The Netherlands, 2003; p. 52.
79. Ranieri, G.; Calcina, S.V.; Piroddi, L. Preventive geo-physical surveys for the evaluation of the archaeological risk: Examples from the region of the ancient Pylos (western Peloponnese, Greece). In Proceedings of the 21st International Conference on Computational Science and Its Applications (ICCSA), Cagliari, Italy, 13–16 September 2021; IEEE: New York, NY, USA, 2021; pp. 242–250.
80. Trogu, A.; Ranieri, G.; Calcina, S.; Piroddi, L. The ancient Roman aqueduct of Karales (Cagliari, Sardinia, Italy): Applicability of geophysics methods to finding the underground remains. *Archaeol. Prospect.* **2014**, *21*, 157–168. [CrossRef]
81. Drahor, M.G. Integrated geophysical studies in the upper part of Sardis archaeological site, Turkey. *J. Appl. Geophys.* **2006**, *59*, 205–223. [CrossRef]
82. Bayrak, M.; Gürer, A.; Gürer, Ö.F.; İlkışık, O.M. Delineation of the Acemhöyük settlement mound in Turkey using 2-D and pseudo-3-D VLF imaging. *Arab. J. Geosci.* **2021**, *14*, 1–15. [CrossRef]
83. Karastathis, V.K.; Papamarinopoulos, S.P. The detection of King Xerxes' Canal by the use of shallow reflection and refraction seismics—Preliminary results. *Geophys. Prospect.* **1997**, *45*, 389–401. [CrossRef]
84. Deidda, G.P.; Balia, R. An ultrashallow SH-wave seismic reflection experiment on a subsurface ground model. *Geophysics* **2001**, *66*, 1097–1104. [CrossRef]
85. Balia, R. Shallow reflection survey in the Selinunte National Archaeological Park (Sicily, Italy). *Boll. Geofis. Teor. Appl.* **1992**, *34*, 121–131.
86. Karastathis, V.K.; Papamarinopoulos, S.; Jones, R.E. 2-D velocity structure of the buried ancient canal of Xerxes: An application of seismic methods in archaeology. *J. Appl. Geophys.* **2001**, *47*, 29–43. [CrossRef]
87. Nogoshi, M.; Igarashi, T. On the propagation characteristics of microtremors. *J. Seism. Soc. Jpn.* **1970**, *23*, 264–280.
88. Nakamura, Y. A method for dynamic characteristics estimation of subsurface using microtremor on the ground surface. *Railw. Tech. Res. Inst. Q. Rep.* **1989**, *30*, 25–33.
89. Gutenberg, B. Two types of microseisms. *J. Geophys. Res.* **1958**, *63*, 595–597. [CrossRef]
90. Asten, M.W. Geological control on the three-component spectra of Rayleigh-wave microseisms. *Bull. Seismol. Soc. Am.* **1978**, *68*, 1623–1636.
91. Asten, M.W.; Henstridge, J.D. Array estimators and the use of microseisms for reconnaissance of sedimentary basins. *Geophysics* **1984**, *49*, 1828–1837. [CrossRef]
92. Castellaro, S.; Imposa, S.; Barone, F.; Chiavetta, F.; Gresta, S.; Mulargia, F. Georadar and passive seismic survey in the Roman Amphitheatre of Catania (Sicily). *J. Cult. Herit.* **2008**, *9*, 357–366. [CrossRef]
93. Bottari, C.; Urbini, S.; Bianca, M.; D'Amico, M.; Marchetti, M.; Pizzolo, F. Buried archaeological remains connected to the Greek-Roman harbor at Tindari (north-east Sicily): Results from geomorphological and geophysical investigations. *Ann. Geophys.* **2012**, *55*, 223–234. [CrossRef]
94. Wilken, D.; Wunderlich, T.; Majchczack, B.; Andersen, J.; Rabbel, W. Rayleigh-wave resonance analysis: A methodological test on a Viking age pit house. *J. Cult. Herit.* **2015**, *9*, 357–366. [CrossRef]
95. Abu Zeid, N.; Corradini, E.; Bignardi, S.; Morandi, N.; Nizzo, V. The passive seismic technique "HVSR" as a reconnaissance tool for mapping paleo-soils: The case of the Pilastri archaeological site, Northern Italy. *Archaeol. Prospect.* **2017**, *24*, 245–258. [CrossRef]
96. Tsokas, G.N.; Papazachos, C.B.; Vafidis, A.; Loukoyiannakis, M.Z.; Vargemezis, G.; Tzimeas, K. The detection of monumental tombs buried in tumuli by seismic re-fraction. *Geophysics* **1995**, *60*, 1735–1742. [CrossRef]
97. Ranieri, G. The Application of Geophysical methods to resolve a fascinating archaeological query. In Proceedings of the 5th EEGS-ES Meeting, Cape Town, South Africa, 28 September–1 October 1999; European Association of Geoscientists & Engineers: Bunnik, The Netherlands, 1999; p. 35.

98. Forte, E.; Pipan, M. Integrated seismic tomography and ground-penetrating radar (GPR) for the high-resolution study of burial mounds (tumuli). *J. Archaeol. Sci.* **2008**, *35*, 2614–2623. [CrossRef]
99. Polymenakos, L.; Tweeton, D. Reevaluating a seismic traveltime tomography survey at Kastas tumulus (Amphipolis, Greece). *J. Archaeol. Sci. Rep.* **2015**, *4*, 434–446. [CrossRef]
100. Polymenakos, L.; Tweeton, D. Non-invasive characterization of a burial tumulus with use of seismic P-wave velocity and attenuation tomography. *J. Archaeol. Sci. Rep.* **2017**, *13*, 36–48. [CrossRef]
101. Gołębiowski, T.; Pasierb, B.; Porzucek, S.; Łój, M. Complex prospection of medieval underground salt chambers in the village of Wiślica, Poland. *Archaeol. Prospect.* **2018**, *25*, 243–254. [CrossRef]
102. Rabbel, W.; Erkul, E.; Stümpel, H.; Wunderlich, T.; Pašteka, R.; Papco, J.; Niewöhner, P.; Bariş, Ş.; Çakin, O.; Pekşen, E. Discovery of a Byzantine Church in Iznik/Nicaea, Turkey: An educational case history of geophysical prospecting with combined methods in urban areas. *Archaeol. Prospect.* **2015**, *22*, 1–20. [CrossRef]
103. Moussa, M. Gamma-ray spectrometry: A new tool for exploring archaeological sites; a case study from East Sinai, Egypt. *J. Appl. Geophys.* **2001**, *48*, 137–142. [CrossRef]
104. Robinson, V. Atomic archaeology? Using portable gamma surveying techniques to identify buried archaeological. *Spectrosc. Eur.* **2022**, *34*, 20–23. [CrossRef]
105. Robinson, V.; Clark, R.; Black, S.; Fry, R.; Beddow, H. Portable gamma ray spectrometry for archaeological prospection: A preliminary investigation at Silchester Roman Town. *Archaeol. Prospect.* **2022**, *29*, 353–367. [CrossRef]
106. Beni, T.; Borselli, D.; Bonechi, L.; Lombardi, L.; Gonzi, S.; Melelli, L.; Turchetti, M.A.; Fanò, L.; D'Alessandro, R.; Gigli, G.; et al. Laser scanner and UAV digital photogrammetry as support tools for cosmic-ray muon radiography applications: An archaeological case study from Italy. *Sci. Rep.* **2023**, *13*, 19983. [CrossRef] [PubMed]
107. Saracino, G.; Ambrosino, F.; Bonechi, L.; Cimmino, L.; D'Alessandro, R.; D'Errico, M.; Noli, P.; Scognamiglio, L.; Strolin, P. Applications of muon absorption radiography to the fields of archaeology and civil engineering. *Philos. Trans. R. Soc. A Math. Phys. Eng. Sci.* **2019**, *377*, 20180057. [CrossRef] [PubMed]
108. Tsourlos, P.I.; Tsokas, G.N. Non-destructive electrical resistivity tomography survey at the south walls of the Acropolis of Athens. *Archaeol. Prospect.* **2011**, *18*, 173–186. [CrossRef]
109. Angelis, D.; Tsourlos, P.; Tsokas, G.; Vargemezis, G.; Zacharopoulou, G.; Power, C. Combined application of GPR and ERT for the assessment of a wall structure at the Heptapyrgion fortress (Thessaloniki, Greece). *J. Appl. Geophys.* **2018**, *152*, 208–220. [CrossRef]
110. Balia, R.; Pirinu, A. Geophysical surveying of the ancient walls of the town of Cagliari, Italy, by means of refraction and up-hole seismic tomography techniques. *Archaeol. Prospect.* **2018**, *25*, 147–153. [CrossRef]
111. Pirinu, A.; Balia, R.; Piroddi, L.; Trogu, A.; Utzeri, M.; Vignoli, G. Deepening the knowledge of military architecture in an urban context through digital representations integrated with geophysical surveys. The city walls of Cagliari (Italy). In Proceedings of the Metrology for Archaeology and Cultural Heritage (MetroArchaeo), Cassino, Italy, 22–24 October 2018; IEEE: New York, NY, USA, 2018; pp. 211–215.
112. Pérez-Gracia, V.; Caselles, J.O.; Clapes, J.; Osorio, R.; Martínez, G.; Canas, J.A. Integrated near-surface geophysical survey of the Cathedral of Mallorca. *J. Archaeol. Sci.* **2009**, *36*, 1289–1299. [CrossRef]
113. Casas, A.; Cosentino, P.L.; Fiandaca, G.; Himi, M.; Macias, J.M.; Martorana, R.; Muñoz, A.; Rivero, L.; Sala, R. Non-invasive Geophysical Surveys in Search of the Roman Temple of Augustus Under the Cathedral of Tarragona (Catalonia, Spain): A Case Study. *Surv. Geophys.* **2018**, *39*, 1107–1124. [CrossRef]
114. Fiandaca, G.; Martorana, R.; Messina, P.; Cosentino, P.L. The MYG methodology to carry out 3D electrical resistivity tomography on media covered by vulnerable surfaces of artistic value. *Il Nuovo Cimento B* **2010**, *125*, 711–718.
115. Cosentino, P.; Capizzi, P.; Fiandaca, G.; Martorana, R.; Messina, P. Advances in microgeophysics for engineering and cultural heritage. *J. Earth Sci.* **2009**, *20*, 626–639. [CrossRef]
116. Yilmaz, O. Geophysical investigations of historic buildings—A case study of the Great Church of St. Sophia. *Lead. Edge* **2013**, *32*, 292–296. [CrossRef]
117. Yilmaz, O. Geophysical Investigations of Historic Buildings. In *Engineering Seismology with Applications to Geotechnical Engineering*; Yilmaz, Ö., Ed.; Society of Exploration Geo-Physicists: Tulsa, OK, USA, 2013.
118. Piroddi, L.; Rassu, M. Application of GPR Prospection to Unveil Historical Stratification inside Monumental Buildings: The Case of San Leonardo de Siete Fuentes in Santu Lussurgiu, Sardinia, Italy. *Land* **2023**, *12*, 590. [CrossRef]
119. Orlando, L.; De Donno, G.; Di Giambattista, L.; Palladini, L. Investigating the Foundation of the Amphiteatrum Flavium through the Passage of Commodus. *Ann. Geophys.* **2017**, *60*, 0437. [CrossRef]
120. Argote-Espino, D.; Tejero-Andrade, A.; Cifuentes-Nava, G.; Iriarte, L.; Farías, S.; Chávez, R.E.; López, F. 3D electrical prospection in the archaeological site of El Pahñú, Hidalgo State, Central Mexico. *J. Archaeol. Sci.* **2013**, *40*, 1213–1223. [CrossRef]
121. Chávez, R.E.; Tejero-Andrade, A.; Cifuentes, G.; Argote-Espino, D.L.; Hernández-Quintero, E. Karst detection beneath the pyramid of El Castillo, Chichen Itza, Mexico, by non-invasive ERT-3D methods. *Sci. Rep.* **2018**, *8*, 15391. [CrossRef]

122. Pazzi, V.; Tapete, D.; Cappuccini, L.; Fanti, R. An electric and electromagnetic geophysical approach for subsurface investigation of anthropogenic mounds in an urban environment. *Geomorphology* **2016**, *273*, 335–347. [CrossRef]
123. Pašteka, R.; Pánisová, J.; Zahorec, P.; Papčo, J.; Mrlina, J.; Fraštia, M.; Vargemezis, G.; Kušnirák, D.; Zvara, I. Microgravity method in archaeological prospection: Methodical comments on selected case studies from crypt and tomb detection. *Archaeol. Prospect.* **2020**, *27*, 415–431. [CrossRef]
124. Padín, J.; Martín, A.; Anquela, A.B. Archaeological microgravimetric prospection inside don church (Valencia, Spain). *J. Archaeol. Sci.* **2012**, *39*, 547–554. [CrossRef]
125. Fais, S.; Radogna, P.V.; Romoli, E.; Matta, P.; Klingele, E.E. Microgravity for detecting cavities in an archaeological site in Sardinia (Italy). *Near Surf. Geophys.* **2015**, *13*, 495–504. [CrossRef]
126. Alvarez, L.W.; Anderson, J.A.; Bedwei, F.E.; Burkhard, J.; Fakhry, A.; Girgis, A.; Goneid, A.; Hassan, F.; Iverson, D.; Lynch, G.; et al. Search for Hidden Chambers in the Pyramids: The structure of the Second Pyramid of Giza is determined by cosmic-ray absorption. *Science* **1970**, *167*, 832–839. [CrossRef] [PubMed]
127. Gòmez, H.; Carloganu, C.; Gibert, D.; Marteau, J.; Niess, V.; Katsanevas, S.; Tonazzo, A. Feasibility study of archaeological structures scanning by muon tomography. In *AIP Conference Proceedings*; AIP Publishing LLC.: Melville, NY, USA, 2015; Volume 1672.
128. Gomez, H.; Carloganu, C.; Gibert, D.; Jacquemier, J.; Karyotakis, Y.; Marteau, J.; Niess, V.; Katsanevas, S.; Tonazzo, A. Studies on muon tomography for archaeological internal structures scanning. *J. Phys. Conf. Ser.* **2016**, *718*, 052016. [CrossRef]
129. Morishima, K.; Kuno, M.; Nishio, A.; Kitagawa, N.; Manabe, Y.; Moto, M.; Takasaki, F.; Fujii, H.; Satoh, K.; Kodama, H.; et al. Discovery of a big void in Khufu's Pyramid by observation of cosmic-ray muons. *Nature* **2017**, *552*, 386–390. [CrossRef]
130. Baccani, G.; Bonechi, L.; Bongi, M.; Brocchini, D.; Casagli, N.; Ciaranfi, R.; Cimmino, L.; Ciulli, V.; D'Alessandro, R.; Del Ventisette, C.; et al. Muon radiography of ancient mines: The San Silvestro archaeo-mining park (Campiglia Marittima, Tuscany). *Universe* **2019**, *5*, 34. [CrossRef]
131. Biondi, F.; Malanga, C. Synthetic Aperture Radar Doppler Tomography Reveals Details of Undiscovered High-Resolution Internal Structure of the Great Pyramid of Giza. *Remote Sens.* **2022**, *14*, 5231. [CrossRef]
132. Margottini, C.; Spizzichino, D.; Orlando, L.; Marsella, M.; Renzi, B.; Sonnessa, A.; Pandolfi, O.; Soddu, P. Geotechnical and geophysical characterization of Moai statues—Rapa nui easter Island (Chile). In *Geotechnical Engineering for the Preservation of Monuments and Historic Sites, Proceedings of the 2nd International Symposium on Geotechnical Engineering for the Preservation of Monuments and Historic Sites, Napoli, Italy, May 2013*; Taylor & Francis Group: London, UK, 2013; pp. 539–547.
133. Abd-el-Maguid, M.M. Underwater Archaeology in Egypt and the Protection of its Underwater Cultural Heritage. *J. Mari. Arch.* **2012**, *7*, 193–207. [CrossRef]
134. Barstad, J.F. Underwater Archaeology in the 20th Century. In *International Handbook of Underwater Archaeology*; Ruppé, C.V., Barstad, J.F., Eds.; The Springer Series in Underwater Archaeology; Springer: Boston, MA, USA, 2002. [CrossRef]
135. Donati, J.; Sarris, A. Geophysical survey in Greece: Recent developments, discoveries and future prospects. *Archaeol. Rep.* **2016**, *62*, 63–76. [CrossRef]
136. Tusa, S. Research, protection and evaluation of Sicilian and Mediterranean marine cultural heritage. *Conserv. Sci. Cult. Herit.* **2009**, *9*, 79–112. [CrossRef]
137. Ding, W.; Dineng, Z.; Mingwei, W.; Zhihao, L. Chapter 4 Side-scan Sonar and Sub-bottom Profiler Surveying. In *High-Resolution Seafloor Survey and Applications*; Anthropogenic Geomorphic Fingerprints Identification, Evolution and Hydrodynamic Response of the Inner Lingding Bay in the Last 100 Years 2020; NSFC No.41906069; Springer: Berlin/Heidelberg, Germany; Science Press: Beijing, China, 2020.
138. Mattei, G.; Giordano, F. Integrated geophysical research of Bourbonic shipwrecks sunk in the Gulf of Naples in 1799. *J. Archaeol. Sci. Rep.* **2015**, *1*, 64–72. [CrossRef]
139. Özdas, H.; Kizildağ, N. Archaeological and Geophysical Investigation of Submerged Coastal Structures in Kekova, Southern Coast of Turkey. *Geoarchaeology Int. J.* **2013**, *28*, 504–516. [CrossRef]
140. Capozzoli, L.; Giampaolo, V.; De Martino, G.; Perciante, F.; Lapenna, V.; Rizzo, E. ERT and GPR prospecting applied to unsaturated and subwater analogue archaeological site in a full scale laboratory. *Appl. Sci.* **2022**, *12*, 1126. [CrossRef]
141. Passaro, S. Marine electrical resistivity tomography for shipwreck detection in very shallow water: A case study from Agropoli (Salerno, southern Italy). *J. Archaeol. Sci.* **2010**, *37*, 1989–1998. [CrossRef]
142. Oikonomou, D.; Papadopoulos, N.; Simyrdanis, K.; Cantoro, G.; Beck, J.; Loke, M.H. Processing strategies for 3-D marine dynamic electrical resistivity tomography data. In Proceedings of the 13th International Conference on Archaeological Prospection, Sligo, Ireland, 28 August–1 September 2019.
143. Papadopoulos, N. Shallow Offshore Geophysical Prospection of Archaeological Sites in Eastern Mediterranean. *Remote Sens.* **2021**, *13*, 1237. [CrossRef]
144. Loke, M.H.; Papadopoulos, N.; Wilkinson, P.B.; Oikonomou, D.; Simyrdanis, K.; Rucker, D.F. The inversion of data from very large three-dimensional electrical resistivity tomography mobile surveys. *Geophys. Prospect.* **2020**, *68*, 2579–2597. [CrossRef]

145. Cocchi, L.; Stefanelli, P.; Carmisciano, C.; Caratori Tontini, F.; Taramaschi, L.; Cipriani, S. Marine Archaeogeophysical Prospection of Roman Salapia Settlement (Puglia, Italy): Detecting Ancient Harbour Remains. *Archaeol. Prospect.* **2012**, *19*, 89–101. [CrossRef]
146. Ludeno, G.; Capozzoli, L.; Rizzo, E.; Soldovieri, F.; Catapano, I. A Microwave Tomography Strategy for Underwater Imaging via Ground Penetrating Radar. *Remote Sens.* **2018**, *10*, 1410. [CrossRef]
147. *EN 1998–1*; Eurocode 8: Design of Structures for Earthquake Resistance—Part 1: General Rules, Seismic Actions and Rules for Buildings. CEN (European Committee for Standardization): Brussels, Belgium, 2004.
148. *EN 1998–3*; Eurocode 8: Design of Structures for Earthquake Resistance—Part 3: Assessment and Retrofitting of Buildings. CEN (European Committee for Standardization): Brussels, Belgium, 2005.
149. Crispino, M.; D'Apuzzo, M. Measurement and prediction of traffic-induced vibrations in a heritage building. *J. Sound Vibrat.* **2001**, *246*, 319–335. [CrossRef]
150. Jakubczyk-Galczynska, A.; Jankowski, R. Traffic-induced vibrations. The impact on buildings and people. In Proceedings of the 9th International Conference Environmental Engineering, Vilnius, Lithuania, 22–23 May 2014. [CrossRef]
151. D'Amico, S.; Imposa, S.; Panzera, F.; Lombardo, G.; Betti, M.; Muscat, R.; Borg, R.; Grassi, S. Evaluating dynamic behavior of historical buildings through ambient seismic noise measurement and numerical modelling. In Proceedings of the IMEKO International Conference on Metrology for Archaeology and Cultural Heritage, Lecce, Italy, 23–25 October 2017.
152. Iannucci, R.; Martino, S.; Paciello, A.; D'Amico, S.; Galea, P. Investigation of cliff instability at Għajn Ħadid Tower (Selmun Promontory, Malta) by integrated passive seismic techniques. *J. Seismol.* **2020**, *24*, 897–916. [CrossRef]
153. Gentile, C.; Saisi, A. Ambient vibration testing of historic masonry towers for structural identification and damage assessment. *Constr. Build. Mater.* **2007**, *21*, 1311–1321. [CrossRef]
154. Saisi, A.; Gentile, C. Post-earthquake diagnostic investigation of a historic masonry tower. *J. Cult. Herit.* **2015**, *16*, 602–609. [CrossRef]
155. Bernardeschi, K.; Padovani, C.; Pasquinelli, G. Numerical modelling of the structural behavior of Buti's bell tower. *J. Cult. Herit.* **2004**, *5*, 371–378. [CrossRef]
156. Carpinteri, A.; Invernizzi, S.; Lacidogna, G. Numerical assessment of three medieval 1085 masonry towers subjected to different loading conditions. *Mason. Int.* **2006**, *19*, 65–76.
157. Girardi, M.; Padovani, C.; Pagni, A.; Pasquinelli, G. Numerical modeling of masonry towers: The case study of the Rognosa Tower in San Gimignano. In Proceedings of the Fourth International Conference on Structural Engineering, Mechanics and Computation, SEMC 2010, Cape Town, South Africa, 6–8 September 2010.
158. Micelli, F.; Cascardi, A. Structural assessment and seismic analysis of a 14th century masonry tower. *Eng. Fail. Anal.* **2019**, *107*, 104198. [CrossRef]
159. Facchini, L.; Betti, M. An efficient Bouc & Wen approach for seismic analysis of masonry tower. *Fract. Struct. Integr.* **2014**, *29*, 139–149. [CrossRef]
160. Bartoli, G.; Betti, M.; Galano, L.; Pieraccini, M. Seismic Assessment of Historic Masonry Towers: Non-invasive Techniques and Analysis Methodologies. In *Handbook of Cultural Heritage Analysis*; Springer International Publishing: Cham, Switzerland, 2022; pp. 1221–1268.
161. Acito, M.; Bocciarelli, M.; Chiesi, C.; Milani, G. Collapse of the clock tower in finale Emilia after the May 2012 Emilia Romagna earthquake sequence: Numerical insight. *Eng. Struct.* **2014**, *72*, 70–91. [CrossRef]
162. Augenti, N.; Parisi, F. Learning from construction failures due to the 2009 L'Aquila, Italy, earthquake. *J. Perform. Constr. Facil.* **2010**, *24*, 536–555. [CrossRef]
163. Atzeni, C.; Bicci, A.; Dei, D.; Fratini, M.; Pieraccini, M. Remote Survey of the Leaning Tower of Pisa by Interferometric Sensing. *IEEE Geosci. Remote Sens. Lett.* **2010**, *7*, 185–189. [CrossRef]
164. Calcina, S.V.; Piroddi, L.; Ranieri, G. Fast dynamic control of damaged historical buildings: A new useful approach for Structural Health Monitoring after an earthquake. *ISRN Civ. Eng.* **2013**, *2013*, 527604. [CrossRef]
165. Calcina, S.V.; Piroddi, L.; Ranieri, G. Vibration analysis of historic bell towers by means of contact and remote sensing measurements. *Nondestruct. Test. Eval.* **2016**, *31*, 4–331. [CrossRef]
166. Castagnetti, C.; Bassoli, E.; Vincenzi, L.; Mancini, F. Dynamic Assessment of Masonry Towers Based on Terrestrial Radar Interferometer and Accelerometers. *Sensors* **2019**, *19*, 1319. [CrossRef]
167. Marchisio, M.; Piroddi, L.; Ranieri, G.; Calcina, S.V.; Farina, P. Comparison of natural and artificial forcing to study the dynamic behaviour of bell towers in low wind context by means of ground-based radar interferometry: The case of the Leaning Tower in Pisa. *J. Geophys. Eng.* **2014**, *11*, 055004. [CrossRef]
168. Montuori, A.; Luzi, G.; Stramondo, S.; Casula, G.; Bignami, C.; Bonali, E.; Bianchi, M.G.; Crosetto, M. Combined use of ground-based systems for Cultural Heritage conservation monitoring. In Proceedings of the 2014 IEEE Geoscience and Remote Sensing Symposium, Quebec City, QC, Canada, 13–18 July 2014; IEEE: New York, NY, USA, 2014.

169. Nico, G.; Masci, O.; Panidi, E. Non-destructive monitoring strategies of historical constructions and tangible Culturale Heritage based on Ground-based SAR Interferometry. In Proceedings of the International Conference InterCarto/InterGIS, GI Support of Sustainable Development of Territories, Petrozavodsk (Russia), Bonn (Germany), Anchorage (USA), Anchorage, AL, USA, 19 July–1 August 2018; pp. 528–535.
170. Pieraccini, M.; Fratini, M.; Dei, D.; Atzeni, C. Structural testing of Historical Heritage Site Towers by microwave remote sensing. *J. Cult. Herit.* **2009**, *10*, 174–182. [CrossRef]
171. Pieraccini, M.; Dei, D.; Betti, M.; Bartoli, G.; Tucci, G.; Guardini, N. Dynamic identification of historic masonry towers through an expeditious and no-contact approach: Application to the "Torre del Mangia" in Siena (Italy). *J. Cult. Herit.* **2014**, *15*, 275–282. [CrossRef]
172. Porco, G.; Costanzo, A.; Montuori, A.; Casula, G.; Luzi, G. Material damage assessment and Structural Health Monitoring of historical heritages by using NDT techniques and proximal remote sensing tools. In Proceedings of the 8th National Conference NDT of the Hellenic Society of NDT—HSNT Athens, National Hellenic Research Foundation, Athens, Greece, 8–9 May 2015.
173. Luzi, G.; Montuori, A.; Bignami, C.; Crosetto, M.; Stramondo, S. Radar Interferometry for Cultural Heritage Monitoring. In Proceedings of the 11th International Conference on Non-Destructive Investigations and Microanalysis for the Diagnostics and Conservation of Cultural and Environmental Heritage—ART-2014, Madrid, Spain, 11–13 June 2014.
174. Fratini, M.; Pieraccini, M.; Atzeni, C.; Betti, M.; Bartoli, G. Assessment of vibration reduction on the Baptistery of San Giovanni in Florence (Italy) after vehicular traffic block. *J. Cult. Herit.* **2011**, *12*, 323–328. [CrossRef]
175. Piroddi, L.; Calcina, S.V. Integrated Vibration Analysis for Historical Dome Structures: A Complementary Approach Based on Conventional Geophysical Methods and Remote Sensing Techniques. In *Computational Science and Its Applications—ICCSA 2020*; Gervasi, O., Ed.; Lecture Notes in Computer Science; Springer: Cham, Switzerland, 2020; Volume 12255. [CrossRef]
176. Atzeni, C.; Barla, M.; Pieraccini, M.; Antolini, F. Early Warning Monitoring of Natural and Engineered Slopes with Ground-Based Synthetic-Aperture Radar. *Rock Mech. Rock Eng.* **2015**, *48*, 235–246. [CrossRef]
177. Pieraccini, M.; Miccinesi, L. Ground-based Radar Interferometry: A Bibliographic Review. *Remote Sens.* **2019**, *11*, 1029. [CrossRef]
178. Pratesi, F.; Nolesini, T.; Bianchini, S.; Leva, D.; Lombardi, L.; Fanti, R.; Casagli, N. Early Warning GBInSAR-Based Method for Monitoring Volterra (Tuscany, Italy) City Walls. *IEEE J. Sel. Top. Appl. Earth Obs. Remote Sens.* **2015**, *8*, 4–1753. [CrossRef]
179. Frodella, W.; Ciampalini, A.; Gigli, G.; Lombardi, L.; Raspini, F.; Nocentini, M.; Scardigli, C.; Casagli, N. Synergic use of satellite and ground based remote sensing methods for monitoring the San Leo rock cliff (Northern Italy). *Geomorphology* **2016**, *264*, 80–94. [CrossRef]
180. Tapete, D.; Casagli, N.; Luzi, G.; Fanti, R.; Gigli, G.; Leva, D. Integrating radar and laser-based remote sensing techniques for monitoring structural deformation of archaeological monuments. *J. Archaeol. Sci.* **2013**, *40*, 176–189. [CrossRef]
181. Chen, F.; Guo, H.; Tapete, D.; Cigna, F.; Piro, S.; Lasaponara, R.; Masini, N. The role of imaging radar in cultural heritage: From technologies to applications. *Int. J. Appl. Earth Obs. Geoinf.* **2022**, *112*, 102907. [CrossRef]
182. Moscatelli, M.; Piscitelli, S.; Piro, S.; Stigliano, F.; Giocoli, A.; Zamuner, D.; Marconi, F. Integrated geological and geophysical investigations to characterize the anthropic layer of the Palatine hill and Roman Forum (Rome, Italy). *Bull. Earthq. Eng.* **2014**, *12*, 1319–1338. [CrossRef]
183. Capozzoli, L.; De Martino, G.; Capozzoli, V.; Duplouy, A.; Henning, A.; Rizzo, E. The pre-Roman hilltop settlement of Monte Torretta di Pietragalla: Preliminary results of the geophysical survey. *Archaeol. Prospect.* **2020**, *30*, 33–46. [CrossRef]
184. Menci, L. StereoSpace: An idea for photogrammetric data collection. *Int. Arch. Photogramm. Remote Sens.* **2000**, *33*, 395–400.
185. Menci, L.; Ceccaroni, F. Digital photogrammetry. In *Information Technology and Project Automation*; Biagini, C., Ed.; University Press: Florence, Italy, 2002; pp. 115–138.
186. Pisa, C.; Zeppa, F.; Fangi, G. Spherical photogrammetry for cultural heritage—San Galgano Abbey and the Roman Theater, Sabratha. *J. Comput. Cult. Herit. (JOCCH)* **2011**, *4*, 1–15. [CrossRef]
187. Remondino, F.; El-Hakim, S. Image-based 3D modeling: A review. *Photogramm. Rec.* **2006**, *21*, 269–291. [CrossRef]
188. Soudarissanane, S.S.; Lindenbergh, R.C.; Gorte, B.G.H. Reducing the error in terrestrial laser scanning by optimizing the measurement set-up. In Proceedings of the XXI ISPRS Congress, Commission I-VIII, Beijing, China, 3–11 July 2008; International Society for Photogrammetry and Remote Sensing: Hannover, Germany, 2008.
189. Lai, L.; Sordini, M.; Campana, S.; Usai, L.; Condò, F. 4D recording and analysis: The case study of Nuraghe Oes (Giave, Sardinia). *Digit. Appl. Archeol. Cult. Herit.* **2015**, *2*, 233–239. [CrossRef]
190. Gabrielli, R.; Greco, G. Umm Ar-Rasas: The Application of Integrated Methodologies for the Valorization of a Unesco Site. *Glob. J. Arch. Anthropol.* **2018**, *6*, 555688. [CrossRef]
191. .Angelini, A.; Cozzolino, M.; Gabrielli, R.; Gentile, V.; Mauriello, P. Geophysical and Geomatic Methods for the Knowledge, Conservation, and Management of Jordanian Cultural Heritage. *Geosciences* **2023**, *13*, 349. [CrossRef]
192. Barsanti, S.G.; Remondino, F.; Visintini, D. Photogrammetry and laser Scanning for archaeological site 3D modeling–Some critical issues. In Proceedings of the 2nd Workshop on the New Technologies for Aquileia, Aquileia, Italy, 25 June 2012; Roberto, V., Fozzat, L., Eds.

193. Arias, P.; González-Aguilera, D.; Riveiro, B.; Caparrini, N. Documentation based on orthographic images of archaeological structures: The case of a medieval wall in Pontevedra, Spain. *Archaeometry* **2011**, *53*, 858–872. [CrossRef]
194. Lambers, K.; Eisenbeiss, H.; Sauerbier, M.; Kupferschmidt, D.; Gaisecker, T.; Sotoodeh, S.; Hanusch, T. Combining photogrammetry and laser scanning for the recording and modelling of the Late Intermediate Period site of Pinchango Alto, Palpa, Peru. *J. Archaeol. Sci.* **2007**, *34*, 1702–1712. [CrossRef]
195. Lerma, J.L.; Navarro, S.; Cabrelles, M.; Villaverde, V. Terrestrial laser scanning and close range Photogrammetry for 3D archaeological documentation: The Upper Palaeolithic Cave of Parpalló as a case study. *J. Archaeol. Sci.* **2010**, *37*, 499–507. [CrossRef]
196. Dell'Unto, N.; Landeschi, G.; Touati, A.M.L.; Dellepiane, M.; Callieri, M.; Ferdani, D. Experiencing ancient buildings from a 3D GIS perspective: A case drawn from the Swedish Pompeii Project. *J. Archaeol. Method Theory* **2016**, *23*, 73–94. [CrossRef]
197. Sauerbier, M.; Eisenbeiss, H. UAVs for the documentation of archaeological Excavations. *Int. Arch. Photogramm. Remote Sens. Spat. Inf. Sci.* **2010**, *38*, 526–531.
198. McClinton, K.E. Applications of Photogrammetric Modeling to Roman Wall Painting: A Case Study in the House of Marcus Lucretius. *Arts* **2019**, *8*, 89. [CrossRef]
199. Danese, M.; Sileo, M.; Masini, N. Geophysical Methods and Spatial Information for the Analysis of Decaying Frescoes. *Surv. Geophys.* **2018**, *39*, 1149–1166. [CrossRef]
200. Cozzolino, M.; Di Meo, A.; Gentile, V.; Mauriello, P.; Zullo, E. Combined Use of 3D Metric Survey and GPR for the Diagnosis of the Trapezophoros with Two Griffins Attacking a Doe of Ascoli Satriano (Foggia, Italy). *Geosciences* **2020**, *10*, 307. [CrossRef]
201. Kersten, T.P.; Hinrichsen, N.; Lindstaedt, M.; Weber, C.; Schreyer, K.; Tschirschwitz, F. Architectural Historical 4D Documentation of the Old-Segeberg Town House by Photogrammetry, Terrestrial Laser Scanning and Historical Analysis. In *Digital Heritage. Progress in Cultural Heritage: Documentation, Preservation, and Protection*; Ioannides, M., Magnenat-Thalmann, N., Fink, E., Žarnić, R., Yen, A.Y., Quak, E., Eds.; Lecture Notes in Computer Science; Springer: Cham, Switzerland, 2014; Volume 8740. [CrossRef]
202. Fawzy, H.E.-D. 3D laser scanning and close-range photogrammetry for buildings documentation: A hybrid technique towards a better accuracy. *Alex. Eng. J.* **2019**, *58*, 4–1191. [CrossRef]
203. Cozzolino, M.; Di Meo, A.; Gentile, V. The contribution of indirect topographic surveys (photogrammetry and laser scanner) and GPR investigations in the study of the vulnerability of the Abbey of Santa Maria a Mare, Tremiti Islands (Italy). *Ann. Geophys.* **2019**, *62*, 3. [CrossRef]
204. Cozzolino, M.; Gabrielli, R.; Galata', P.; Gentile, V.; Greco, G.; Scopinaro, E. Combined use of 3D metric surveys and non-invasive geophysical surveys at the Stylite Tower (Umm ar-Rasas, Jordan). *Ann. Geophys.* **2019**, *62*, 3. [CrossRef]
205. Angelini, A.; Cozzolino, M.; Gabrielli, R.; Gentile, V.; Mauriello, P. Three-Dimensional Modeling and Non-Invasive Diagnosis of a Huge and Complex Heritage Building: The Patriarchal Basilica of Santa Maria Assunta in Aquileia (Udine, Italy). *Remote Sens.* **2023**, *15*, 2386. [CrossRef]
206. Angelini, A.; Cozzolino, M.; Foschi, B.; Gabrielli, R.; Gentile, V.; Mauriello, P.; Scopinaro, E. Joint Use of Geomatic and Geophysical Methods for the Survey and Documentation of the Vespasian's Thermal Baths (Cittaducale, Rieti, Italy). In *International Conference on Computational Science and Its Applications*; Springer: Cham, Switzerland, 2024; pp. 388–405.
207. Capper, J.E. Photographs of Stonehenge as seen from a War Balloon. *Archaeologia* **1907**, *60*, 571. [CrossRef]
208. Verhoeven, G. Providing an archeological bird'seye view—An overall picture of ground-based means to execute low-altitude aerial photography (LAAP) in Archeology. *Archaeol. Prospect.* **2009**, *16*, 233–249. [CrossRef]
209. Campana, S. Drones in archaeology. State-of-the-art and future perspectives. *Archaeol. Prospect.* **2017**, *24*, 275–296. [CrossRef]
210. Colosi, F.; Fangi, G.; Gabrielli, R.; Orazi, R.; Angelini, A.; Bozzi, C.A. Planning the Archaeological Park of Chan Chan (Peru) by means of satellite images, GIS and photogrammetry. *J. Cult. Herit.* **2009**, *10*, e27–e34. [CrossRef]
211. Gabrielli, R.; Angelini, A.; Portarena, D. The Shawbak Castle from a balloon. An integrated methodological approach for the study of archaeological emergencies. *Archeol. Aerea* **2019**, *11*, 50–58.
212. Altan, M.O.; Celikoyan, T.M.; Kemper, G.; Toz, G. Balloon photogrammetry for cultural heritage. *Int. Arch. Photogramm. Remote Sens. Spat. Inf. Sci.* **2004**, *35*, 964–968.
213. Ahmet, K. The Western Papagueria from the air: Digital imagery using kite and balloon aerial photography. In *Enter the Past. The E-Way into the Four Dimensions of Cultural Heritage. CAA 2003. Computer Applications and Quantitative Methods in Archaeology, Proceedings of the 31st Conference*; Wien, M.d.S., Erbe, R.K., Wien, S., Eds.; Archaeo Press: Oxford, UK; pp. 46–49.
214. Bogacki, M.; Malkowski, W.; Misiewicz, K. Kite aerial photography (KAP) as a tool for completing GIS models. Ptolemais (Libya) case study. In *Remote Sensing for Archaeology and Cultural Heritage Management. Proceedings of the 1st International EARSeL Workshop, CNR, Rome*; Lasaponara, R., Masini, N., Eds.; Aracne: Rome, Italy, 2008; pp. 329–332.
215. Vannini, G.; Nucciotti, M.; Gabrielli, R. Stratigraphy and virtual modeling: An interdisciplinary approach to the study of the archaeological site of Santa Maria di Rescamone (France-Corsica). In *The Reconstruction of Archaeological Landscapes through Digital Technologies. Proceedings of the 2nd Italy-United States Workshop, Rome, Italy, 3–5 November 2003*; Berkeley, USA, May 2005; Forte, M., Ed.; Archaeo Press: Oxford, UK, 2005; pp. 139–146.

216. Eisenbeiss, H.; Lambers, K.; Sauerbier, M.; Li, Z. Photogrammetric documentation of an archaeological site (Palpa, Peru) Using an Autonomous Model Helicopter. In Proceedings of the CIPA 2005 XX International Symposium, Torino, Italy, 26 September 2005; Hailey TI; The Powered Parachute as an Archaeological Reconnaissance Vehicle; Archaeological Prospection; Camera and Imaging Products Association: Tokyo, Japan, 2005; Volume 12, pp. 69–78.
217. Seitz, C.; Altenbach, H. Project Archeye—The quadrocopter as the archaeologist's eye, ISPRS Zurich 2011 Workshop, 14–16 September 2011, Zurich. *Int. Arch. Photogramm. Remote Sens. Spat. Inf. Sci.* **2011**, *XXXVIII*, 297–302.
218. Remondino, F.; Barazzetti, L.; Nex, F.; Scaioni, M.; Sarazzi, D. UAV photogrammetry for mapping and 3D modelling—Current status and future perspectives. *Int. Arch. Photogramm. Remote Sens. Spat. Inf. Sci.* **2011**, *XXXVIII*, 25–31.
219. Rinaudo, F.; Chiabrando, F.; Lingua, A.; Spanò, A. Archaeological site monitoring: UAV photogrammetry could be an answer. *Int. Arch. Photogramm. Remote Sens. Spat. Inf. Sci.* **2012**, *39*, 583–588. [CrossRef]
220. Campana, S.; Sordini, M.; Rizzi, A. 3D Modeling of a Romanesque church in Tuscany: Archaeological aims and geomatic techniques. In Proceedings of the 3rd International Workshop on the 3D Virtual Reconstruction and Visualization of Complex Architectures, Trento, Italy, 25–28 February 2009.
221. Fiorillo, F.; Jiménez Fernández-Palacios, B.; Remondino, F.; Barba, S. 3d Surveying and modelling of the archaeological area of Paestum, Italy. *Virtual Archaeol. Rev.* **2013**, *4*, 55–60. [CrossRef]
222. Fiorillo, F.; Remondino, F.; Barba, S.; Santoriello, A.; De Vita, C.B.; Casellato, A. 3D digitization and mapping of heritage monuments and comparison with historical drawings. In Proceedings of the XXIV International CIPA Symposium, Strasbourg, France, 2–6 September 2013; ISPRS Annals of the Photogrammetry, Remote Sensing and Spatial Information Sciences II(5/W1); pp. 133–138.
223. Pueschel, H.; Sauerbier, M.; Eisenbeiss, H. A 3D model of Castle Landenberg (CH) from combined photogrammetric processing of terrestrial and UAV-based images. *Int. Arch. Photogramm. Remote Sens. Spat. Inf. Sci.* **2008**, *XXXVII*, 93–98.
224. Remondino, F.; Gruen, A.; Von Schwerin, J.; Eisenbeiss, H.; Rizzi, A.; Sauerbier, M.; Richards-Rissetto, H. Multisensors 3D documentation of the Maya site of Copan. In Proceedings of the 22nd CIPA Symposium, Kyoto, Japan, 11–15 October 2009.
225. Bendea, H.; Chiabrando, F.; Tonolo, F.G.; Marenchino, D. Mapping of archaeological areas using a low-cost UAV. The Augusta Bagiennorum test site. In *AntiCIPAting the Future of the Cultural Past. Proceedings of the CIPA 2007 XXI International Symposium, Athens, Greece, 1–6 October 2007*; National Technical University of Athens: Athens, Greece, 2007.
226. Chiabrando, F.; Nex, F.; Piatti, D.; Rinaudo, F. UAV and RPV systems for photogrammetric surveys in archeological areas: Two tests in the Piedmont Region (Italy). *J. Archaeol. Sci.* **2011**, *38*, 697–710. [CrossRef]
227. Sonnemann, T.F.; Malatesta, E.H.; Hofman, C.L. Applying UAS photogrammetry to analyze spatial patterns of indigenous settlement sites in the northern Dominican Republic. In *Archaeology in the Age of Sensing*; Forte, M., Campana, S., Eds.; Springer: New York, NY, USA, 2016.
228. Orihuela, A.; Molina-Fajardo, M.A. UAV Photogrammetry Surveying for Sustainable Conservation: The Case of Mondújar Castle (Granada, Spain). *Sustainability* **2021**, *13*, 24. [CrossRef]
229. Campana, S.; Sordini, M.; Remondino, F. Integration of geomatics techniques for the digital documentation of heritage areas. In Proceedings of the 1st European Association of Remote Sensing Laboratories (EARSeL) International Workshop on 'Advances in Remote Sensing for Archaeology and Cultural Heritage Management', Rome, Italy, 30 September–4 October 2008.
230. Guidi, G.; Russo, M. Reality-based and reconstructive models: Digital media for cultural heritage valorization. *SCIRES-IT-SCIentific RESearch Inf. Technol.* **2011**, *1*, 71–86.
231. Eisenbeiss, H.; Zhang, L. Comparison of DSMs generated from mini UAV imagery and terrestrial laser scanner in a cultural heritage application. *Int. Arch. Photogramm. Remote Sens. Spat. Inf. Sci.* **2006**, *XXXVI*, 90–96.
232. Pierdicca, R.; Frontoni, E.; Malinverni, E.S.; Colosi, F.; Orazi, R. Virtual reconstruction of archaeological heritage using a combination of photogrammetric techniques: Huaca Arco Iris, Chan Chan, Peru. *Digit. Appl. Archaeol. Cult. Herit.* **2016**, *3*, 3–80. [CrossRef]
233. Shaw, R.; Corns, A. Recording archaeological excavation using terrestrial laser scanning and low cost balloon based photogrammetry. In Proceedings of the CAA 2008. Computer Applications and Quantitative Methods in Archaeology, Budapest, Hungary, 2–6 April 2008.
234. Liang, H.; Li, W.; Lai, S.; Zhu, L.; Jiang, W.; Zhang, Q. The integration of terrestrial laser scanning and terrestrial and unmanned aerial vehicle digital Photogrammetry for the documentation of Chinese classical gardens–A case study of Huanxiu Shanzhuang, Suzhou, China. *J. Cult. Herit.* **2018**, *33*, 222–230. [CrossRef]
235. Fabbri, S.; Chiarini, V.; Ercolani, M.; Sansavini, G.; Santagata, T.; De Waele, J. Terrestrial laser scanning, geomorphology and archaeology of a Roman gypsum quarry (Vena del Gesso Romagnola area, Northern Apennines, Italy). *J. Archaeol. Sci. Rep.* **2021**, *36*, 102810. [CrossRef]
236. Guidi, G.; Russo, M.; Ercoli, S.; Remondino, F.; Rizzi, A.; Menna, F. A multi-resolution methodology for the 3D modeling of large and complex archaeological areas. *Int. J. Archit. Comput.* **2009**, *7*, 39–55.

237. Barone, P.M.; Ruffell, A.; Tsokas, G.N.; Rizzo, E. Geophysical Surveys for Archaeology and Cultural Heritage Preservation. *Heritage* **2019**, *2*, 2814–2817. [CrossRef]
238. Luo, L.; Wang, X.; Guo, H.; Lasaponara, R.; Zong, X.; Masini, N.; Wang, G.; Shi, P.; Khatteli, H.; Chen, F. Airborne and spaceborne remote sensing for archaeological and cultural heritage applications: A review of the century (1907–2017). *Remote Sens. Environ.* **2019**, *232*, 111280. [CrossRef]
239. Adamopoulos, E.; Rinaudo, F. UAS-Based Archaeological Remote Sensing: Review, Meta-Analysis and State-of-the-Art. *Drones* **2020**, *4*, 46. [CrossRef]
240. Agudo, P.; Pajas, J.; Pérez-Cabello, F.; Redón, J.; Lebrón, B. The Potential of Drones and Sensors to Enhance Detection of Archaeological Cropmarks: A Comparative Study between Multi-Spectral and Thermal Imagery. *Drones* **2018**, *2*, 29. [CrossRef]
241. McLeester, M.; Casana, J.; Schurr, M.R.; Hill, A.C.; Wheeler, J.H. Detecting prehistoric landscape features using thermal, multi-spectral, and historical imagery analysis at Midewin National Tallgrass Prairie, Illinois. *J. Archaeol. Sci. Rep.* **2018**, *21*, 450–459.
242. Uribe, P.; Angás, J.; Pérez-Cabello, F. Aerial mapping and multi-sensor approaches from remote sensing applied to the Roman Archaeological Heritage. Int. Arch. Photogramm. *Remote Sens. Spat. Inf. Sci.* **2015**, *XL-5/W4*, 461–467.
243. Brooke, C.; Clutterbuck, B. Mapping Heterogeneous Buried Archaeological Features Using Multisensor Data from Unmanned Aerial Vehicles. *Remote Sens.* **2019**, *12*, 41. [CrossRef]
244. Calleja, J.F.; Pagés, O.R.; Díaz-Álvarez, N.; Peón, J.; Gutiérrez, N.; Martín-Hernández, E.; Relea, A.C.; Melendi, D.R.; Álvarez, P.F. Detection of buried archaeological remains with the combined use of satellite multispectral data and UAV data. *Int. J. Appl. Earth Obs. Geoinf.* **2018**, *73*, 555–573. [CrossRef]
245. Casella, V.; Franzini, M.; Gorrini, M.E. Crop marks detection through optical and multi-spectral imagery acquired by UAV. In Proceedings of the 2018 Metrology for Archaeology and Cultural Heritage (MetroArchaeo), Cassino, Italy, 22–24 October 2018; pp. 173–177.
246. Cowley, D.; Moriarty, C.; Geddes, G.; Brown, G.; Wade, T.; Nichol, C. UAVs in Context: Archaeological Airborne Recording in a National Body of Survey and Record. *Drones* **2017**, *2*, 2. [CrossRef]
247. González, J.F.; Hernández, F.V. NDVI Identification and Survey of a Roman Road in the Northern Spanish Province of Álava. *Remote Sens.* **2019**, *11*, 725. [CrossRef]
248. Garzia, F.; Lombardi, M.; Papi, L. Analysis and data acquisition methodology based on flying drones for the implementation of the internet of everything to smart archaeological areas. *Int. J. Herit. Arch. Stud. Repairs Maintence* **2017**, *2*, 383–394. [CrossRef]
249. Gehrke, R.; Greiwe, A. RGBI images with UAV and o_-the-shelf compact cameras: An investigation of linear sensor characteristics. *EARSel Eproc.* **2014**, *13*, 53–58.
250. González, J.J.F.; González, J.I.F. Prospección arqueológica en NDVI con drones. El uso de geoEuskadi como herramienta de ponderación de un nuevo método. *Rev. Mapp.* **2018**, *29*, 24–29.
251. Hill, A.C.; Laugier, E.J.; Casana, J. Archaeological Remote Sensing Using Multi-Temporal, Drone-Acquired Thermal and Near Infrared (NIR) Imagery: A Case Study at the Enfield Shaker Village, New Hampshire. *Remote Sens.* **2020**, *12*, 690. [CrossRef]
252. Hill, A.C.; Rowan, Y.; Kersel, M.M. Mapping with Aerial Photographs: Recording the Past, the Present, and the Invisible at Marj Rabba, Israel. *Near East. Archaeol.* **2014**, *77*, 182–186. [CrossRef]
253. Koucká, L.; Kopăcková, V.; Fárová, K.; Gojda, M. UAV Mapping of an Archaeological Site Using RGB and NIR High-Resolution Data. *Proceedings* **2018**, *2*, 351. [CrossRef]
254. Lehmann, J.R.K.; Smithson, K.Z.; Prinz, T. Making the invisible visible: Using UAS-based high-resolution color-infrared imagery to identify buried medieval monastery walls. *J. Unmanned Veh. Syst.* **2015**, *3*, 58–67. [CrossRef]
255. Ramón, A.G.M.; Barba, L.; Ortiz, A.; Blancas, J. Geophysical prospection at the formative site of Altica in the Teotihacan Valley Piedmont. *Anc. Mesoam.* **2019**, *30*, 267–278. [CrossRef]
256. Moriarty, C.; Cowley, D.C.; Wade, T.; Nichol, C.J. Deploying multi-spectral remote sensing for multi-temporal analysis of archaeological crop stress at Ravenshall, Fife, Scotland. *Archaeol. Prospect.* **2019**, *26*, 33–46. [CrossRef]
257. Šedina, J.; Hulková, M.; Pavelka, K.; Pavelka, K., Jr. RPAS for documentation of Nazca aqueducts. Eur. *J. Remote. Sens.* **2019**, *52*, 174–181.
258. Raeva, P.; Pavelka, K.; Hanuš, J.; Gojda, M. Using of both hyperspectral aerial sensing and RPAS multi-spectral sensing for potential archaeological sites detection. In *Multispectral, Hyperspectral, and Ultraspectral Remote Sensing Technology, Techniques and Applications VII.*; Larar, A.M., Suzuki, M., Wang, J., Eds.; SPIE: Honolulu, HI, USA, 2018; p. 47.
259. Carmona, J.Á.S.; Quirós, E.; Mayoral, V.; Charro, C. Assessing the potential of multi-spectral and thermal UAV imagery from archaeological sites. A case study from the Iron Age hillfort of Villasviejas del Tamuja (Cáceres, Spain). *J. Archaeol. Sci. Rep.* **2020**, *31*, 102312.
260. Abate, N.; Frisetti, A.; Marazzi, F.; Masini, N.; Lasaponara, R. Multitemporal–Multispectral UAS Surveys for Archaeological Research: The Case Study of San Vincenzo Al Volturno (Molise, Italy). *Remote Sens.* **2021**, *13*, 2719. [CrossRef]

261. Brumana, R.; Oreni, D.; Van Hecke, L.; Barazzetti, L.; Previtali, M.; Roncoroni, F.; Valente, R. Combined geometric and thermal analysis from UAV platforms for archaeological heritage documenation. *ISPRS Ann. Photogramm. Remote Sens. Spat. Inf. Sci.* **2013**, *II-5/W1*, 49–54.
262. Liu, C.; Cao, Y.; Yang, C.; Zhou, Y.; Ai, M. Pattern identification and analysis for the traditional village using low altitude UAV-borne remote sensing: Multifeatured geospatial data to support rural landscape investigation, documentation and management. *J. Cult. Herit.* **2020**, *44*, 185–195. [CrossRef]
263. Magnini, L.; Bettineschi, C.; De Guio, A.; Burigana, L.; Colombatti, G.; Bettanini, C.; Aboudan, A. Multisensor-multiscale approach in studying the proto-historic settlement of Bostel in northern Italy. *Archeol. Calc.* **2019**, *30*, 347–365.
264. Parisi, E.I.; Suma, M.; Güleç Korumaz, A.; Rosina, E.; Tucci, G. Aerial platforms (UAV) surveys in the VIS and TIR range. Applications on archaeology and agriculture. *Int. Arch. Photogramm. Remote Sens. Spat. Inf. Sci.* **2019**, *XLII-2/W11*, 945–952. [CrossRef]
265. Šedina, J.; Housarová, E.; Raeva, P. Using RPAS for the detection of archaeological objects using multi-spectral and thermal imaging. *Eur. J. Remote Sens.* **2019**, *52*, 182–191. [CrossRef]
266. Skarlatos, D.; Vlachos, M. Vegetation removal from UAV derived DSMs, using combination of RGB and NIR imagery. *ISPRS Ann. Photogramm. Remote Sens. Spat. Inf. Sci.* **2018**, *IV-2*, 255–262. [CrossRef]
267. Casana, J.; Wiewel, A.; Cool, A.; Hill, A.C.; Fisher, K.D.; Laugier, E.J. Archaeological Aerial Thermography in Theory and Practice. *Adv. Archaeol. Pract.* **2017**, *5*, 310–327. [CrossRef]
268. Levin, S.; Yuan, M.; Adler, M. Thermographic Quantification for Archaeological Prospection at Picuris Pueblo, New Mexico. In Proceedings of the 2018 3rd Digital Heritage International Congress (DigitalHERITAGE) Held Jointly with 2018 24th International Conference on Virtual Systems & Multimedia (VSMM 2018), San Francisco, CA, USA, 26–30 October 2018; pp. 1–8.
269. Thomas, H. Some like it hot: The impact of next generation FLIR Systems thermal cameras on archaeological thermography. *Archaeol. Prospect.* **2018**, *25*, 81–87. [CrossRef]
270. Thomas, H.; Williams, E. High resolution terrestrial thermography of archaeological sites. *Archaeol. Prospect.* **2019**, *26*, 189–198. [CrossRef]
271. Walker, S. Low-altitude aerial thermography for the archaeological investigation of arctic landscapes. *J. Archaeol. Sci.* **2020**, *117*, 105126. [CrossRef]
272. Poirier, N.; Hautefeuille, F.; Calastrenc, C. Low Altitude Thermal Survey by Means of an Automated Unmanned Aerial Vehicle for the Detection of Archaeological Buried Structures: Thermal Archaeological Survey by Automated Unmanned Aerial Vehicle. *Archaeol. Prospect.* **2013**, *20*, 303–307. [CrossRef]
273. Piga, C.; Piroddi, L.; Pompianu, E.; Ranieri, G.; Stocco, S.; Trogu, A. Integrated geophysical and aerial sensing methods for archaeology: A case history in the Punic Site of Villamar (Sardinia, Italy). *Remote Sens.* **2014**, *6*, 10986–11012. [CrossRef]
274. Casana, J.; Kantner, J.; Wiewel, A.; Cothren, J. Archaeological aerial thermography: A case study at the Chaco-era Blue J community, New Mexico. *J. Archaeol. Sci.* **2014**, *45*, 207–219. [CrossRef]
275. Barazzetti, L.; Brumana, R.; Oreni, D.; Cuca, B.; Previtali, M.; Roncoroni, F. Finding Buried Remains Using Thermal Images. *Int. J. Herit. Digit. Era* **2015**, *4*, 295–306. [CrossRef]
276. Adamopoulos, E.; Rinaudo, F. Enhancing Image-Based Multiscale Heritage Recording with Near-Infrared Data. *ISPRS Int. J. Geo-Inf.* **2020**, *9*, 269. [CrossRef]
277. Evers, R.; Masters, P. The application of low-altitude near-infrared aerial photography for detecting clandestine burials using a UAV and low-cost unmodified digital camera. *Forensic Sci. Int.* **2018**, *289*, 408–418. [CrossRef]
278. Colombatti, G.; Aboudan, A.; Bettanini, C.; Magnini, L.; Bettineschi, C.; Deotto, G.; Toninello, L.; Debei, S.; Guio, A.D.; Zanovello, P.; et al. Horus—A drone project for visual and IR imaging. In Proceedings of the 2017 IEEE International Workshop on Metrology for AeroSpace (MetroAeroSpace), Padua, Italy, 21–23 June 2017; pp. 589–592.
279. Khan, S.; Aragão, L.; Iriarte, J. A UAV–lidar system to map Amazonian rainforest and its ancient landscape transformations. *Int. J. Remote Sens.* **2017**, *38*, 2313–2330. [CrossRef]
280. Murtha, T.M.; Broadbent, E.N.; Golden, C.; Scherer, A.; Schroder, W.; Wilkinson, B.; Zambrano, A.A. Drone-Mounted Lidar Survey of Maya Settlement and Landscape. *Lat. Am. Antiq.* **2019**, *30*, 630–636. [CrossRef]
281. Risbøl, O.; Gustavsen, L. LiDAR from drones employed for mapping archaeology—Potential, benefits and challenges. *Archaeol. Prospect.* **2018**, *25*, 329–338. [CrossRef]
282. VanValkenburgh, P.; Cushman, K.C.; Butters, L.J.C.; Vega, C.R.; Roberts, C.B.; Kepler, C.; Kellner, J. Lasers Without Lost Cities: Using Drone Lidar to Capture Architectural Complexity at Kuelap, Amazonas, Peru. *J. Field Archaeol.* **2020**, *45*, S75–S88. [CrossRef]
283. Pisciotta, A.; Vitale, G.; Scudero, S.; Martorana, R.; Capizzi, P.; D'Alessandro, A. A lightweight prototype of a magnetometric system for unmanned aerial vehicles. *Sensors* **2021**, *21*, 4691. [CrossRef]

284. Garcia-Fernandez, M.; Alvarez-Lopez, Y.; Heras, F.L.; Gonzalez-Valdes, B.; Rodriguez-Vaqueiro, Y.; Pino, A.; Arboleya-Arboleya, A. GPR system on-board a UAV for non-invasive detection of buried objects. In Proceedings of the 2018 IEEE International Symposium on Antennas and Propagation & USNC/URSI National Radio Science Meeting, Boston, MA, USA, 8–13 July 2018; pp. 1967–1968.
285. Ludeno, G.; Catapano, I.; Renga, A.; Vetrella, A.R.; Fasano, G.; Soldovieri, F. Assessment of a micro-UAV system for microwave tomography radar imaging. *Remote Sens. Environ.* **2018**, *212*, 90–102. [CrossRef]
286. Linck, R.; Kaltak, A. Drone radar: A new survey approach for Archaeological Prospection? In Proceedings of the 13th International Conference on Archaeological Prospection, Sligo, Ireland, 28 August–1 September 2019; Bonsall, J., Ed.; pp. 268–271.
287. Accomando, F.; Florio, G. Drone-Borne Magnetic Gradiometry in Archaeological Applications. *Sensors* **2024**, *24*, 4270. [CrossRef]
288. Niccolucci, F.; Felicetti, A.; Hermon, S. Populating the data space for cultural heritage with heritage digital twins. *Data* **2022**, *7*, 105. [CrossRef]
289. Luther, W.; Baloian, N.; Biella, D.; Sacher, D. Digital twins and enabling technologies in museums and cultural heritage: An overview. *Sensors* **2023**, *23*, 1583. [CrossRef]
290. Shabani, A.; Skamantzari, M.; Tapinaki, S.; Georgopoulos, A.; Plevris, V.; Kioumarsi, M. 3D simulation models for developing digital twins of heritage structures: Challenges and strategies. *Procedia Struct. Integr.* **2022**, *37*, 314–320. [CrossRef]
291. Gabellone, F. Digital Twin: A new perspective for cultural heritage management and fruition. *Acta Imeko* **2022**, *11*, 7. [CrossRef]
292. Dang, X.; Liu, W.; Hong, Q.; Wang, Y.; Chen, X. Digital twin applications on cultural world heritage sites in China: A state-of-the-art overview. *J. Cult. Herit.* **2023**, *64*, 228–243. [CrossRef]
293. Council of Europe (1992) European Convention on the Protection of the Archaeological Heritage (Revised) (ETS No. 143), Valletta 16/01/1992—Treaty Open for Signature by the Member States and the Other States Parties to the European Cultural Convention and for Accession by the Other Non-Member States and by the EU. Available online: https://www.coe.int/en/web/culture-and-heritage/valletta-convention (accessed on 5 February 2025).
294. Cerato, I.; Pescarin, S. Reconstructing past landscapes for virtual museums. In *Good Practice in Archaeological Diagnostics: Non-Invasive Survey of Complex Archaeological Sites*; Springer International Publishing: Cham, Switzerland, 2013; pp. 285–296.
295. Ranieri, G.; Trogu, A.; Loddo, F.; Piroddi, L.; Cogoni, M. Digital museum from integrated 3D aerial photogrammetry, laser scanner and geophysics data. In Proceedings of the 24th European Meeting of Environmental and Engineering Geophysics, Porto, Portugal, 9–12 September 2018; European Association of Geoscientists & Engineers: Bunnik, The Netherlands, 2018; Volume 2018, No. 1, pp. 1–5.
296. Trizio, I.; Savini, F.; Giannangeli, A.; Fiore, S.; Marra, A.; Fabbrocino, G.; Ruggieri, A. Versatil tools: Digital survey and virtual reality for documentation, analysis and fruition of cultural heritage in seismic areas. *Int. Arch. Photogramm. Remote Sens. Spat. Inf. Sci.* **2019**, *42*, 377–384. [CrossRef]
297. Rababeh, S.; Hanaqtah, R.; Abu-Khafajah, S. Leveraging Digitized Heritage Technologies for Smart Fruition: Heritage Understanding and Enhancement Framework. *Heritage* **2024**, *7*, 6891–6915. [CrossRef]
298. Sharma, P.V. *Environmental and Engineering Geophysics*; Cambridge University Press: Cambridge, UK, 1997.
299. Butler, D.K. *Near-Surface Geophysics*; Society of Exploration Geophysicists: Houston, TX, USA, 2005.
300. Reynolds, J.M. *An Introduction to Applied and Environmental Geophysics*; John Wiley & Sons: Hoboken, NJ, USA, 2011.
301. Everett, M.E. *Near-Surface Applied Geophysics*; Cambridge University Press: Cambridge, UK, 2013.

Disclaimer/Publisher's Note: The statements, opinions and data contained in all publications are solely those of the individual author(s) and contributor(s) and not of MDPI and/or the editor(s). MDPI and/or the editor(s) disclaim responsibility for any injury to people or property resulting from any ideas, methods, instructions or products referred to in the content.